

INAUGURAL - DISSERTATION

Zur Erlangung der Doktorwürde
der
Naturwissenschaftlich-Mathematischen Gesamtfakultät
der
Ruprecht - Karls - Universität
Heidelberg

vorgelegt von

MRes Biomedical Science – Sahana Suresh Babu

aus Tumkur, India

Molecular mechanism of wall tension-induced zyxin activation in endothelial cells

Gutachter: Prof. Dr. Stephan Frings
PD Dr. Marco Cattaruzza

Tag der Mündlichen Prüfung:.....

ZUSAMMENFASSUNG

Eine chronische arterielle Hypertonie führt aufgrund mechanischer Überlastung zu dysfunktionalen Blutgefäßen, d. h. auf Zellebene zu einer endothelialen Dysfunktion und zu einem synthetischen Phänotyp glatter Gefäßmuskelzellen. Nicht überraschend ist deshalb, dass sie ein klassischer Risikofaktor für Arteriosklerose und hypertophen/hyperplastischen Gefäßwandumbau ist. Trotz ihrer klinischen Bedeutung sind die Mechanismen früher Phasen druckinduzierter Phänotypänderungen vaskulärer Zellen bisher wenig untersucht.

In dieser Arbeit wurden zum ersten Mal die molekularen Mechanismen der druck- bzw. dehnungsinduzierten Aktivierung des spezifischen *Mechanotransducer*-Proteins Zyxin *in vitro* und *in situ* untersucht. Darüber hinaus konnte gezeigt werden, dass Zyxin eigene Transkriptionsfaktoraktivität besitzt.

Die Aktivierung von Zyxin wird durch eine hierarchisch organisierte Signaltransduktionskaskade induziert, an deren Anfang die Aktivierung des Kationenkanals TRPC3 steht. Dies führt zu einer Ausschüttung von Endothelin-1 (ET-1) und danach, vermittelt durch den B-Typ Rezeptor von ET-1, von atrialem natriuretischem Peptid (ANP). ANP schließlich aktiviert seinen Guanylatzyklase-rezeptor GC-A was zu einer cGMP-vermittelten Phosphorylierung von Zyxin an Serin 142 durch die cGMP-abhängige Proteinkinase G führt. Diese Phosphorylierung ist notwendig für die Translokation von Zyxin in den Zellkern. Die wahrscheinlich zentrale Bedeutung von Zyxin für den (frühen) druckinduzierten Gefäßwandumbau wird dadurch unterstrichen, dass das Protein annähernd 70% aller dehnungssensitiven Gene reguliert indem es an ein neues Bindungsmotiv dehnungssensitiver Genpromotoren, die PyPu-box, bindet.

Die detaillierte Charakterisierung dieses komplexen dehnungsspezifischen Signalweges eröffnet in Zukunft die Möglichkeit schon während früher Phasen des druckinduzierten Gefäßumbaus in den Prozess einzugreifen. Neben eher pleiotropen Möglichkeiten die Zyxinaktivierung zu unterbinden, etwa eine pharmakologische Hemmung des B-Typ ET-1 Rezeptors, soll vor allem eine direkte Hemmung der Transkriptionsfaktoraktivität von Zyxin durch Decoy-Oligonukleotide versucht werden.

SUMMARY

Hypertension is a major predisposing factor for developing chronic endothelial dysfunction and a predominantly synthetic vascular smooth muscle cell phenotype. Therefore, the disease is one of the classical risk factors for atherosclerosis, arterial hypertrophy/hyperplasia and, consequently, cardiac hypertrophy.

Despite these severe clinical consequences, surprisingly little is known about the primary signalling events leading to pressure or wall tension-induced phenotype changes of vascular cells.

For the first time, the mechanisms of wall tension or stretch-induced activation of the specific mechanotransducer protein zyxin and its action as a transcription factor could be delineated in endothelial cells *in vitro* and *in situ* at the molecular level. Activation of zyxin is mediated by a hierarchical chain of events starting with the cation channel TRPC3, TRPC3-mediated or reinforced release of the autacoids ET-1 and, consecutively, ANP and, finally, the ANP receptor GC-A/cyclic GMP/ protein kinase G mediated phosphorylation of zyxin at serine-142. This phosphorylation enables zyxin to translocate to the nucleus where it affects the expression of approximately 70% of all stretch-sensitive genes in endothelial and smooth muscle cells by binding to a novel stretch-sensitive promoter motif, the PyPu-box. This motif is found in all zyxin-dependent genes so far analysed.

The detailed characterization of this complex pathway, specifically activated in response to mechanical overload in vascular cells, opens the possibility to interfere with early phases of pressure-/stretch-induced vascular remodelling process *in vivo* at several levels. Besides targeting the, quite pleiotropic, main mediators of zyxin activation, ET-1 and ANP, zyxin may be targeted directly, e.g., by use of decoy-oligonucleotides that specifically prevent it from acting as a transcription factor.

PUBLICATIONS*Journal articles*

Wójtowicz A*, **Babu SS***, Li L, Gretz N, Hecker M, Cattaruzza M (2010). Zyxin mediation of stretch-induced gene expression in human endothelial cells. *Circ Res* **107**(7): 898-902.

Babu SS, Wojtowicz A, Freichel M, Birnbaumer L, Hecker M, Cattaruzza M. Molecular mechanism of stretch-induced cellular mechanotransduction. *Submitted*.

Conference presentations

Suresh S, Wojtowicz A, Kuhn M, Hecker M and Cattaruzza M. Role of focal adhesion protein zyxin in wall-tension induced endothelial signaling. *Experimental Biology 2011*, Washington DC, US (April 2011).

Suresh S, Wojtowicz A, Kuhn M, Hecker M and Cattaruzza M. Role of focal adhesion protein zyxin in wall-tension induced endothelial signaling. *90th Annual German Physiological conference*, Regensburg, Germany (March 2011).

Suresh S, Wojtowicz A, Hecker M, Cattaruzza M. Mechanisms of wall tension induced vascular signaling. *Joint meeting of Scandinavian and German Physiological Societies*, Copenhagen, Denmark (March 2010).

Suresh S, Wojtowicz A, Hecker M, Cattaruzza M. Wall tension-induced signaling in endothelial cells. *88th Annual German Physiological Conference*, Giessen, Germany (March 2009).

CONTENTS

Abbreviations	V
1. INTRODUCTION.....	1
1.1 Hemodynamic forces and vascular homeostasis.....	1
1.2 Pathways of mechanically induced cardiovascular disease	2
1.3 Short term vs. chronic increases in wall tension.....	4
1.4 Known molecular mediators of wall tension-induced signalling	4
1.4.1 Stretch-induced transcription factors and pro-inflammatory gene expression in endothelial and smooth muscle cells	4
1.4.2 Endothelin-1 (ET-1).....	5
1.4.3 Atrial natriuretic peptide (ANP)	6
1.4.4 Transient receptor potential channels (TRP channels)	7
1.4.5 Specific versus non-specific vascular stretch-signalling	9
1.5 Focal adhesions in mechanotransduction.....	10
1.6 Structure of zyxin.....	11
1.7 Zyxin in vascular mechanotransduction	12
1.8 Aims of the project.....	12
2. MATERIALS	13
2.1 Synthetic oligonucleotide primers for PCR	13
2.2 Kits	15
2.3 Bacterial strains and plasmids.....	16
2.4 Cell culture.....	17
2.5 Reagents	17
2.6 Buffers and solutions	18
2.7 Microbiological media.....	19
2.8 Small interfering RNAs	19
2.9 Antibodies	20
2.10 Mouse strains	21
2.11 Software	22

3. METHODS	23
3.1 Molecular techniques	23
3.1.1 Expression plasmids.....	23
3.1.2 Site-directed mutagenesis	23
3.1.3 Plasmid cloning for RT-PCR standards.....	24
3.1.4 TOPO cloning	24
3.1.4.1 Transformation of competent bacteria.....	24
3.1.4.2 Plasmid mini/maxi-cultures and plasmid purification	25
3.1.5 Polymerase chain reaction (PCR)	25
3.1.6 Reverse transcription PCR (RT-PCR)	25
3.1.7 PCR amplification of DNA fragments.....	26
3.1.8 Quantitative real-time PCR.....	26
3.1.9 Agarose gel electrophoresis	27
3.1.10 Isolation of total DNA from cultured cells and mouse tails	28
3.1.11 Isolation of total RNA from cultured cells and femoral arteries	29
3.1.12 Measurement of RNA/cDNA concentration.....	29
3.2 Cell culture.....	29
3.2.1 Isolation and culture of human umbilical vein endothelial cells (HUVEC)	29
3.2.2. Culture of mouse smooth muscle cells	30
3.2.3 siRNA transfection into HUVEC.....	30
3.2.4 Transfection of zyxin expression plasmids into HUVEC.....	31
3.2.5 Incubation of cells with various drugs	32
3.2.6 Application of mechanical strain	32
3.3 Immunofluorescence analysis	33
3.3.1 Cell fixation	33
3.3.2 Immunostaining of fixed cells	33
3.4 Immunohistochemistry	34
3.4.1 Tissue preparation for paraffin embedding.....	34
3.4.2 Staining of paraffin sections	34
3.5 Confocal microscopy	35
3.6 Chromatin immunoprecipitation (ChIP).	35
3.7 Protein biochemistry	36
3.7.1 Isolation of total cellular protein.....	36
3.7.1 Separation of cytoplasmic and nuclear proteins	36
3.7.2 Sodium dodecylsulfate polyacrylamide gel electrophoresis (SDS-PAGE).....	36

3.7.3 Western blot analysis	38
3.7.4 Enzyme-linked immunosorbent assay (ELISA)	39
3.8 <i>Ex-vivo</i> blood vessel perfusion	39
3.8.1 Isolation and preparation of murine femoral arteries for perfusion	39
3.8.2 Perfusion of isolated murine femoral arteries	39
3.9 Statistical analysis	41
4. RESULTS	42
4.1 Effect of cyclic stretch on cellular localisation of zyxin (<i>in vitro</i>)	42
4.2 Pressure-induced zyxin translocation in mouse arteries (<i>in situ</i>).....	44
4.3 Role of zyxin in stretch-induced gene expression	45
4.4 Mechanism of zyxin-induced gene expression	47
4.4.1 Zyxin association with the PyPu box:.....	48
4.4.2 PyPu box mimicking decoy oligonucleotide (decoy ODN)	50
4.4.3 Optimisation of the stretch protocol	51
4.5 Components of the signalling cascade activated by wall tension	53
4.5.1 Effect of mechanosensitive pathway inhibitors on zyxin translocation	53
4.5.2 Effect of ANP and ET-1 on zyxin translocation	56
4.5.3 Effect of the TRP blocker gadolinium on stretch induced	
ANP and ET-1 expression in endothelial cells	56
4.6 Hierarchy of TRPs, ANP and ET-1 in zyxin translocation pathway in	
endothelial cells	58
4.7 Zyxin translocation in smooth muscle cells.....	61
4.8 TRP channels in endothelial cells	62
4.9 <i>In situ</i> perfusion analysis of femoral arteries derived from	
TRP- deficient mice	63
4.10 TRPC3 mediates zyxin activation.....	64
4.10.1 <i>In situ</i> analysis of TRP KO femoral arteries	64
4.10.2 Analysis of TRP deficient SMC for zyxin translocation	64
4.11 GC-A mediates zyxin phosphorylation by PKG.....	67
4.11.1 <i>In situ</i> analysis of GC-A deficient femoral arteries	67
4.11.2 Analysis of GC-A deficient smooth muscle cell.....	68
4.12 Analysis of phosphorylated amino acid residues in zyxin	
targeted by PKG.....	70
4.12.1 Generation eGFP-zyxin constructs	71
4.12.2 Transfection of zyxin expression plasmids into HUVEC.....	71

4.12.3 Effects of ANP on cells transfected with zyxin-wildtype and mutant constructs	71
4.12.4 Effect of cyclic stretch on cells transfected with zyxin-wildtype and mutant constructs	73
4.13 Effect of Rho associated protein kinase (ROCK) on zyxin translocation .	75
5. DISCUSSION	77
5.1 Models used to apply wall tension.....	77
5.2 Gene expression regulated by zyxin	78
5.3 The endothelial cell response to stretch – a defined signalling cascade	80
5.4 Stretch-induced zyxin activation and pressure-induced vascular remodelling	86
5.5 Perspective	86
6. REFERENCES.....	88
APPENDIX.....	96
ACKNOWLEDGEMENTS	98

Abbreviations

ANOVA	analysis of variance
ANP	atrial natriuretic peptide
BNP	brain natriuretic peptide
BSA	bovine serum albumin
cGMP	cyclic guanosine monophosphate
ChIP	chromatin immune precipitation
CNP	c-type natriuretic peptide
D142	aspartate 142
DMEM	Dulbecco's modification of eagle's medium
DNA	deoxyribonucleic acid
DTT	dithiotreitol
EC	endothelial cells
EDTA	ethylene diamine tetraacetic acid
EGTA	ethylene glycol tetra acetic acid
ELISA	enzyme-linked immunosorbent assay
ET-1	endothelin-1
ET_B-R	Endothelin-1 receptor B type
FA	focal adhesion
FBS	fetal bovine serum
FSS	fluid shear stress
GAPDH	glyceraldehyde-3-phosphate dehydrogenase
GC-A/B	guanylyl cyclase receptor type A/B
Gd³⁺	gadolinium
GSEA	gene set enrichment analysis
HRP	horseradish peroxidase
HUVEC	human umbilical vein endothelial cells
ICAM-1	intercellular adhesion molecule-1
IFA	immunofluorescence analysis
IL-8	interleukin 8
MCP-1	monocyte chemoattractant protein-1
NES	nuclear export signal
ng	nano-gram
NO	nitric oxide
NOS-3	type 3 (endothelial) nitric oxide synthase
NPR-C	C-type ANP receptor
Nu	nucleus
PBS	phosphate buffered saline

PCR	polymerase chain reaction
PKG	protein kinase G
PVDF	polyvinylidene fluoride
RNA	ribonucleic acid
ROCK	rho-associated protein kinase
Rp8pGPT-cGMPS	guanosine, 3',5'-cyclic monophosphorothioate, 8--(4-chlorophenylthio)-, Rp-isomer
RPM	revolutions per minute
RT	reverse transcriptase
RT-PCR	reverse transcription-polymerase chain reaction
S142	serine -142
S-1-P	spingocine-1-phosphate
SDS	sodium dodecylsulfate
SDS-PAGE	sodium dodecylsulfate-polyacrylamide gel electrophoresis
SF	stress fibres
siRNA	small interfering RNA
SMA	smooth muscle actin
SMC	smooth muscle cell
TRP	transient receptor potential channel
VASP	vasodilator-stimulated phosphoprotein
VCAM-1	vascular cell adhesion molecule-1
VEGF	vascular endothelial growth factor
WT	wall tension

1. INTRODUCTION

1.1 Hemodynamic forces and vascular homeostasis

The balance between circumferential wall tension (WT) and laminar fluid shear stress (FSS), the two principle hemodynamic forces to which vascular cells are exposed to, governs their phenotype (Davies 1995; Lehoux 2006, Fig. 1). FSS, by its stimulatory effect on endothelial nitric oxide (NO) production with its multiple effects on endothelial cell and smooth muscle cell signalling (Hermann 1997), has generally been defined as an anti-inflammatory and homeostatic force (Uematsu 1995; Kawashima 2004; Malek 1999). In contrast, WT has been marked as a potentially detrimental pro-inflammatory force causing, among others, a prolonged increase in intracellular free calcium concentrations, formation of reactive oxygen species and activation of other stress-pathways (Hishikawa 1997; Cheng 2001).

Shifting the balance between these two forces towards WT, e.g., due to inadequately low FSS, or increased WT, consequently leads to both adaptive and maladaptive vascular remodelling processes. Whereas adaptive processes like a limited growth of medial smooth muscle cells re-adjust the aforementioned balance and then stop (see the Laplace equation, Figure 1), maladaptive processes are characterised by an excessive and lasting phenotype change in vascular cells, include atherosclerosis and hypertension-induced hypertrophic arterial remodelling.

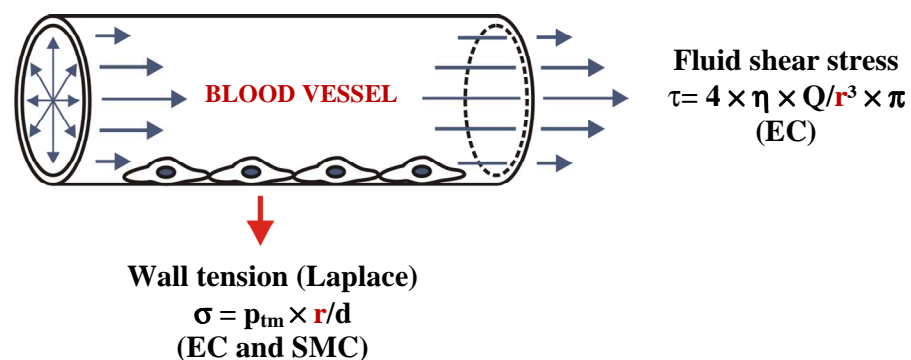


Figure 1: Hemodynamic forces in the arterial system. Wall tension (σ) is a tensile force or stretch sensed by smooth muscle cells (SMC) and endothelial cells (EC) and depends on transmural pressure (p_{tm}), vessel radius (r) and wall thickness (d) in blood vessels (represented as: $\sigma = p_{tm} \times r/d$). Fluid shear stress (τ), viscous drag parallel to the longitudinal axis of the blood vessel, is sensed by EC only and is expressed as $\tau = 4 \times \eta \times Q/r^3 \times \pi$ where η is the viscosity, Q the blood flow and r the vessel radius. Suggestively, as the radius is part of the numerator in WT and denominator in FSS, both forces may be regarded to be functionally antagonistic.

1.2 Pathways of mechanically induced cardiovascular disease

Although several vascular pathologies caused by an imbalance of FSS and WT possess similar or even identical patho-mechanisms at the cellular level, the primary cause of the imbalance, low FSS or high WT, mostly defines the actual nature of vascular dysfunction. This may be due to the fact that FSS has a *direct* effect only on endothelial cells (EC), whereas increased WT acts on both SMC and EC.

For example, an intrinsic anatomical feature of the vascular tree, the necessity for arterial bifurcations, leads to endothelial dysfunction defined locations. Here, merely due to the geometry of the vascular bed, laminar FSS decreases and, additionally, systolic pulse waves cause a somewhat increased WT in the vessel wall (Glagov 1988; Sharma 2010, Figure 2).

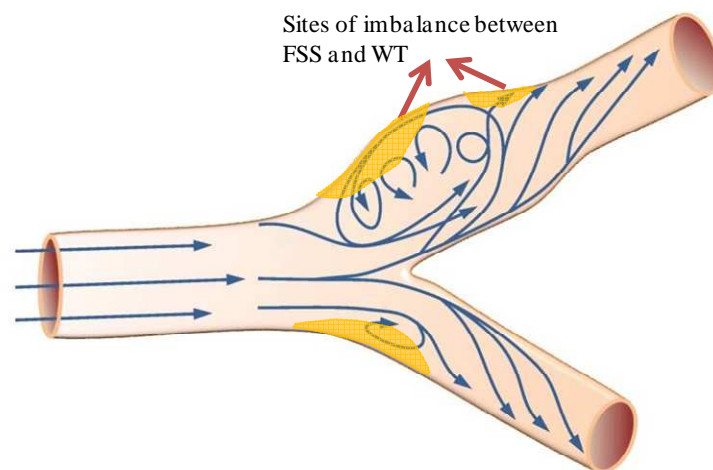


Figure 2: Arterial bifurcations are prone to hemodynamic stress: Scheme of typical flow profiles at arterial bifurcations, the sites where fluid shear stress (FSS) and wall tension (WT), without any pathological transformation, are in imbalance. (modified from Cattaruzza 2011). Atherosclerosis-prone locations are highlighted in yellow.

Therefore, because of chronic deficiency in NO formation (low FSS) and stress-signalling (Klotz 2002, increased WT) not only the EC will be dysfunctional, but also the underlying medial SMC will develop a synthetic, hence pro-inflammatory and proliferative and/or hypertrophic, phenotype already in young and healthy individuals (Wung 1997; Guest 2006). Not surprisingly, it is here where first signs of atherosclerosis, can be found suggesting that a lasting force shift dominated by a decrease in FSS leads to a chronic inflammatory response.

In contrast, chronically increased WT in hypertension is dominated by a phenotype shift of SMC from the contractile to the synthetic state (Lehoux 2006). Also here, however, EC play an important role as, besides a moderately decreased FSS and, consequently NO production, WT also alters the phenotype of EC in a particular way (Sumpio 1990). However, this process, although fed by pro-inflammatory pathways, finally does not result in a predominantly inflammatory response but causes a hypertrophic (conduit arteries) or hyperplastic (resistance arteries) remodelling (Heagerty 1993; Lehoux 1998). This process, as outlined for the limited response above, is aimed to diminish WT via an increase in wall thickness (see Figure 1) but, unfortunately, if exaggerated and generalized, causes in parallel a critical increase in total peripheral resistance and, therefore fixation of the elevated blood pressure level with its consequences such as cardiac remodelling (Figure 3; MacMohan 1990; Pasterkamp 2000; Pohl 2009).

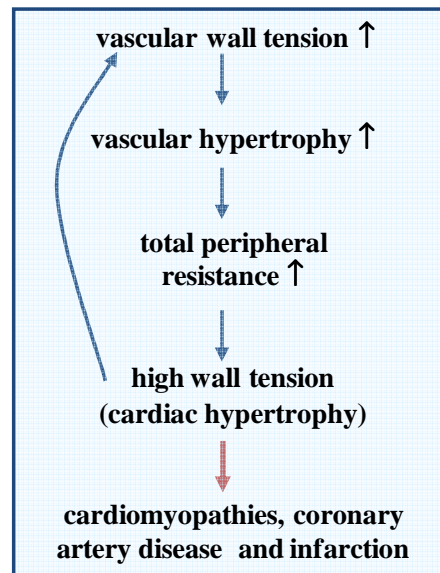


Figure 3: Vicious circle of pressure-induced cardiovascular remodelling. Pressure-induced vascular remodelling causes a similar process in the heart. Again, WT is a major determinant as the myocardium responds with a hypertrophic growth to increased afterload. However, normalization of cardiac WT inevitably comes along with increased ejection pressure and/or volume, thus, triggering a new response and so forth. The process is terminated (red arrow), when the critical heart weight is reached (dilative cardiomyopathies) or, alternatively, cardiac perfusion becomes insufficient because of (WT-induced) atherosclerosis (coronary artery disease/myocardial infarction).

As in this thesis WT and the specific signalling mechanism activated in EC and SMC by this force are the major focus, the vascular response to acute and lasting increases in WT will be shortly discussed. A critical point in this discussion will be that actually little is known about specific WT-induced mechanotransduction in EC and SMC and, hence, the early phase of WT-induced vascular remodelling.

1.3 Short term vs. chronic increases in wall tension

A first line response of arteries to pressure-induced supra-physiological WT levels is the release of vasoactive mediators such as the vasoconstrictor endothelin-1 (ET-1) from endothelial cells aimed at offloading the overt mechanical strain by active vasoconstriction (Schiffrin 1999). However, when this initial response is insufficient, i.e., local regulation of the vascular tone cannot be reinstated against the high transmural pressure, a next phase is initiated. Then, the lasting WT-induced release of ET-1 and many other trophic factors released from EC as well as SMC such as chemokines like IL-8 or MCP-1 (Yue 1994; Porecca 1997), or platelet-derived growth factor (Kida 2010) cause the above mentioned pressure-induced remodelling process. However, what is the switch from constriction to remodelling? What is the initial signal?

1.4 Known molecular mediators of wall tension-induced signalling

Wall tension is basically a tensile force which is experienced as stretch exerted at the cellular level. Therefore, stretch will further on be used synonymous to wall tension.

1.4.1 Stretch-induced transcription factors and pro-inflammatory gene expression in endothelial and smooth muscle cells

As mentioned above, chronic increases in cyclic stretch possess a marked pro-inflammatory component and, thus, promote the expression of several pro-inflammatory gene products such as vascular endothelial growth factors (VEGF; Black 2004), cell adhesion molecules (ICAM-1, VCAM-1; Sung 2007) and chemokines (interleukin-8, MCP-1, Schepers 2006).

This change in pro-inflammatory gene expression has been thought to be mainly caused by the activation of several kinases such as c-Jun N-terminal kinases and p38 MAPK (mitogen activated protein kinase p38; Tsuda 2002; Li 2003). These

and other kinases are known to activate transcription factors such as activator protein-1 (AP-1), CAAT/enhancer binding protein (C/EBP) or nuclear factor- κ B (NF- κ B) (Hishikawa 1997; Wagner 2000; De Martin 2000; Li 2003; Demicheva 2008). Indeed, the stretch-dependent activation of AP-1 is critical for the up-regulation of preproET-1 gene expression, the precursor of ET-1 (Lauth 2000) pointing towards a role of these common proliferation and inflammation-related pathways in stretch-induced activation of vascular cells.

Another well defined factor in stretch-induced endothelial and smooth muscle cell-signalling is NADPH oxidase, an enzyme that catalyses the formation of superoxide anions (Molavi and Mehta, 2004). Superoxide anions and degradation products of this reactive oxygen derivative, NO-derived peroxynitrite (Kawashima and Yokoyama 2004) and hydrogen peroxide have all been implicated in stretch-induced remodelling (Kinlay 2001; Libby 2007). Indeed, several of the above mentioned transcription factors can be indirectly activated by these mediators suggesting oxidative stress as a factor in stretch-induced gene expression and phenotype changes in vascular cells. Nevertheless, NADPH-oxidase, most of the transcription factors and gene products discussed above have been shown to be activated and play a role in several cellular stress responses (Schiffrin 2003; Black 2004), especially in inflammation (Griendling 2000).

Thus, although principally the stretch-induced activation of these factors is not controversial, all these factors are not specific for stretch or WT and cannot explain the unique response of vascular cells to chronic stretch.

So, what specific stretch-induced factors are known?

1.4.2 Endothelin-1 (ET-1)

The local vasoconstrictor peptide ET-1 is secreted by endothelial cells in response to increased WT (Yamasaki 1995, Sadoshima & Izumo 1997). It is expressed by endothelial cells as a precursor peptide (preproET-1) that is first cleaved to bigET-1 and then to the mature 21-amino acid peptide. Although the cellular mechanism of action via two G protein-coupled receptors, ET_A-R and ET_B-R, appears to be similar to systemic vasoconstrictors such as angiotensin II and norepinephrine, its expression is controlled exclusively at the local level defining ET-1 as the major local vasoconstrictor (Yanagisawa 1994; Salvator 2010). Besides its short-time

vasoconstrictor effects, chronically increased ET-1 secretion has trophic effects on SMC (Touyz 2004; Piechota 2010). Interestingly, ET-1 is able to induce cardiac ANP release (Mäntymaa 1990, Shirakami 1993) linking these two stretch-inducible autacoids together (see below).

1.4.3 Atrial natriuretic peptide (ANP)

ANP is known as the heart-derived hormone that is released by the atrial cardiomyocytes in response to supra-physiological distension of the atria thus stretch caused by hypervolemia. The stretch-sensing cells seem to be the atrial endothelial cells (Mäntymaa 1990, Shirakami 1993) which, in response to that stimulus release ET-1. ET-1, in turn, seems to bind to myocyte ET_A-R (Thibault 1994) which, then, causes ANP secretion (Taskinen 2000). The increased secretion of ANP results in reduced sodium (Na⁺) and water retention by increasing the rate of glomerular filtration, inhibiting sodium re-absorption by the kidney (natriuresis) and decreasing hypothalamic release of the anti-diuretic hormone/vasopressin. Consequently, the reduced salt/water re-absorption causes a volume loss in this way helping to return blood volume, hence, atrial wall tension, back to normal (Guyton & Hall 1996).

ANP, B-type natriuretic peptide (BNP) and C-type natriuretic peptide (CNP) are the types of natriuretic peptides found in mammals. Natriuretic peptides bind to three functionally distinct receptors, two membrane-bound guanylyl cyclases, GC-A, GC-B, and NPR-C, a receptor coupled to trimeric G-proteins (Stults 1994; Schulz 2005; Potter 2006). The physiological effects of natriuretic peptides are mostly elicited through the cGMP formed by activation of the two guanylate cyclase receptors and cGMP binding proteins namely the cGMP-dependent effector-kinase PKG (Airhart 2003; Suga 1992). Whereas, ANP and BNP preferentially bind to GC-A resulting in natriuresis and vasorelaxation effects in vascular cells and epithelia (Potter 2006), CNP binds to GC-B resulting in growth regulation in bone cells and fibroblasts (Chrisman 1999). All three peptides bind to NPR-C which seems to mostly act as a clearance receptor by mediating lysosomal degradation of all three natriuretic peptides (Garbers 1991; Cohen 1996; Nussenzveig 1990).

Thus, ANP as ET-1 may be interesting for stretch-induced signalling because of two reasons: the peptide is known to have effects on EC and SMC and ANP is one

of the factors known to be genuinely and specifically released in response to increases in wall tension/stretch.

1.4.4 Transient receptor potential channels (TRP channels)

TRP channels are a complex superfamily of non-selective cation channels which are implicated in a wide range of functions from nociception to the vascular myogenic response (Figure 4; Davis and Hill 1999; Minke 2002; Vennekens 2010). TRP channels have been found in many cell types, including both neuronal cells, such as sensory and primary afferent neurons and non-neuronal tissues such as vascular endothelial cells, epithelial cells, and smooth muscle cells.

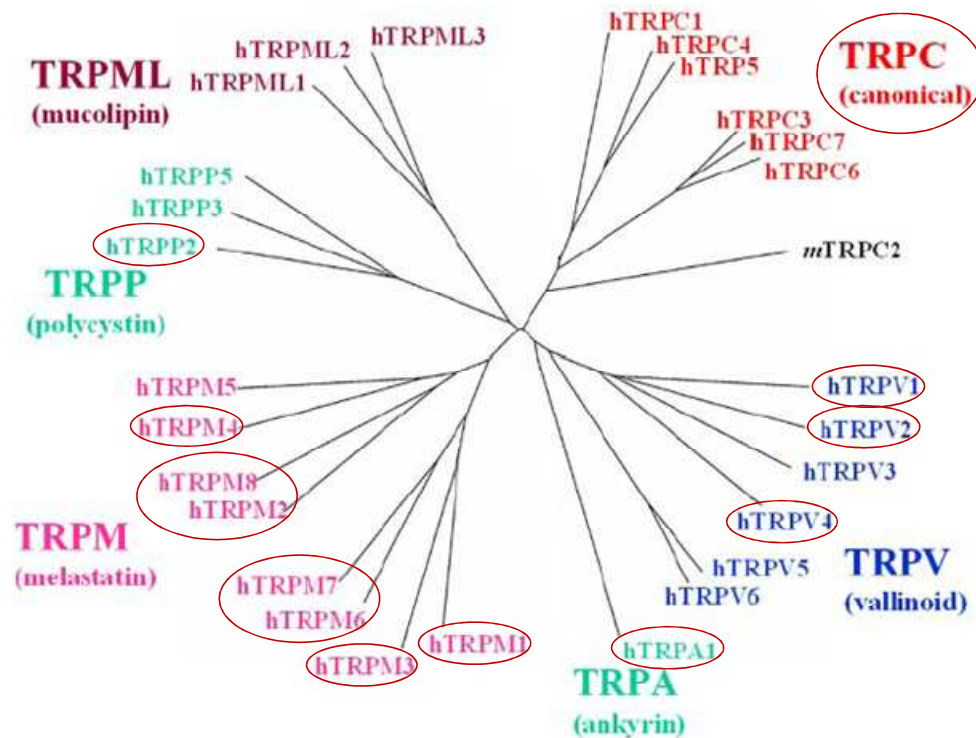


Figure 4: Phylogenetic tree of the mammalian transient receptor potential (TRP) channel superfamily. The 28 mammalian TRP channels can be subdivided into six main subfamilies: TRPC (canonical), TRPM (melastatin), TRPV (vanilloid), TRPA (ankyrin), TRPP (polycystin), and TRPML (mucolipin; adapted from Nilius 2007). TRP channels previously characterised to be expressed in EC and/or SMC are encircled in red.

TRP channel structure

The structure of TRP channels relates them to the superfamily of voltage-gated channel proteins characterised by six transmembrane segments (S1-S6), a pore region (between S5 and S6), and a voltage sensor. The N-terminus of several members of the TRP channel family exhibits ankyrin domains and a coiled-coil domain. The cytosolic C-terminus domain, depending on the TRP subfamily, may display phosphoinositide (PIP2) and/or calmodulin-binding (CaM) domains. In addition, the C-terminal domain may also exhibit a TRP domain that contributes to the association of several single receptor molecules which may build up a “super-channel” (Minke 2002; Figure 5). The molecular domains that are conserved in all members of the TRP family constitute parts of the transmembrane domains and in most members also the ankyrin-like repeats. All of the above features suggest that members of the TRP family are multifunctional “special assignment” channels, which are recruited to diverse signalling pathways (Cases and Montiel 2007).

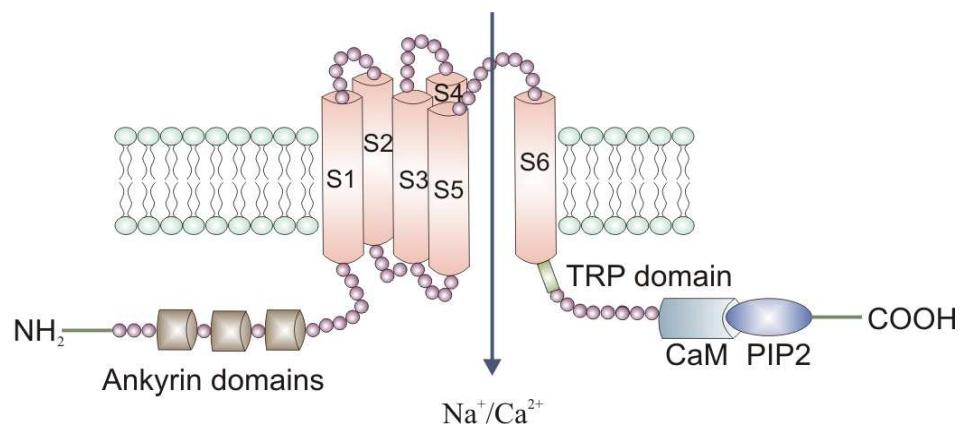


Figure 5: Molecular structure of TRP channels. The Figure displays a membrane domain composed of six transmembrane segments (S1–S6) with an amphipathic region between the fifth and sixth segment that forms the channel conductive pore. The additional domains shown are discussed in the text.

TRP channels in mechanotransduction

TRPM3 was found to be activated by hyper osmotic (“swelling”) stimuli when it was first characterised and it has been suggested to have a role in calcium homeostasis because of its high calcium conductance (Grimm 2003). TRPV1 has been implicated in controlling the response of the bladder urothelium to stretch and TRPV1 knockout mice have defects in bladder voiding (Birder 2002), a

process largely controlled by WT of the bladder. TRPC3 and TRPC6, along with TRPV2 and TRPM4, are implicated in mediating the arterial myogenic response, a major WT-controlled mechanism by which arteries rapidly compensate sudden increases in perfusion pressure (Davis 1999). Knockdown of these TRP channel genes in vascular SMC decreases the mechanically responsive current that is observed in response to experimentally stretching of these cells (Welsh 2002; Dietrich 2005).

TRPM7 has also been implicated in mechanosensing in native vascular SMC at higher pressures (Oancea 2006). However, although involved in the specific response to stretch in several cell types, up to now it is not clear whether TRP channels are real mechanosensors or are only indirectly activated by stretch.

Endothelial TRP channels

Several members of the TRP superfamily have been identified and characterised in the endothelium (for review see Nilius 2007). TRPC1, C4, C6, and M7 have been linked to endothelial barrier dysfunction and perturbed angiogenic processes, TRPC3, C4, M2, and M7 have been suggested to be responsible for oxidative damage and cell death. TRPM2 mediates H₂O₂-induced increases in endothelial permeability through activation of calcium entry (Dietrich 2008; Hecquet 2008). TRPA1 has been implicated as a player in endothelium-dependent vasorelaxation via activation of the endothelial NO synthase (Earley 2009).

1.4.5 Specific versus non-specific vascular stretch-signalling

Thus, the response of EC and SMC to supra-physiological stretch includes several non-specific stress-responses (1.4.1). These signalling pathways may play a role in later phases of vascular remodelling or may be activated by (a) specific response-pathway(s). However, it is difficult to imagine how these (mostly pro-inflammatory) stress-pathways can be responsible for the *onset* of pressure-induced vascular remodelling. On the other hand, not many really specific stretch-response factors are known or, at least, suspected (1.3.2 to 1.3.4). Moreover, these molecules do not necessarily act together.

In this context, the focal adhesion protein zyxin was identified as a highly specific transducer of a stretch-stimulus to the nucleus of SMC (Cattaruzza 2004) and EC

(Wojtowicz 2010 and doctoral thesis of Agnieszka Wojtowicz, Heidelberg, 2008). Moreover, focal adhesion complexes have been shown to integrate a multitude of signal transduction cascades leading to functional changes within the cell (Christopher 2004; Samarel 2005; Lehoux 2006). Using zyxin as the first specific mechanotransducer characterised in EC and SMC, it may be possible to characterise the stretch-induced signalling cascade in these cells.

1.5 Focal adhesions in mechanotransduction

Focal adhesions mediate force transmission from the extracellular matrix to the cytoskeleton, cytoskeletal organization and integrate signal transduction of multiple stimuli. They consist of a complex network of proteins linking the extracellular matrix (ECM) to the actin cytoskeleton as shown in the Figure 6 (Kanchanawong 2010; Guo 2007).

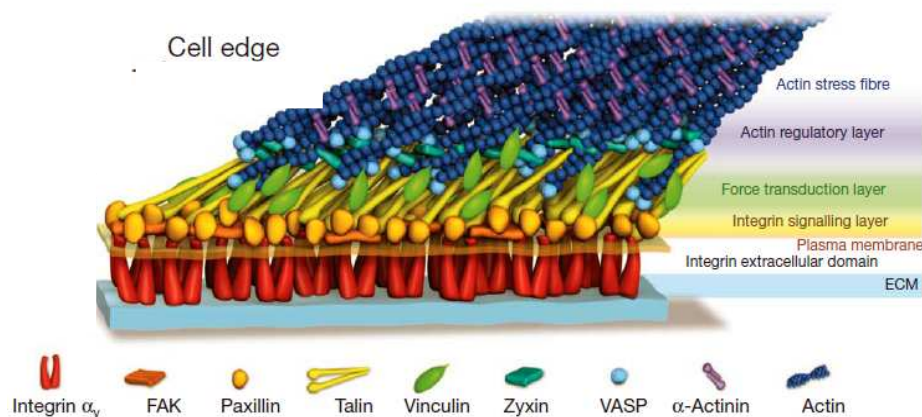


Figure 6: Molecular organisation of focal adhesion proteins in a cell: Integrins mediate the attachment of the cell to the extracellular matrix. The intracellular domain contains 3 functional layers: (i) the force transduction layer consisting of proteins like zyxin, paxillin, talin, vinculin and VASP, (ii) the signalling layer consisting of focal adhesion kinase and intracellular integrin domains involved in signalling cascades controlling adhesion dynamics and (iii) the actin regulatory layer essentially organized by actin filaments and α -actinin (adapted from Kanchanawong 2010).

The above outlined model of focal adhesions places zyxin at an ideal place, namely at the interface between possible force sensing and several signalling pathways. Zyxin, as other members of the family of LIM-domain proteins, Ajuba and the proto-oncogene lipoma-preferred protein (LPP), have indeed been

discussed to be involved in signalling processes due to their domain structure (Beckerle 1997; Kanungo 2000; Petit 2000).

1.6 Structure of zyxin

Zyxin is a zinc-binding phospho-protein originally identified in chicken fibroblasts as a protein associated with the actin cytoskeleton, cell-cell adherens junctions and integrins at sites of cell–substratum attachment (Macalma 1996; Reinhard 1999; Rottner 2001). A proline-rich region of zyxin mediates its association with α -actinin, three consecutive actA-domains interact with proteins of the Ena/VASP family that are important for the assembly and integrity of the actin cytoskeleton. At the C-terminus of zyxin three specific zinc finger structures, LIM domains, have been characterised. These domains have been shown to participate in specific protein–protein interactions, signal transduction and may also have the capacity to bind nucleic DNA (Figure 7; Wang and Gilmore 2003, Nix 1997). The functional nuclear export signal in the conserved leucine-rich region of zyxin (corresponding to the amino acids 322-331) is required to exclude zyxin from the nucleus (Nix 1997). Zyxin and its partners have been implicated in the spatial control of actin filament assembly as well as in pathways important for cell differentiation (Reinhard 1999). Thus, zyxin displays a tandem array of domains that mediate protein-protein interactions (Schmeichel and Beckerle, 1994).

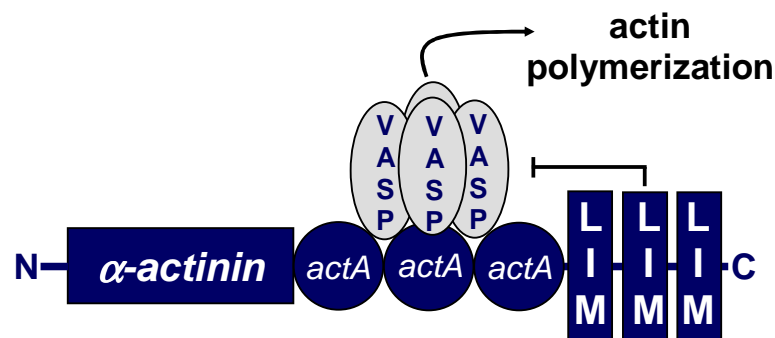


Figure 7: Molecular structure of zyxin indicating different domains required to interact with other focal adhesion proteins such as VASP. Zyxin is composed of three C-terminal zinc finger containing LIM domains, a proline-rich N-terminal region and at least one nuclear export signal (Nix 1997; taken from the doctoral thesis of Agnieszka Wojtowicz, Heidelberg, 2008).

1.7 Zyxin in vascular mechanotransduction

Several expression constructs of zyxin missing the nuclear export signal were found to shuttle between focal adhesions and the nucleus when overexpressed in chicken fibroblasts (Nix 1997). In cardiomyocytes, zyxin as whole protein is capable of translocating into the nucleus (Kato et al, 2005).

For a signalling protein to be a specific transducer of WT (i) the molecule must be associated with the actual sensor for WT, e.g. integrin-containing structures like focal adhesions, (ii) this ‘mechanotransducer’ has to be sensitive to activation and capable of transducing the signal, i.e. an increase in WT must lead to a signal to the cell nucleus and (iii) a specific mechanotransducer should orchestrate the first steps in adapting the cellular phenotype to the altered haemodynamic situation.

Zyxin in response to stretch is phosphorylated (doctoral thesis of Agnieszka Wojtowicz, Heidelberg, 2008) and enters the nucleus in its phosphorylated state in order to regulate the expression of several stretch-induced gene products. Therefore, the protein fulfils the above criteria to be a true mechanotransducer (Cattaruzza 2004; doctoral thesis of Agnieszka Wojtowicz, Heidelberg, 2008, Wojtowicz 2010).

1.8 Aims of the project

Zyxin is a specific mechanotransducer protein in EC and SMC. Using zyxin activation and zyxin-induced gene expression in stretched EC and SMC as functional read-outs, the following questions have been addressed to elucidate the specific mechanotransduction pathway in EC and SMC in which zyxin is implicated:

1. Additionally, what is the mechanism through which zyxin alters gene expression in these cells.
2. What is the causal chain of events leading to wall tension-induced zyxin activation in EC?
3. Which is the amino acid residue in zyxin that is phosphorylated during wall tension/stretch?

2. MATERIALS

2.1 Synthetic oligonucleotide primers for PCR

Synthetic oligonucleotides used for cloning, chromatin immunoprecipitation (ChIP) and for real time (r.t.) RT-PCR and genotype analysis are listed in table 1 along with Fragment size/position and gene identification numbers (Gene ID). Oligonucleotides were dissolved in water to a final concentration of 1 nmol/ μ l.

Table 1. Synthetic oligonucleotide primers

Gene product	Sequence (5' - 3')	Official Symbol/ Gene ID position (size)
Calponin (RT-PCR)	GAGGAGGGAAGAGTGTGCAG GTTGGCCTCAAAAATGTCGT	CNN1/ID: 1264 72/491 (420 bp)
Clusterin (CLU) (ChIP)	ACCAAACGTGGATCTGCAAG GTTGTGGGCACTGGGAGG	NC_000008.10 81/-632 (713 bp)
Endothelin-1 (ET-1)	AGCCGGCAGAGAGCTGTCCA GAGAAGGCAGCGAGCGGAGC	NM_001955.3 42/170 (129 bp)
e-Selectin	CGCCATCCCTCAGCCTCAGA GGCCCTGCAACGTGAAACT	NM_011345.2 1054/1170 (117 bp)
ET-1 (ChIP)	CCGCGTGCCTGCAGAC TCATGAGCAAATAATCCATTC	NC_000006.11 19/-202 (221 bp)
ET-1 receptor B type (ET _B -R)	TCCCACTGGCGCGAAACTT GGTCAGCTGCCCGAGCCAAG	NM_001122659.1 70/171 (102 bp)
GAPDH (RT-PCR, all species)	TCACCATCTTCCAGGAGCG CTGCTTACCACCTTCTTGA	GAPDH/ID: 2597 273/844 (582 bp)
Glyceraldehyde dehydrogenase (GAPDH) (r.t. RT-PCR)	GACCACAGTCCATGCCATCACTGC ATGACCTTGCCACAGCCTTGG	GAPDH/ID: 2597 627/764 (138 bp)
guanylate cyclase-1 β (Gucy1B3) (ChIP)	AGGCACTGGAGCGCAGCAGC CATGGTGTCTGCACCGGGGAG	NC_000004.11 2/-275 (277 bp)
hairy/enhancer-of-split related (HEY-1)	TGAGAAGCAGGTAATGGAGC AAGTAACCTTTCCCTCCTGC	NM_012258.3 440/550 (111 bp)
Hemicentin	GATGTGCTAGTTCCACCCAC ATATCAGGAAAGGGAGTGCC	NM_031935.2 4568/4683 (115 bp)
Hemicentin (ChIP)	GTAGGATTCAAACCTGCTCAG CTCTCAGCCCACAACCTCGGC	NC_000001.10 -776/-1146 (371 bp)
Hey-1 (ChIP)	CTGGTGGCCACTGTGGACG CTCTGTCCAGCCTGCACTC	NC_000008.10 -395/-991 (597 bp)
HMG-CoA reductase HMGCR (ChIP)	CATTTTCAGAGAGAATCCAG CAGTAGGAGGCAGTGATAG	NC_000005.9 -657/-957 (301 bp)
ICAM-1 (ChIP)	GTGCATGAGCCTGGGTTT GGCGTCCCTCTCTACAC	NC_000019.9 -699/-1043 (345 bp)
Inter-Cellular Adhesion Molecule 1 (ICAM-1)	TGATGGGCAGTCAACAGCTA GGGTAAGGTTCTTGCCCACT	NM_000201.2 610/716 (107 bp)
Interleukin-6 (CXCL-6; Chemokine CXC ligand6) (RT-PCR; mouse)	CTGATGCTGGTGACAACCACGG TTAAGCCTCCGACTTGTGAAGTGGT	IL6/ID: 16193 20/134 (115 bp)
Interleukin-8 (r.t. RT-PCR; human)	TAGCCAGGATCCACAAGTCC GCTTCCACATGTCTACAA	IL8/ID: 3576 879/995 (117 bp)

Gene product	Sequence (5' - 3')	Official Symbol/ Gene ID position (size)
JAM-2 (ChIP)	CTCAGCTTCGCCCCTTGGGC CTCTGAGGAGGTCGAGGGTC	NC_000021.8 -24/-623 (600 bp)
Junctional adhesion molecule -2 (JAM2)	ATCCGGATCAAAAATGTGAC GCTGGAGCCACTAATACTTCC	NM_021219.2 825/949 (125 bp)
Laminin- γ	ATCTGATGGACCAGCCTCTC CCTCTCTCCAGCTCTGACA	NM_005562.2 3634/3758 (125 bp)
Matrix Metalloproteinase-3 (MMP-3;RT-PCR, mouse)	TGGGAGGAGGTGACCCCACT AGCCAAGACTGTTCCAGGCC	Mmp3/ID: 17392 423/548 (126 bp)
Mice NEO zyxin (genotyping)	GACCGCTTCCTCGTCTTTAC TGGACGAAGTTTCCGTGTGTTG	ZYX/ID: 7791 N.A (473 bp)
Mice TRPC3 Knockout (genotyping)	GAATCCACCTGCTTACAACCATGTG GGTGGAGGTAACACACAGCTAAGCC	TRPC3/ID: 7222 N.A (300 bp)
Mice TRPC6 Knockout (genotyping)	ACGAGACTAGTGAGACGTGCTACTTCC GGGTTTAAATGCTGTATCACTAAAGCCTCC	TRPC6/ID: 7225 N.A (339 bp)
Mice WT TRPC3 (genotyping)	GCTATGATTAATAGCTCATACCAAGAGATC GGTGGAGGTAACACACAGCTAAGCC	TRPC3/ID: 7222 N.A (300 bp)
Mice WT TRPC3 (genotyping)	GAATCCACCTGCTTACAACCATGTG GGTGGAGGTAACACACAGCTAAGCC	TRPC3/ID: 7222 N.A (800 bp)
Mice WT TRPC6 (genotyping)	CAGATCATCTCTGAAGGTCTTTATGC TGTGAATGCTTCATTCTGTTTTCGCGCC	TRPC6/ID: 7225 N.A (234 bp)
Mice WT zyxin (genotyping)	TACAAGGGCGAAGTCAGGGCGAGTG TGGACGAAGTTTCCGTGTGTTG	ZYX/ID: 7791 N.A (327 bp)
Thrombomodulin (RT-PCR, mouse)	ATGAACCCAGATGCCTCTGCCC ATGCTCGCAGAGTTCTGTTGCAC	Thbd/ID: 21824 771/871 (101 bp)
Transient Receptor Potential Channel (Canonical) 3- TRPC3 (RT-PCR)	GATCTGGAATCAGCAGAGCC GTTGGGATGAGCCCAAACCT	TRPC3/ID: 7222 871/988 (108 bp)
TRPC4 (RT-PCR)	CAGGCTGGAGGAGAAGACAC GACCTGTGATGTGCTGAGA	TRPC4/ID: 7223 1191/1404 (214 bp)
TRPC5 (RT-PCR)	GACAGCCTGCGCCACTCTCG GAGCTCCCAGCCAGACGGA	TRPC5/ID: 7224 1481/1600 (120 bp)
TRPC6 (RT-PCR)	TTTGCTGAAGCAAGAGGTT TGGAGTCACATCATGGGAGA	TRPC6/ID: 7225 981/1091 (111 bp)
TRPC7 (RT-PCR)	CGAGCTGAAGGAAATCAAGC CTTGTTCCACCCTCAGGTGGT	TRPC7/ID:57113 2295/2448 (154 bp)
TRPV4 (RT-PCR)	CGGATTCCAGCGAAGGCCCC CGGTGAGGGCGAAAGGGAGC	TRPV4/ID:59341 36/184(149 bp)
Vascular cell Adhesion Molecule (VCAM-1)	CATGGAATTCGAACCCAAACA GACCAAGACGGTTGTATCTCTGG	NM_001078.2 1593/1674 (82 bp)
VCAM-1 (ChIP)	GATTCCAGACCTCAGCTATG GTATTTCAGCTCCTGAAGCC	NC_000001.10 -77/-1430 (1506 bp)
Zyxin (Full length cDNA)	CAGCCCGGCCCGCCATGGC CTGAAGAGGGCCTGTCTCACTCAGGT	ZYX/ID: 7791 143-1895 (1753)
Zyxin (S142G)	CAGGGAGAAGGTGGGCAGTATGATTTG CAAATCAATACTGCCACCTTCTCCCTG	ZYX/ID: 7791 566 N.A.
Zyxin (S142D)	CAGGGAGAAGGTGGACAGTATTGATTTG CAAATCAATACTGTCCACCTTCTCCCTG	ZYX/ID: 7791 566 N.A.
Zyxin (S142E)	CAGGGAGAAGGTGGAGAGTATTGATTTG CAAATCAATACTTCCACCTTCTCCCTG	ZYX/ID: 7791 566 N.A.
Zyxin (S344A)	AACCAGGTGCGCGCCCTGGGGCCC GGGCCCCAGGGGCGCGCACCTGGTT	ZYX/ID: 7791 1173 N.A.
Zyxin (S344D)	AACCAGGTGCGCGACCTGGGGCCC GGGCCCCAGGGTTCGCGCACCTGGTT	ZYX/ID: 7791 1173 N.A.
Zyxin (S344E)	AACCAGGTGCGCGAGCCTGGGGCCC GGGCCCCAGGCTCGCGCACCTGGTT	ZYX/ID: 7791 1173 N.A.
Zyxin (T352A)	CCAGGGCCCTGGCTCTGAAGGAGGTG CACCTCCTTCAGAGCCAGGGCCCTGG	ZYX/ID: 7791 1197 N.A.
Zyxin (T352D)	CCAGGGCCCTGGATCTGAAGGAGGTG CACCTCCTTCAGATCCAGGGCCCTGG	ZYX/ID: 7791 1197 N.A.
Zyxin (r.t. RT-PCR, human)	CTGTCCTCACTGTGGATG GAGTTGGACCTGAGGCTTG	ZYX/ID: 7791 609/867 (259 bp)

2.2 Kits

Table 2: Kits

Name	Company
(A) ELISA Kits	
Human CXCL8/IL-8 ELISA Kit	R&D Systems (Wiesbaden, Germany)
Human Endothelin-1 ELISA Kit	R&D Systems
Human pro-ANP ELISA kit	Biomedica (Graz, Austria)
(B) Nucleic acid extraction analysis and purification	
QIAquick Gel Extraction Kit	Qiagen (Hilden, Germany)
Qiagen DNeasy kit	Qiagen
QIAGEN Maxi-Prep Plasmid Kit	Qiagen
Qiagen Maxi-prep plasmid Kit	Qiagen
QIAprep Mini Plasmid Kit	Qiagen
Rneasy Mini Kit	Qiagen
(C) RT-PCR Kits	
QuantiTect SYBR Green [®] Kit	Qiagen
Sensiscript RT Kit	Qiagen
(D) Protein purification kit	
ReadyPrep Protein Extraction Kit (Cytoplasmic/Nuclear)	BioRad (München, Germany)
(E) TOPO cloning kits	
TOPO mammalian expression vector kit	Invitrogen (Karlsruhe, Germany)
TOPO TA cloning Kit	Invitrogen
(F) Mutagenesis Kit	
Quickchange II site directed mutagenesis kit	Stratagene (U.K)

Name	Company
(G) DNA and Protein Standards/Markers	
DNA standards- O'GeneRuler™ DNA Ladder	Fermentas (Germany)
Protein standard – Precision Plus Protein™ standards (Dual colour)	Biorad

2.3 Bacterial strains and plasmids

Bacterial strains and plasmid vectors used for cloning and maintenance of plasmids constructs are listed in Table 3 and 4.

Table 3: Plasmids

Vector	Characteristic	Source
pCR 2.1-TOPO 3.9 kb	pUC origin, lacZ α reporter fragment; T7 promoter/priming site, f1 origin; ampiciline resistance ORF; kanamycin resistance ORF	Invitrogen (Karlsruhe, Germany)
pcDNA 6.2/N-EmGFP/YFP TOPO 5.9 kb	N-terminal GFP expression vector. pUC origin, CMV promoter/priming site, f1 origin; ampiciline resistance ORF	Invitrogen
pcDNA 6.2/C-EmGFP/YFP TOPO 5.8 kb	C-terminal GFP expression vector. pUC origin, CMV promoter/priming site, f1 origin; ampiciline resistance ORF	Invitrogen

Table 4: Chemically competent *E. coli* cells

Bacterial cells	Genotype	Source
One Shot TOP10F'	<i>mcrA</i> $\Delta(mrr-hsdRMS-mcrBC)$ $\Phi 80lacZ\Delta M15$ $\Delta lacX74$ <i>recA1</i> <i>araD139</i> $\Delta(ara-leu)7697$ <i>galU</i> <i>galK</i> <i>rpsL</i> <i>endA1</i> <i>nupG</i>	Invitrogen (Karlsruhe, Germany)

2.4 Cell culture

Table 5: Cell culture media, buffers, antibiotics and supplements

Name of product	Company
Collagenase	Sigma Aldrich (Steinheim, Germany)
Dispase	Böhringer (Mannheim, Germany)
D-MEM + GlutaMAX-I	Invitrogen (Karlsruhe, Germany)
Endothelial cell growth medium	Promocell (Karlsruhe, Germany)
Endothelial cell growth supplement (ECGS)	Promocell
FBS	Invitrogen
Gelatine	Sigma Aldrich
Hank's BSS	PAA (Cölbe, Germany)
M199 + GlutaMAX-I	Invitrogen
OPTIMEM I	Promocell
Penicillin	Invitrogen
SMC growth media	Promocell
Streptomycin	Invitrogen
Supplemental Mix	Promocell

2.5 Reagents

Table 6: Regularly used reagents and substances

Substance	Company
®-(-)Phenylephrine hydrochloride	Sigma Aldrich
Acetylcholine chloride, minimum 99% TLC	Sigma Aldrich
Atrial Natriuretic Factor 1-28, human	Calbiochem

Substance	Company
Bio-Lyte 3-10 Ampholyte	BioRad
BQ-788	Sigma Aldrich
ECL Plus Western Blotting Detection reagent	Amersham (Buckinghamshire, UK)
Endothelin 1, human and porcine,	Calbiochem
Endothelin 1, rat and porcine	Sigma Aldrich
Gadolinium chloride	Sigma Aldrich
Lanthanum chloride	Sigma Aldrich
MATra-A Reagent	IBA (Göttingen, Germany)
Phosphatase Inhibitors	Active Motif (Rixensart, Belgium)
Proteinase K	Sigma Aldrich
RNAlater RNA stabilization reagent	Qiagen
Rock inhibitor (Y27632)	Calbiochem
Rp8pGPT-cGMPS	Calbiochem
Taq Polymerase	Bioron (Ludwigshafen, Germany)

All standard chemicals were purchased from Roth (Karlsruhe, Germany) or Sigma-Aldrich (Steinheim, Germany).

2.6 Buffers and solutions

Phosphate Buffered Saline (10×) pH 7.4:

130.0 mM	NaCl
2.7 mM	KCl
7.0 mM	Na ₂ HPO ₄ x 2H ₂ O
4.0 mM	KH ₂ PO ₄

Tris Buffered Saline, pH 7.4:

25.0 mM	Tris-HCl
137.0 mM	NaCl
2.7 mM	KCl

2.7 Microbiological media

Luria-Bertani (LB) Medium, pH 7.0:

1.0 % (w/v)	Bacto-tryptone
0.5 % (w/v)	Yeast extracts
1.0 % (w/v)	NaCl

LB-Agar Plates:

1.0 % (w/v)	Bacto-tryptone
0.5 % (w/v)	Yeast extracts
1.0 % (w/v)	NaCl
1.5 % (w/v)	Agar

The Luria-Bertani medium was prepared with distilled water, autoclaved and stored at room temperature. LB agar was melted at 50°C using a microwave and the temperature was brought down to 37°C. The warm media were supplemented with 50 µg/ml ampicillin and poured into Petri dishes. The dishes were stored at 4°C.

2.8 Small interfering RNAs

Table 7: siRNA target sequences constructed by Qiagen

siRNA	Target sequence	Source
Hs_ZYX_1_HP Validated	AAG GTG AGC AGT ATT GAT TTG	Qiagen (Hilden, Germany)
All Stars Negative Control (scrambled siRNA)	N/A	Qiagen

2.9 Antibodies

Table 8: Primary antibodies: WB: antibodies used for Western blot, ICC: antibodies used for Immunocytochemistry, IHC: antibodies used for Immunohistochemistry,

Primary antibody and specification	Use	Dilution	Source
Mouse anti-human eNOS /NOS-3	WB	1:1000	BD Transduction Laboratories (California, USA)
Rat anti-mouse CD31 clone MEC 13.3, polyclonal	IHC	1:25	Santa Cruz Biotechnology (Heidelberg, Germany)
Mouse anti - β -actin	WB	1:5000	Sigma Aldrich
Rabbit anti-human B72 LH-ZyxinPLAG (against peptide CDFPLPPPLAGDGDDAEGAL, zyxin amino acids 70 to 89)	WB/ICC/IHC	1:2500/1:250	Mary Beckerle, (Huntsman Cancer Research Centre, University of Utah)
Rabbit anti-human B71 LH-ZyxinNES (against peptide CSPGAPGPLTKEVEELEQLT, zyxin amino acids 344 to 363)	ICC/IHC	1:250	Mary Beckerle, Huntsman Cancer Research Centre, University of Utah
Mouse anti-human Atrial Natriuretic Peptide, monoclonal	ICC	1:50	Chemicon Europe (Hampshire, UK)
Mouse anti- Paxillin (165 Paxillin, monoclonal)	WB/ICC	1:1000/1:100	BD Transduction Laboratories
Mouse anti- Vinculin (SPM227, monoclonal)	ICC	1:100	Abcam
Mouse anti-smooth muscle actin (1A4, asm-1, monoclonal)	ICC	1:50	Dianova
Mouse anti-Zyxin 164 ID4	ICC	1:100	Mary Beckerle, Huntsman Cancer Research Centre, University of Utah
Rabbit- Transient Receptor Potential Channel 3 (TRPC3, polyclonal)	WB	1:250	Alomone labs
Mouse anti-GAPDH (Clone GAPDH - 71.1, monoclonal)	WB	1:1000	Sigma
Mouse anti-human CD31	ICC	1:50	Dako (Glostrup, Denmark)
Mouse anti-Ku80 (Ku15, monoclonal)	WB/ICC	1:1000/1:100	Novus biological (Cambridge, UK)
Sheep anti-TRPM6 (polyclonal)	WB	1:300	Novus Biologicals

Table 9: Regularly used secondary antibodies WB: antibodies used for Western blot, ICC: antibodies used for Immunocytochemistry, IHC: antibodies used for Immunohistochemistry,

Secondary antibody and specification	Use	Dilution	Source
Cy2 donkey anti-mouse and anti-rat IgG	ICC	1:50	Jackson laboratories via Dianova (Hamburg, Germany)
Cy3 donkey anti-rabbit IgG	ICC	1:50	Jackson laboratories via Dianova (Hamburg, Germany)
Goat anti-rabbit IgG peroxidase	WB	1:5000	Sigma
Goat anti-mouse IgG peroxidase	WB	1:5000	Sigma

2.10 Mouse strains

C57BL/6J mice were initially ordered from Charles River Laboratories, Sulzfeld, Germany.

Table 10: Mouse strains

Strain	Source
C57BL/6J	Charles River Laboratories, Sulzfeld, Germany
C57BL/6J zyxin (-/-) null (line 185)	Dr. Laura Hoffman and Prof. Mary Beckerle Huntsman Cancer Research Centre, University of Utah, Salt Lake City /JBF
TRPC3(-/-), TRPC6(-/-), TRPC3/C6 double knockout, TRPC1/C4/C5 triple knockout mice	Dr. Marc Freichel Experimental and Clinical Pharmacology and toxicology, University of Saarland, Homburg, Germany
GC-A (-/-) mice	Prof. Michaela Kuhn Institute of Physiology, University of Würzburg, Germany

2.11 Software

Table 11: Frequently used software and programs

Software/Program	Use	Company
(A) Software		
analySIS ^{AD} version 5.0 Imaging analysis	Image analysis	Olympus Soft Imaging Systems GmbH
Cell ^{AR} Imaging analysis	Image analysis	Olympus (Hamburg, Germany)
Corel Draw 14.0	Drawing tool	Corel
KCjunior TM Software	ELISA measurements	BIO-TEK Instruments (Winooski, Vermont, USA)
LightCycler TM software version 3.5.3	Real time RT-PCR	Roche (Mannheim, Germany)
MetaMorph [®] imaging system version 3.5	Image analysis	Universal Imaging Corporation (Marlow Buckinghamshire, UK)
MyoView TM Pressure Myograph software	<i>In situ</i> perfusion	Danish Myo Technology (Atlanta, USA)
NanoDrop [®] software	Nucleic acid measurement	NanoDrop (Wilmington, USA)
Quantity One [®] 1-D analysis software	Western blot analysis	BioRad (USA)
Quantity One [®] image acquisition software	Image analysis	BioRad
(B) Online tools		
BLAST (Basic Local Alignment Search Tool) www.ncbi.nlm.nih.gov	Sequence analysis	National Center for Biotechnology Information (NCBI)
ExpASy tool www.expasy.ch	Protein structure analysis	SwissProt
http://www.phosphosite.org	Phosphorylation site prediction	Protein modification resource

3. METHODS

3.1 Molecular techniques

3.1.1 Expression plasmids

Zyxin expression plasmids were constructed by sub-cloning the PCR amplified fragment into EmGFP-Topo-vector. To enable directional cloning, primers were designed for human Zyxin (the complete coding region from pos. 143 to pos. 1895 with a stop codon can be found in appendix) PCR was carried out at 94 °C (90 s), 63 °C (30 s), and 72 °C (4 min) for 35 cycles. After amplification with Taq polymerase, the fragment was cloned into the N-terminal GFP- fluorescing vector (pcDNA 6.2/N-EmGFP/YFP TOPO 5.9 kb) using TOPO cloning reaction according to the manufacturer's recommendations (TOPO mammalian expression vector kit, Invitrogen).

3.1.2 Site-directed mutagenesis

Site-directed mutagenesis was performed to generate phosphorylation-resistant mutants by converting serine to glycine/alanine (S142G/S344A/T352A). These constructs were further converted to phosphorylation-mimetic mutants by replacing a glycine or alanine residue by negatively charged residue such as glutamate/aspartate (S142E/S344E/T352D). The primers used for mutagenesis is listed in Table 1. The QuickChange II site directed mutagenesis kit was used according to the manufacturer's protocol (Stratagene, UK). Briefly, for the mutant strand synthesis, the expression plasmids were subjected to PCR with appropriate primer pair containing the mutation of interest. The high fidelity DNA polymerase, Pfu Turbo DNA polymerase was used to extend and incorporate the mutagenic primers (Table 1). The reaction mixture as follows;

- 5 µl 10 × reaction buffer
- 50 ng dsDNA template
- 125 ng oligonucleotide primers carrying the mutation
- 1 µl of dNTP mix
- 50 µl ddH₂O to a final volume
- 1 µl of Pfu Turbo DNA polymerase (2.5 U/µl)

The reaction mixture was then subjected to the PCR reaction (Table 12).

Table 12: PCR program for site-directed mutagenesis

PCR step	Temperature (in °C)	Time	
Pre-denaturation	95°C	5 minutes	
Denaturation	95°C	30 seconds	18 cycles
Annealing	55°C	1 minute	
Synthesis	68°C	7 minutes (1 minute/Kb of plasmid length)	

Following temperature cycling, the reaction was placed on ice for 2 minutes to cool the reaction to $\leq 37^{\circ}\text{C}$. To digest all non-mutated parental supercoiled dsDNA, 1 μl DpnI (10 U/ μl) restriction enzyme was added to the amplification reaction and incubated at 37 °C for 1 hour. The reaction was then used for the transformation into the competent bacteria.

3.1.3 Plasmid cloning for RT-PCR standards

For the construction of specific real-time RT-PCR standards (ref 3.1.8), PCR fragments were ligated into the pCR® TOPO 2.1 vector (3.9 Kb) using the TOPO TA Cloning® Kit according to the manufacturer's instructions. Plasmids containing the inserts were amplified further (3.1.5.4).

3.1.4 TOPO cloning

TOPO cloning was used to clone the amplified DNA fragments in to the vectors. Briefly, 2 μl of PCR product was mixed with 1 μl of the appropriate topo vector and 1 μl salt solution (200 mM NaCl, 10 mM MgCl₂) to prevent topoisomerase I from re-binding to DNA and to obtain higher transformation efficiency. The mixture was diluted to a final volume of 6 μl and incubated on ice for 30 minutes for ligation of the DNA to the topo vector. The reaction mixture was further taken for transformation into competent bacteria.

3.1.4.1 Transformation of competent bacteria

2 μl of the reaction mixtures containing the topo vector with the fragment were mixed with 20 μl of Top10F™ competent cells and incubated on ice for 30 min. Thereafter, cells were subjected to the heat shock at 42°C for 40 s, and

immediately placed on ice. 250 μ l of SOC medium was added to the cells and the suspension was incubated at 37°C for 1 h with shaking at 300 rpm. Sterile LB-agar medium with 20 μ g/ml of ampicillin in petri-dishes was pre-warmed to 37°C. 30 μ l and 230 μ l of transformed competent cells were plated onto the separate petri-dishes. Plates were then incubated at 37°C overnight to allow bacterial colonies to grow.

3.1.4.2 Plasmid mini/maxi-cultures and plasmid purification

Transformed colonies of Top10FTM competent cells were picked by using a sterile pipette tip and added to 7 ml of LB Broth (with appropriate antibiotic) in 15 ml falcon tubes. Caps of the falcon tubes were perforated to allow air to circulate through the tube. These cultures were then incubated at 37°C with shaking overnight. Plasmids grown in mini-cultures were purified using the QIAprep® Spin Miniprep Kit according to the manufacturer's instructions.

200 μ l of the mini-culture broth was then transferred in to 250 ml LB Broth (with appropriate antibiotic) in 500 ml conical flasks for maxi culture. Plasmids grown in maxi-cultures were purified using the QIAprep® Maxiprep Kit according to the manufacturer's instructions. All clones were sequenced.

3.1.5 Polymerase chain reaction (PCR)

The polymerase chain reaction (PCR) is a sensitive and powerful technique used to exponentially amplify a specific DNA sequence in vitro by using sequence-specific synthetic oligonucleotides and a thermo-stable DNA-polymerase (Mullis 1983). This method was used for the amplification of cDNA for determination of mRNA expression levels of stretch-inducible gene products.

3.1.6 Reverse transcription PCR (RT-PCR)

RT-PCR was performed to synthesize cDNA from RNA templates from cultured cells. 0.5-2 μ g of total RNA was mixed with RNase free water to a total volume of 13 μ l. The mixture was heated to 70°C for 10 minutes following the addition of 1 μ l of oligo (dT) 18 primer (10 pmol/ μ l) to facilitate hybrid formation of the oligo dT-primers with polyA-tails of mRNA.

For the first strand cDNA synthesis, the following was added to the mixture:

4 μ l of 5x First strand buffer

1 μ l of 0.1 M reverse transcriptase enzyme (RT)

1 μ l of 10 mM dNTPs

The content of the tube was mixed and incubated at 42°C for 50 minutes. Then, the reaction was inactivated by incubating the mixture at 70°C for 10 minutes, and 180 μ l of RNase-free water was added to dilute the resulting cDNA. Sensiscript kit (Qiagen) was used to generate cDNA from the isolated mouse arteries according to the manufacturer's instructions. These samples were further used for the PCR reactions.

3.1.7 PCR amplification of DNA fragments

To detect the amount of final amplified product at the endpoint semi-quantitative PCR was performed by normalizing to the relative amount of cDNA of an invariant endogenous control. The house keeping gene, glyceraldehyde-3-phosphate dehydrogenase (GAPDH) was chosen as an internal standard. The PCR reaction was performed in an automatic thermocycler (Biometra) programmed (as shown in Table 15).

Table 13: PCR programme for semi-quantitative PCR

PCR step	Temperature (in °C)	Time	
Pre-denaturation	95°C	5 minutes	
Denaturation	95°C	30 seconds	30-40 cycles
Annealing	56°- 60°C (depending on the primers used)	60 seconds	
Synthesis	72°C	2 minutes	
Extension	72°C	5 minutes	

3.1.8 Quantitative real-time PCR

Real-time PCR was carried out in a LightCycler instrument (Roche Diagnostics, Penzberg, Germany) by using the QuantiTect SYBR Green® kit according to the manufacturer's instructions. Principally, it quantitates the initial amount of template cDNA specifically and sensitively (Freeman 1999; Raeymaekers 2000). So, for the quantitative analysis of changes in gene expression real-time RT-PCR analysis was used. The standard cDNA probes for the gene products to be

measured were cloned into TOPO vectors (ref 3.1.3) and the number of molecules per reaction was calculated according to size (bp) and uv-absorption. The number of plasmid templates used as standards per reaction varied between 10^1 to 10^8 depending on the expected abundance of the gene product to be determined as number of copies per ng of total RNA. As control gene products for the normalization of the cDNA amount added to the reaction, GAPDH was used.

3.1.9 Agarose gel electrophoresis

Agarose gel electrophoresis was used for the separation of nucleic acids. Depending on the size of the DNA fragment to be analysed 1-2% agarose gels were used along with 4% of the ethidium bromide for the visualization of the DNA fragment. Agarose was melted in 100 ml TBE buffer followed by the addition of 4 μ l ethidium bromide and poured onto an electrophoresis chamber. Samples were mixed with 0.2 volumes of 5X of loading buffer before loading. Electrophoresis was carried out at a steady voltage of 110-140 V. The size of the DNA fragments in the agarose gels was determined using appropriate size standards (O'GeneRuler™ DNA Ladder, Fermentas). The band intensities were analysed using a GelDoc XR unit and the Quantity One software package version 4.06 (Biorad, Munich, Germany) and normalized to the respective intensities of GAPDH expression.

5X TBE buffer

450 mM	Tris base
450 mM	Boric acid
20 mM	EDTA, pH 8.0

6X Glycerol loading buffer

10 mM	Tris/HCl, pH 7.5
10 mM	EDTA, pH 8.0
30.00 %	Glycerol
0.01 %	Bromophenol blue
0.01 %	Xylene green

3.1.10 Isolation of total DNA from cultured cells and mouse tails

To isolate total DNA from cultured cells Qiagen DNeasy kit was used according to the manufacturer's protocol. Genotyping of the TRP deficient smooth muscle cells were performed with the primers (Table 1; WT TRPC and TRPC KO) using the following PCR programme.

Table 14: PCR program for genotyping (TRP knockout mice)

PCR step	Temperature (in °C)	Time	
Pre-denaturation	95°C	90 seconds	
Denaturation	95°C	30 seconds	36 cycles
Annealing	60°C	30 seconds	
Synthesis	72°C	60 seconds	
Final Elongation	72°C	5 minutes	

DNA isolation from the mouse tails was performed according to a standard protocol (Hogan 1993). The mouse tail of 0.7-1 cm length was incubated in 150 µl digestion buffer containing proteinase K (1 mg/ml) at 55°C overnight to facilitate. Thereafter, the digestion mixture was incubated at 95°C for 10 – 20 minutes, gently mixed and centrifuged at 13000 rpm for 10 minutes at ambient temperature to collect undigested tail debris. Finally, the DNA containing supernatant was stored at -20°C for further PCR analysis (see 3.1.4). The genotype analysis zyxin mice were performed with the primers (Table 1; mice WT zyxin and mice NEO zyxin) using the following programme;

Table 15: PCR programme for genotyping (zyxin knockout mice)

PCR step	Temperature (in °C)	Time	
Denaturation	95°C	60 seconds	30 cycles
Annealing	58°C	30 seconds	
Synthesis	72°C	50 seconds	
	95°C	1 minute	
Final elongation	72°C	3 minutes	

Digestion buffer for tail DNA:

670.0 mM	Tris/HCl, pH 8.8
166.0 mM	Ammonium sulphate
65.0 mM	MgCl ₂
1.0 %	β-mercaptoethanol
0.5 %	Triton X-100

3.1.11 Isolation of total RNA from cultured cells and femoral arteries

Total RNA was isolated from cultured cells and individually excised mouse femoral arteries using the RNeasy kit according to the manufacturer's instructions. In order to avoid any RNase activity, RNase-free water and RNase-free reaction tubes were used. Total RNA was extracted by adding 350 µl and 250 µl of lysis buffer containing 1% β-mercaptoethanol to the cultured cells and femoral artery respectively. The femoral artery was then homogenized by a short (~25 seconds) sonification (cycle 1, 100%, Dr. Hielscher GmbH). An equal volume of 70% ethanol was added to the homogenized lysates and the samples were carefully mixed. The mixture was then transferred to the mini spin column, centrifuged for 25 seconds at 13000 rpm followed by two washing steps. Finally, the RNA was eluted with 30 µl RNase-free water. An aliquot of 13 µl of RNA was used to generate single-stranded (ss) cDNA for RT-PCR reactions.

3.1.12 Measurement of RNA/cDNA concentration

Measurement of RNA and cDNA concentrations was performed by using the NanoDrop ND-1000 spectrophotometer. For quantitative real-time PCR analysis 1-20 ng of cDNA was used.

3.2 Cell culture**3.2.1 Isolation and culture of human umbilical vein endothelial cells (HUVEC)**

Human umbilical vein endothelial cells were routinely isolated from freshly collected umbilical cords (closed with a clip) with the consent of parents. Umbilical veins were flushed with Hank's buffer solution until the veins were blood-free. The veins were then filled with dispase solution (3.1 g/l) until the cords were swollen (~10 ml) and incubated for 30 minutes at 37°C. Veins were again flushed with Hank's buffer and the isolated cells were collected in a 50-ml tube and centrifuged at 1000 rpm for 5 min. The pellet containing the HUVEC

was re-suspended in endothelial cell growth medium (Promega, Germany) medium containing 5% fetal bovine serum, 50 U/ml penicillin, 50 µg/ml streptomycin and 0.25 µg/ml Fungizone® antimycotic. The cells were routinely cultured on standard plastic dishes or collagen type I BioFlex elastomer plates (Flexcell® International Corporation) additionally coated with 2% (w/v) gelatine in 0.1 N HCl. Culture medium was changed every other day.

3.2.2. Culture of mouse smooth muscle cells

Mouse smooth muscle cells were isolated from mouse aortic artery. The artery was dissected, cut into fragments, washed several times with Hank's BSS solution and transferred to a 40 mm petri-dish containing 1.4 ml D-MEM/SMC growth medium 2 (1:1, Promocell, Heidelberg, Germany) supplemented with 5% FBS and containing 250 µl collagenase solution (1%, Sigma). The tissue was digested overnight at 37°C, 5% CO₂. The resulting cell suspension was centrifuged for 5 minutes at 1000 rpm. The pellet was resuspended in 2 ml of SMC growth medium (50% D-MEM + GlutaMAX-I Medium, 50% Smooth Muscle Cell Growth Medium, supplemented with 5% FBS, 50 U/ml penicillin, 50 µg/ml streptomycin and 0.25 µg/ml fungizone antimycotic) and seeded into a 6 cm petri-dish. After passage one, the SMC growth medium was replaced by SMC culture medium (D-MEM, supplemented with 15% FBS, 50 U/ml penicillin, 50 µg/ml streptomycin and 0.25 µg/ml fungizone antimycotic). Cells were incubated at 37°C, 5% CO₂, in a humidified atmosphere. Every batch of isolated and cultured mouse aortic smooth muscle cells was tested for the expression of the specific SMC marker, α -actin by immunofluorescence analysis. Routinely, 95% were found to be α -actin positive.

3.2.3 siRNA transfection into HUVEC

To transfect one well of a 6-well plate, 3 µg of plasmid was diluted in OPTIMEM I medium to give a final volume of 200 µl for each well to be transfected. For the formation of the transfection complex, 3 µl of MATra-si reagent (IBA, Göttingen) was added to the diluted siRNA, carefully mixed and allowed to incubate at ambient temperature for 20-30 minutes. HUVEC were once washed in OPTIMEM I, the medium was discarded and then fresh OPTIMEM I (2 ml per well) was added to the cells. The siRNA/magnetic beads were then layered drop wise onto

the cells (200 μ l per well). Cells were incubated with the transfection complex on a custom-made magnetic plate (Universal Magnet Plate, IBA) for 30 minutes in the cell incubator to allow beads to penetrate the target cells. A sufficient knockdown of zyxin ($80 \pm 5\%$ of control) was achieved after 72 hours of transfection (Figure 8).

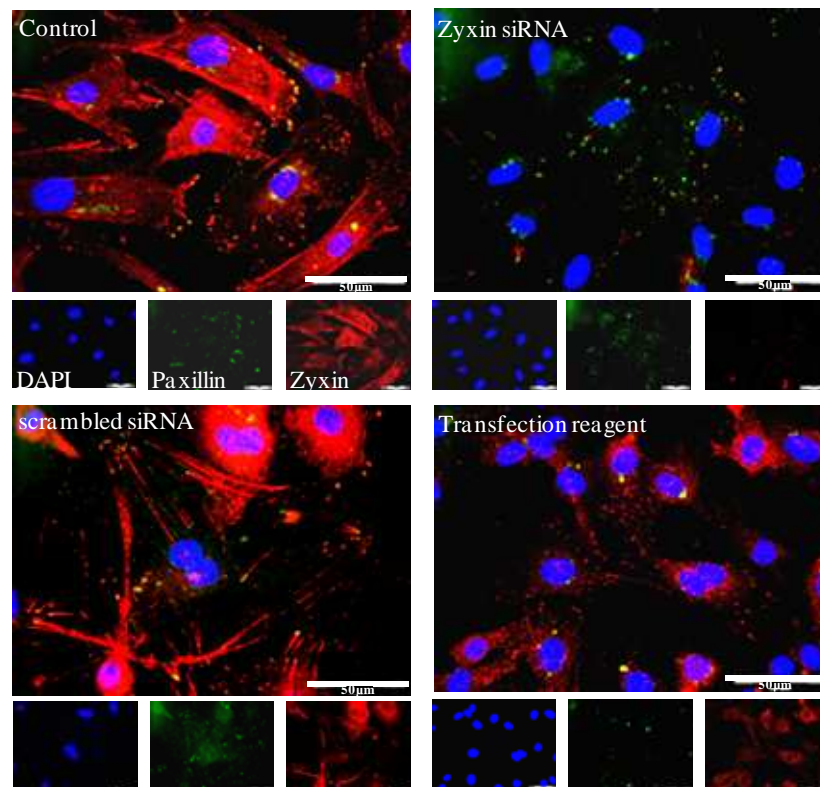


Figure 8: Representative confocal immunofluorescence analysis (IFA) showing reduction in zyxin protein level after magnetofection. Endothelial cells (HUVEC) were transfected using the MaTra transfection reagent with siRNA directed against zyxin. Seventy two hours post transfection the protein was analysed by IFA. Zyxin levels in the siRNA zyxin transfected cells were reduced by 75-85% as compared to the untransfected control cells, scrambled siRNA transfected cells and the cells treated with just transfection reagents. The cells were stained with using the B72 antiserum, Paxillin and DAPI. Scale bar: 50 μ m.

3.2.4 Transfection of zyxin expression plasmids into HUVEC

Transient transfection of HUVEC with the wild type or mutant eGFP-Zyxin constructs (ref 3.1) was performed using polyethylenimine (PEI). PEI has polycationic property. DNA, as a poly-anion, forms complexes with PEI driven by electrostatic interaction. For each well to be transfected plasmid (2 μ g) was incubated with PEI (0.32 g/l) in OptiMEM I (Invitrogen, Darmstadt, Germany) to

a final volume of 200 μ l at ambient temperature for 30 minutes. HUVEC were washed in Hank's BSS solution for 2 times and incubated with fresh Endothelial cell media without antibiotics and FCS (1 ml/well). The transfection mixture was then layered drop wise onto the HUVEC followed by the 6 hours incubation at 37 °C and 5% CO₂. After termination of the procedure by adding normal EC growth media (2 ml/well), transfection efficiency was found to be 35 \pm 5%. 24 hours post transfection, HUVEC were transferred to a BioFlex membrane for stretch experiments; the amount of transfected cells on the Bioflex plates typically dropped to 15 \pm 5%.

3.2.5 Incubation of cells with various drugs

Upon reaching confluence, the HUVEC were incubated with or without 1 nM Atrial Natriuretic Peptide (Calbiochem, San Diego USA), 10 nM Endothelin-1 (Calbiochem), 100 μ M Rp8GPT-cGMP (Calbiochem), 1 μ M BQ-788 (Sigma Aldrich, Deisenhofen, Germany) and 200 μ M Gadolinium (Sigma). After treatment, cells were kept at static conditions or exposed to mechanical strain (cyclic stretch).

3.2.6 Application of mechanical strain

EC and SMC were plated on BioFlexTM collagen I elastomers (Flexercell Inc., Hillsborough, NC, USA) and exposed to cyclic stretch of elongation with 10% and 15% respectively at 0.5 Hz with a sinusoidal profile in a Flexercell FX-3000 strain unit (Figure 9). This protocol is well established method to mimic an increase in circumferential wall tension as previously described (Cattaruzza 2004). The cells were incubated to the stretch medium (M199 medium supplemented with 120 mM TES-HEPES pH 7.3, 20% fetal bovine serum, 50 U/ml penicillin, 50 μ g/ml streptomycin, 0.25 μ g/ml Fungizone antimycotic) and the required drugs (3.2.5) before the application of mechanical strain.

After the stretch protocol, cell culture media were collected and frozen at -80°C for further analysis. Cells were either lysed with RLT buffer (Qiagen) for mRNA isolation fixed (with acetone:methanol or 4% paraformaldehyde, ref 3.3.1) for fluorescence analysis or collected by centrifugation (3000 rpm, 4°C) for cell fractionation and Western blot analysis.

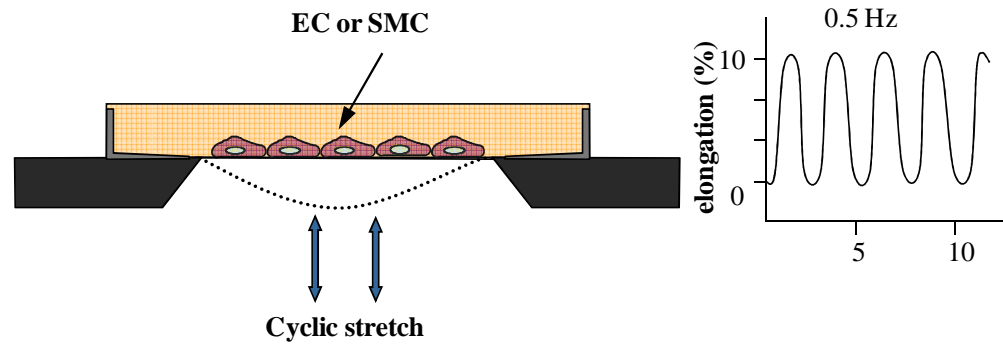


Figure 9: Schematic diagram of the FlexCell model. (A) The computer-controlled flex device applies mechanical strain to the cells by using regulated vacuum pressure to deform the flexible-bottomed culture plates producing substrate elongation and (B) a typical strain profile applied to EC or SMC in culture.

3.3 Immunofluorescence analysis

3.3.1 Cell fixation

For analysis of the localisation of zyxin and other proteins, cells grown on BioFlex membranes or coverslips were fixed in methanol/acetone (1:1) for 20 minutes at -20°C . Thereafter, the cells were dried for 2hrs. Enhanced-GFP-Zyxin transfected cells were fixed with 4% paraformaldehyde for 20 minutes at room temperature and further processed for immunostaining.

3.3.2 Immunostaining of fixed cells

The fixed cells were permeabilized with 0.1% Triton X-100/PBS and nonspecific binding was blocked using Casein blocking serum for 45 minutes. The membranes/coverslips were then incubated cell side down with 15 μL of primary antibodies (Table 8) diluted in casein blocking serum for 2 hours at room temperature. After 5 wash steps (5 minutes each, PBS), cells were incubated cell side down with Cy2- and/or Cy3-conjugated secondary antibodies (Table 9) depending on the primary antibodies used for 1 hour at room temperature. The cells were then washed 2 times with PBS followed by a nuclear stain with DAPI (1 $\mu\text{g}/\text{mL}$) for 10 minutes at room temperature. After the final wash step (PBS, 2 times for 5 minutes), the cells were mounted on to a large coverslip with ProLong (Invitrogen, Oregon, USA).

Permiabilisation buffer

Phosphate-buffered saline per L: pH 7.6

8.0 g	NaCl
0.2 g	KCl
1.44 g	Na ₂ HPO ₄
0.24 g	KH ₂ PO ₄

Casein blocking serum

0.25 %	Casein
0.1 %	BSA
15 mM	NaN ₃
50 mM	Tris pH 7.6

3.4 Immunohistochemistry**3.4.1 Tissue preparation for paraffin embedding**

The freshly isolated femoral arteries were fixed in zinc to retain their morphological structure and dehydrated by passing the tissue through an increasing alcohol gradient i.e. 70%, 80% and 96% ethanol for 90 minutes in each ethanol gradient. The ethanol was removed from the tissue by incubating the femoral artery in isopropanol for 1 hour. Finally, the tissue was embedded in melted paraffin (Sigma Aldrich) and incubated at 60°C overnight. The tissue in the paraffin was poured on to a metal preheated at 60°C to form a block. The tissue embedded in the paraffin block was allowed to cool down and was further processed for sectioning. The paraffin block was cut into sections (5 µm thick) using a microtome. The tissue sections were transferred on to a glass slides and were dried at 40°C overnight. The tissue sections were then processed further for immunohistological analyses.

Zinc fixation

0.1 M	Tris HCl, pH 7.4
3.2 mM	Ca(CH ₃ COO) ₂ X H ₂ O
22.8 mM	Zn(O ₂ CCH ₃) ₂ (H ₂ O) ₂
35.9 mM	ZnCl ₂

3.4.2 Staining of paraffin sections

For staining, paraffin sections (5 µm) were de-paraffinised by a standard protocol and incubated for 10 minutes in 4% hydrogen peroxide to eliminate endogenous peroxidase activity. The procedure was continued by permeabilisation of tissue for 45 minutes and blocked for 1 hour with the casein blocking serum followed by

incubation with the primary antibody for 12 hours at 4°C (Table 8). The cells were then incubated with a Cy3-coupled secondary antibody (Table 9) for 2 hours diluted 1:100 in blocking buffer. The procedure was terminated by DAPI counterstaining (1 µg/mL) for 10 minutes and mounting in ProLong (Invitrogen).

3.5 Confocal microscopy

For confocal microscopy analysis of immunostained tissue sections and cultured cells, a IX81 microscope equipped with a IX-DSU disk unit and the MT20 multi-wavelength illumination system was used in combination with the cell[^]R software package (Olympus, Hamburg, Germany).

3.6 Chromatin immunoprecipitation (ChIP).

ChIP assays were performed by using the ChIP-IT Express Kit (Active Motif; Rixensart, Belgium) according to the manufacturers' instructions (all buffers and enzymes not defined were provided by the manufacturer). In brief, EC were exposed to cyclic stretch (10% 0.5 Hz for 6 h) as described above. Thereafter, cells were fixed and cross-linked with formaldehyde (1% in PBS), the DNA was isolated and digested with the provided restriction enzyme cocktail and subjected to immunoprecipitation. The antibodies used for this procedure were from Santa Cruz Biotechnology, Heidelberg, Germany (zyxin: rabbit antiserum B71; the antiserum (B72) used for Western blot and other procedures did not yield any reproducible results), Sigma-Aldrich (mouse α -actin as a negative control) and Active Motif (RNA polymerase II/ChIP-certified). The resulting precipitated DNA was subjected to gene-specific PCR and the amount of amplified DNA was densitometrically analysed after agarose gel electrophoresis (Molecular Imager Gel Doc XR System and the Density One densitometry software version 4.6, Biorad Munich, Germany). The optimal number of PCR cycles (95°C/30 s denaturation, 60°C/30 s annealing and 72°C/1 minute synthesis) varied between 28 (Clusterin after RNA polymerase II precipitation) and 37 (most genes after precipitation with B72). The primers were chosen in a way that putatively functional PyPu-boxes were included in the amplified region.

3.7 Protein biochemistry

3.7.1 Isolation of total cellular protein

The cells were collected with a cell scraper (Sarstedt Inc.) in 250 μ l PBS and transferred into a microcentrifuge tube and centrifuged at 3000 rpm for 3 minutes. The pellet was resuspended in 50 μ l protein lysis buffer and was incubated on ice for 30 minutes. The mixture was vortex every 10 minutes. The non-ionic detergent, 0.1% triton-x was added for 10 minutes for permeabilisation of cell membrane.

Components of hypotonic protein lysis buffer

10 mM	Hepes, pH 7.9
10 mM	KCl
0.1 mM	EDTA
0.1 mM	EGTA
0.1 M	DTT
50 μ M	Pefablock
25 μ M	Protease inhibitors

3.7.1 Separation of cytoplasmic and nuclear proteins

For enrichment of the cytoplasmic and nuclear protein fraction from cultured cells, the ReadyPrep protein extraction kit (Cytoplasmic/nuclear; BioRad) was used according to the manufacturer's protocol. Briefly, the cells were collected in 250 μ l PBS and centrifuged at 3000 rpm for 3 minutes. The cell pellet was suspended in CPEB buffer and the cell membrane was disrupted mechanically with the syringe needle (20 gauge). The CPEB buffer containing the cells with disrupted cell membrane was subjected to centrifugation at 1000 \times g for 10mins at 4 $^{\circ}$ C to collect the cytoplasmic protein. The remaining cell pellet containing the nuclear fraction was re-suspended in protein solubilization buffer (PSB) followed by centrifugation at 16000 \times g for 20 minutes at room temperature to obtain the nuclear protein. Thus separated cytoplasmic and nuclear proteins were further used in the SDS-PAGE analysis.

3.7.2 Sodium dodecylsulfate polyacrylamide gel electrophoresis (SDS-PAGE)

SDS-PAGE separates proteins exclusively on the basis of their size (Laemmli 1970). Therefore, analysis of complex protein samples was performed using SDS-

PAGE. Gels from 10 – 12 % were poured between the glass plates depending on the size of the proteins to be separated and overlaid after polymerization with a 4% stacking gel. For the preparation of the gels the solutions (described in Table 16) were freshly prepared. Proteins were denatured by the addition of 4× sample loading buffer (Roth) and heated for 5 minutes at 95°C. Proteins were then separated by electrophoresis in 1× Tris-glycine-SDS running buffer at fixed voltages of 100 V for the stacking gel, and 150 V through the separating gel. The Kaleidoscope Precision Plus protein standard (BioRad Laboratories) was used to monitor the progress of the run and to estimate the molecular mass of protein bands of interest.

Tris-glycine-SDS buffer (1×)

25.0 mM Tris HCl, pH 8.3
 192.0 mM Glycine
 0.1 % SDS

Loading Buffer (4×)

150.0 mM Tris HCl, pH 6.8
 300.0 mM DTT
 6.0 % SDS
 0.3 % Bromophenol blue
 30 % Glycerol

Table 16: Formulations for SDS-PAGE separating and stacking gels

	Separating gel 10%	Separating gel 12%	Stacking gel 4%
Acrylamide stock (30%)	3.3 ml	4.0 ml	0.65 ml
1.5 M Tris HCl, pH 8.8	2.5 ml	2.5 ml	-
0.5 M Tris HCl, pH 6.8	-	-	1.25 ml
dd H ₂ O	4.1 ml	3.35 ml	3.05 ml
20% SDS	50 µl	50 µl	50 µl
10% APS	50 µl	50 µl	25 µl
TEMED	10 µl	10 µl	10 µl

3.7.3 Western blot analysis

The proteins separated by SDS-PAGE were transferred onto a PVDF (Polyvinylidene fluoride) membrane in the transfer buffer using trans-blot transfer cell system (Bio-Rad) at a constant current of 350 mA for 45 minutes. To allow the efficient transfer of all the proteins from gel on to the membrane, both the gel and the membrane was sandwiched between the filter papers and sponges. The PVDF membrane was incubated with 100% methanol for 5 minutes and pre-hydrated in ddH₂O before the protein transfer for 30 minutes to facilitate binding of proteins on to the membrane.

After the transfer, the PVDF membrane was immersed in blocking buffer and rocked for 1 hour at room temperature to block the nonspecific binding. The membrane was then incubated with the appropriate primary antibody (Table 8) diluted in the ratio 1:500 to 1:2500 with blocking buffer for 2hrs at ambient temperature. Thereafter the membrane was washed 3 times for 10 minutes with washing buffer. The blot was then incubated with secondary antibody conjugated to horseradish peroxidase (Table 9) diluted in the ratio 1:5000 for 60 minutes at ambient temperature.

The blot was then washed 3 times with wash buffer for 10 minutes whilst shaking. The membrane was then developed with ECL (equal quantities of ECL reagent A and B- Enhanced Chemiluminescence, substrate; Amersham Pharmacia Biotech, Freiburg, Germany), according to the manufacturer's instructions. The light generated by the enzymatic reaction was detected in a ChemiDoc chamber (BioRad) and the molecular mass of protein bands of interest were analysed.

Transfer buffer

25.0 mM	Tris
19.2 mM	Glycine
20 %	Methanol

Washing Buffer

2.5 g	Triton X-100
1.0 L	PBS 1×

Washing Buffer

5% milk powder in washing buffer

3.7.4 Enzyme-linked immunosorbent assay (ELISA)

Pre-coated enzyme-linked immunosorbent assay (ELISA) was used for quantitative determination of interleukin-8 (R&D Systems, Wiesbaden, Germany), endothelin-1 (R&D Systems) and atrial natriuretic peptide (Biomedica, Graz, Austria) concentrations in cell culture supernatants. All samples were thawed only once at the time of testing and analysed according to the manufacturer's protocol.

3.8 *Ex-vivo* blood vessel perfusion

Ex-vivo blood vessel perfusion was performed according to rules of the Regional Council Karlsruhe and conformed to the Guide for the Care and Use of Laboratory Animals (NIH Publication No. 85-23, revised 1996) Wild type mice (C57BL/6) and mice with the indicated gene defect (zyxin, GC-A, TRP-C1/3/4/5/6 deficiencies) were euthanized in CO₂ chambers.

3.8.1 Isolation and preparation of murine femoral arteries for perfusion

For the isolation of femoral arteries, the hind limb of euthanized mice was excised and immersed under perfusion buffer (ref Table 17). The femoral artery was then separated from the accompanying vein and dissected from connective tissue. Segments of the femoral artery (0.5 - 1 cm) were cut and mounted onto glass capillaries (diameter 120 µm) fitted for the use in the Pressure Myograph System 110P.

The glass capillaries used for perfusion experiments were prepared using a P-87 Flaming/Brown micropipette puller (Sutter Instrument Company, Novato, USA). The capillaries were pulled from 0.15 mm glass cannulas (GB150-8P, Science products GmbH, Hofheim, Germany) with the program optimized according to an operation manual provided by the manufacturer to achieve a final tip-diameter of 120 µm. Thereafter, the capillaries were cut to the appropriate length (approximately 1.5 cm).

3.8.2 Perfusion of isolated murine femoral arteries

The femoral arteries were subjected to *in situ* perfusion using Pressure Myograph System Model 110P (Danish Myo Technology, Copenhagen, Denmark, Figure 10). The pressure transducer together with the MyoView™ system and software allowed continuous control of temperature, pressure and vessel diameter.

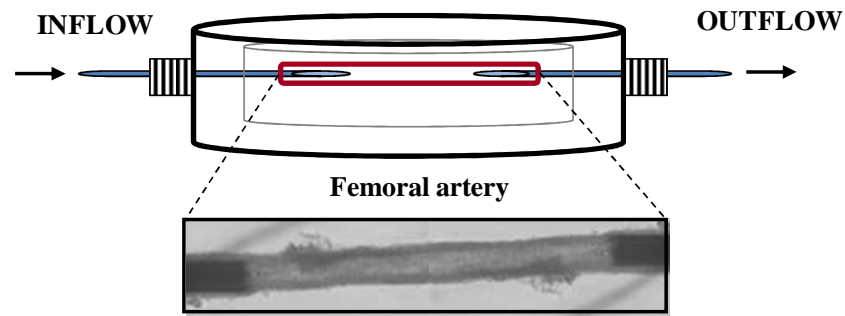


Figure 10: The *in situ* perfusion model. This model mimics the hemodynamic situation of the femoral artery during high wall tension. Perfusion of isolated femoral artery was performed under control conditions ($\Delta p=20$ mm Hg) and under hypertensive conditions ($\Delta p=50$ mm Hg)

The artery was equilibrated at a pressure of 10-30 mmHg for 1 hour. After equilibration, the pressure gradient (Δp) along the femoral artery was gradually raised to 50 mm Hg to mimic hypertensive conditions with an inflow pressure set at 150 mm Hg and a outflow pressure of 100 mm Hg (37 °C, flow 20 to 230 μ l/minute, depending on perfusion pressure). The artery was then perfused at this pressure gradient for the next 4 hours. Changes in vessel diameter were documented after every change in perfusion pressure and in periods of 15 minutes. The vessel chamber was continuously refilled with pre-warmed and equilibrated perfusion buffer. Following the pressure perfusion, the femoral arteries were further processed for immunofluorescence analysis or mRNA/protein analyses. The perfusion buffer was prepared fresh prior to the experiment. 10 ml of 25x solution II was diluted in 800ml distilled water and mixed with 10 ml of solution I and saturated with carbon dioxide and oxygen (95% O₂, 5% CO₂) for 5 minutes. pH was equilibrated to 7.4 and the solution was completed by adding EDTA (260 μ l/l), D-glucose (2 g/l) and 15 % FCS (Fetal Calf Serum).

Table 17: Perfusion buffer pH 7.4 (1×)

Solution I		Solution II	
Chemical	Concentration (mmol/l)	Chemical	Concentration (mmol/l)
NaCl	119.00	NaHCO ₃	2.10
CaCl ₂	1.25	KH ₂ PO ₄	1.18
KCl	4.70		
MgSO ₄ x 7 H ₂ O	1.17		

Table 18: Perfusion buffer pH 7.4 (25×)

Solution I		Solution II	
Chemical	Concentration (g/l)	Chemical	Concentration (g/l)
NaCl	173.850	NaHCO ₃	52.10
CaCl ₂	5.875	KH ₂ PO ₄	4.08
KCl	8.760		
MgSO ₄ x 7 H ₂ O	7.390		

3.9 Statistical analysis

All quantitative data are presented as means \pm SEM of n observations with cells/samples obtained from individual umbilical cords or aorta, respectively. Repeated-measure ANOVA followed by a Tukey-Kramer post-hoc test were performed by using the InStat software package version 3.06 (GraphPad Software, San Diego, USA) with a p-value < 0.05 considered to be significant.

4. RESULTS

Zyxin localisation and function in stretch induced gene expression

The first part of the results deals with the transcriptional changes in human cultured EC in response to stretch, which is induced by zyxin after its translocation to the nucleus and the mechanism of zyxin-induced gene expression.

4.1 Effect of cyclic stretch on cellular localisation of zyxin (*in vitro*)

Human umbilical vein endothelial cells (HUVEC) grown on collagen-coated BioFlex plates were subjected to cyclic stretch (10% elongation, 0.5 Hz, 6 hours) using the Flexercell strain unit to mimic wall tension.

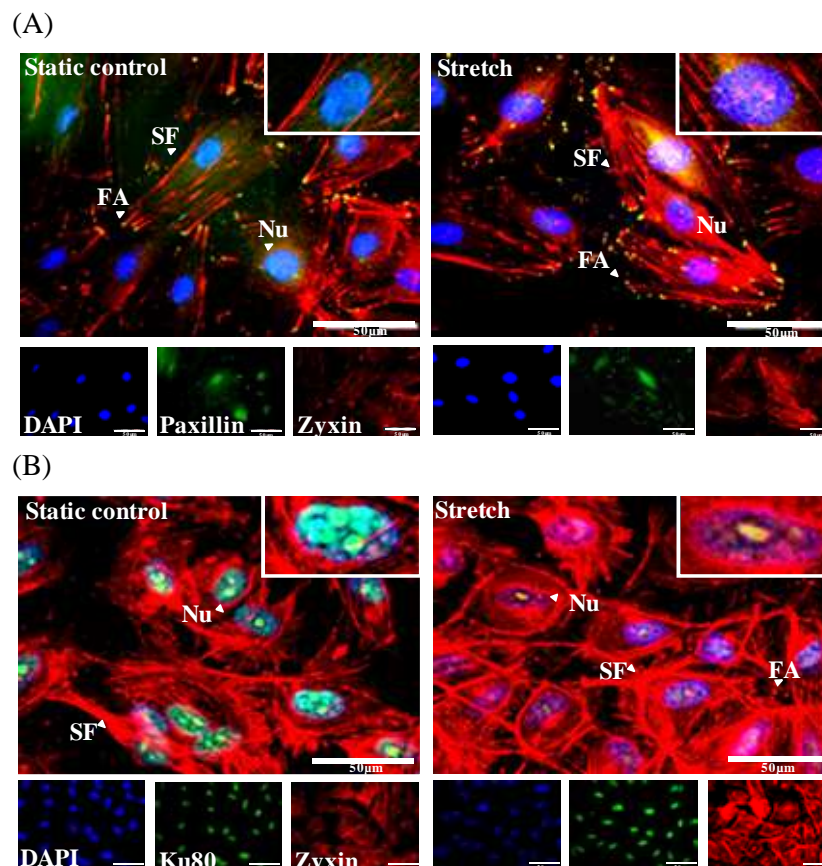


Figure 11: Representative confocal immunofluorescence analysis (IFA) images of zyxin in static and stretched cells. (A) Zyxin is localised in the focal adhesions (FA) in quiescent cells while the nucleus (Nu, inset) is mostly free of zyxin. Cyclic stretch of 6 hours causes nuclear translocation of zyxin. (Cy3/red: Zyxin, Cy2/green: Paxillin). Nuclei were counterstained with DAPI (6-fluoro-diamidin-2-phenylindol: blue). Paxillin colocalises with zyxin exclusively in focal adhesions (FA: yellow) but not in stress fibres (SF) or in the nucleus (after stretch). (B) Partial stretch dependent colocalisation of the nuclear protein Ku80 (Cy2/green) with zyxin (Cy3/red). Whereas nuclei in static cells are virtually devoid of zyxin, significant colocalisation occurs in response to stretch. (insets with magnified exemplary nuclei). For exemplary zyxin negative and zyxin-positive nuclei also see Figure 45 (page 97). Scale bar: 50 μm .

To localise zyxin, the EC were stained with the zyxin specific rabbit antiserum B72 (Figure 11). In quiescent EC, zyxin localises to focal adhesions and stress fibres. After exposure to cyclic stretch, although partly remaining in the focal adhesions, zyxin migrates to the nucleus. In the nucleus, it partially colocalises with the nuclear protein Ku80.

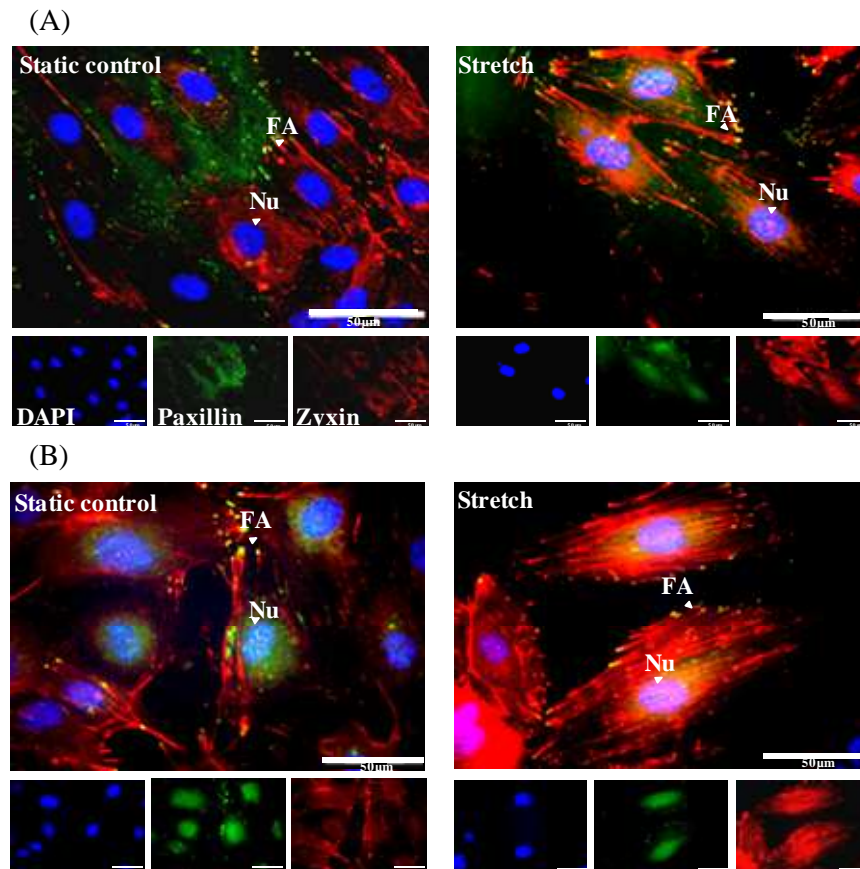


Figure 12: Representative confocal IFA images of zyxin in static and stretched aortic EC (A) and coronary EC (B). In both the cell types, zyxin is localised in the focal adhesions (FA) of quiescent cells. Cyclic stretch causes nuclear (Nu) translocation of zyxin. Paxillin colocalises with zyxin exclusively in focal adhesions (FA) (yellow) but not in the nucleus (after stretch). The cells were stained for zyxin (Cy3/red), paxillin (Cy2/green) and nuclei (DAPI/blue). Scale bar: 50 μm .

In order to exclude HUVEC-specific effects, because of their venous and embryonic origin, immunofluorescence analysis of coronary and aortic cultured endothelial cells was performed that showed zyxin translocation to the nucleus upon stretch in these cell types too (Figure 12).

In line with the immunofluorescence analysis, Western blot analysis of cytosolic and nuclear endothelial cell fractions of HUVEC also showed the translocation of zyxin into nucleus upon stretch (Figure 13).

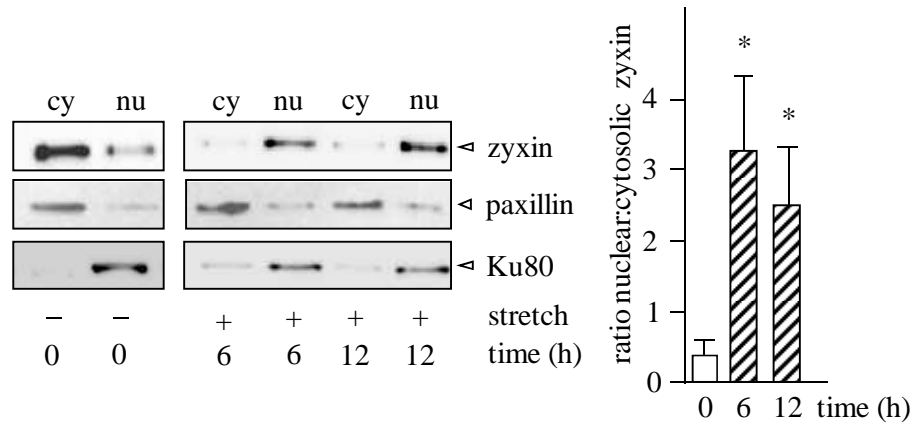


Figure 13: Western blot analysis of nuclear translocation of zyxin. Nuclei and the cytosol of static and stretched (6 and 12 hours) EC were subjected to Western blot analysis. Left panel: exemplary Western blot. Right panel: Statistical summary (* $p < 0.05$ vs. static control, $n = 5$). As control proteins, Ku80 and paxillin were used.

4.2 Pressure-induced zyxin translocation in mouse arteries (*in situ*)

Freshly isolated mouse femoral arteries were subjected to perfusion with oxygen-saturated physiological Krebs-Henseleit buffer at 20 mm Hg (low wall tension) or 150 mm Hg (high wall tension) for 6 h followed by analysis of zyxin translocation by way of immunohistochemistry. Zyxin accumulated in the nucleus of the endothelial cells of arteries perfused under conditions of high pressure, hence stretch (Figure 14A). This also occurs in native SMC, albeit only at even higher perfusion levels (200 mm Hg, Figure 14B).

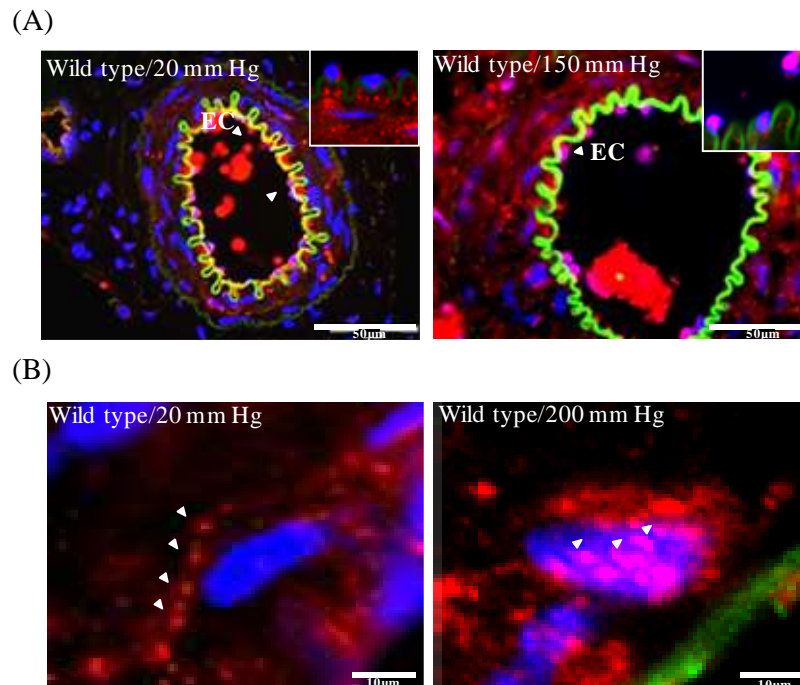


Figure 14: Representative confocal IFA showing localisation of zyxin *in situ*. (A) EC surrounding the lumen of the unperfused femoral artery showing nuclei free of zyxin. Pressure perfused femoral arteries (150 mm Hg) showed zyxin localisation in the nucleus. (B) Enlarged pictures of exemplary SMC in segments perfused at 20 mm Hg (left) and segments perfused at 200 mm Hg (only single cells are shown as, under these conditions, the segments are strongly dilated and partially destroyed). Whereas under low pressure conditions zyxin is located at the cell borders similar to the appearance in cultured cells under static conditions, nuclear accumulation of zyxin is much more prominent in SMC exposed to high wall tension. The arrowheads depict zyxin-positive sites at the cell border (left) and in the nucleus (right). Scale bar: (A) 50 μm (B) 10 μm.

4.3 Role of zyxin in stretch-induced gene expression

The downregulation of zyxin affects stretch-induced-gene expression in rat vascular smooth muscle cells (Cattaruzza 2004). Testing of genes known to be stretch-sensitive revealed that chemokines like interleukin-8 (IL-8) and CXCL1 but not endothelin-1-receptor ET_B -R were regulated by zyxin in cultured EC (doctoral thesis of Agnieszka Wojtowicz, Heidelberg, 2008). To get the full picture of stretch-induced changes in gene expression and the role of zyxin therein, a genome-wide microarray analysis was performed (Wojtowicz 2010) comparing quiescent and stretched HUVEC with and without siRNA-mediated knockdown of zyxin. A total of 592 genes (with $P < 0.02$) turned out to be stretch-sensitive of which 402 (67.9%) were regulated by zyxin. The outcome of this microarray analysis revealed that zyxin is involved in the regulation of rather distinct pathways such as suppression of apoptosis or chemokine release. A similar

analysis of mouse aortic primary cultured SMC from wildtype and zyxin-deficient mice revealed an even more complex albeit partially similar pattern of zyxin controlled genes in stretched SMC. As an overview a comparison of zyxin regulated pathways in SMC and EC is given in Table 19.

Table 19. Comparison of zyxin-controlled stretch-sensitive genes (pathways defined by KEGG or Gene Ontology) in EC and SMC with and without zyxin expression. Only pathways regulated in a highly significant manner in at least one cell type have been included. + to +++: moderately to strongly induced pathways; - to ---: moderately to strongly repressed pathways; \emptyset : pathway not altered. Pathways regulated only in one cell type are highlighted in blue, pathways regulated differentially between cell types are highlighted in green.

	Pathway Functional Description	EC	SMC
Stretch-induced pathways activated by zyxin			
1	CYTOKINE_CYTOKINE_RECEPTOR_INTERACTION	+++	+++
2	LEUKOCYTE_MIGRATION	+	+++
3	CHEMOKINE_RECEPTOR_BINDING	+++	+++
4	CHEMOKINE_ACTIVITY	+++	+++
5	CYTOKINE_ACTIVITY	+++	+++
6	PROTEIN_KINASE_ACTIVITY	+++	++
7	NEGATIVE_REGULATION_OF_PROGRAMMED_CELL_DEATH	++	+++
8	FOCAL_ADHESION	+++	++
9	AMINO_ACID_TRANSMEMBRANE_TRANSPORTER_AC.	+++	++
10	G_PROTEIN_COUPLED_RECEPTOR_BINDING	++	+++
11	TRANSCRIPTION_COREPRESSOR_ACTIVITY	+++	++
12	COMPLEMENT_AND_COAGULATION_CASCADES	++	\emptyset
13	TOLL_LIKE_RECEPTOR_SIGNALLING_PATHWAY	++	\emptyset
14	TGF_BETA_SIGNALLING_PATHWAY	++	\emptyset
15	PROTEIN_SECRETION	\emptyset	+++
16	SMOOTH_MUSCLE_CONTRACTION	\emptyset	+++
17	CALCIUM_MEDIATED_SIGNALLING	\emptyset	+++
18	POSITIVE_REGULATION_OF_CELL_ADHESION	\emptyset	+++
19	POLYMERASE_II_TRANSCRIPTION_FACTOR_ACTIVITY	+++	---
Stretch-induced pathways repressed by zyxin			
20	LIPID_TRANSPORTER_ACTIVITY	---	---
21	OXIDOREDUCTASE_ACTIVITY	---	---
22	CELL_CYCLE*	---	---
23	DNA_POLYMERASE	---	---
24	PYRIMIDINE_METABOLISM	--	---
25	STRUCTURAL_CONSTITUENT_OF_CYTOSKELETON	---	---
26	GAP_JUNCTION	--	\emptyset
27	LYASE_ACTIVITY	---	\emptyset
28	P53_SIGNALLING_PATHWAY	---	\emptyset
29	ORGANELLE_LOCALISATION	\emptyset	---
30	NEGATIVE_REGULATION_OF_PHOSPHORYLATION	\emptyset	---
31	VALINE_LEUCINE_ISOLEUCINE_DEGRADATION	---	+++

As an example for zyxin-regulated stretch-sensitive genes in SMC, thrombomodulin (TM) and calponin (Cal) have been analysed here. The expression of thrombomodulin significantly increased upon stretch in the wildtype SMC whereas in the zyxin knockout SMC, stretch-induced expression was suppressed. In contrast, calponin expression was generally decreased upon stretch. However, in the zyxin-deficient SMC, the gene is no more stretch-sensitive indicating that zyxin is necessary for stretch-dependent repression of calponin expression (Figure 15).

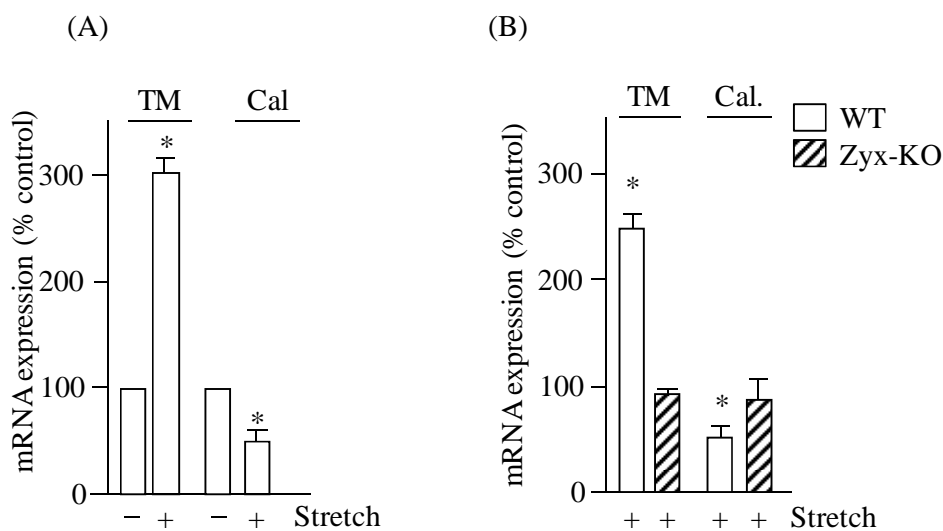


Figure 15: Real time RT-PCR analysis of SMC for thrombomodulin (TM) and calponin (Cal). Cal ($*p < 0.01$ vs. static control, $n = 5$) and TM ($*p < 0.01$ vs. static control, $n = 5$) mRNA expression in response to stretch (12%, 0.5 Hz for 6 h) in cells with (A) a wild type genome (WT) (B) zyxin deficiency.

4.4 Mechanism of zyxin-induced gene expression

To evaluate the mechanism of zyxin-dependent stretch-mediated gene expression, promoter regions of genes identified to be stretch-sensitive were analysed. As described before, zyxin appears to associate with the proximal promoter of the human thrombomodulin gene at a stretch of pyrimidines (PyPu box; position -453 to -481, unpublished observation). On analyzing the promoter regions of stretch-sensitive genes in EC, a comparable motif close to the transcription start site was found solely in the 13 stretch-sensitive genes controlled by zyxin but not in the 11 zyxin-independent genes (Table 20).

Table 20: Alignment of stretch-response element-like sequences. This sequence was found in the subset of zyxin-dependent genes: hairy/enhancer-of-split related with YRPW motif 1 (Hey1), interleukin-8 (IL-8), hemicentin-1 (HMCN1), E74-like factor 4 (ELF4), prepro-endothelin-1 (ET-1), laminin C3 (LAMC3), the transcription factor forkhead box O1 (FOXO1), notch homolog-2 (Notch2), HMG-CoA reductase (HMGCR), E-selectin (SEL-E), ICAM-1, VCAM-1, integrin-6 (ITGB6). Stretch-inducible zyxin-independent genes which have been unsuccessfully analysed for this motif, code for matrix metalloproteases-1 and 12 (MMP-1/12), von Willebrand factor (vWF), clusterin (CLU), guanylate cyclase-1 β (GUCY1B3), frizzled-like-8 (FZD8), heme oxygenase-1 (HMOX1), CD34, the transcription factor forkhead box C1 (FOXC1), leptin receptor (LEPR), matrilin-2 (MATN2), prominin-1 (PROM1) and sulfatase-1 (SULF1).

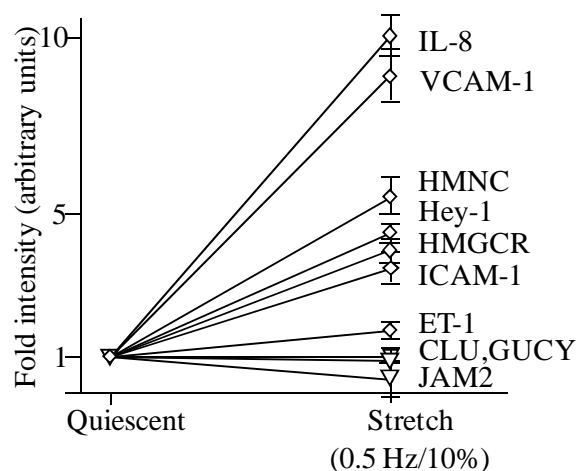
<i>Zyxin-activated genes</i>	
ELF4 (-266):	5'-CTCCCTCCGG CTCTTCCCTC CCTCCCGA-3'
ET-1 (-136):	5'-GGCAGGCGCT TCCTTTTCTC CCCGTAAG-3'
HMCN1 (-670):	5'-GCGTTGTCCT CCCTTCCCTC CCTGCAGA-3'
IL-8 (-685):	5'-GTCCTTACAT TCTTTCTTCT TCTGATAG-3'
LAMC2 (-76):	5'-CCCGGAGCCC TCCTTCTCTC CCGGGGTG-3'
FOXO1 (-597):	5'-AGATTCTGTT TCTCCTTCTC AGAGGTTT-3'
Notch2 (-446):	5'-ATGTGAAATC CTTCCCTTTC TGAGCTGA-3'
HMGCR (-475):	5'-CCGTCGCCGC CTCCTTCCCT TTTTTTAT-3'
<i>Zyxin-repressed genes</i>	
SEL-E (-230):	5'-CTAAAACCTG TCTTTTCTCT TTGACCTG-3'
ICAM-1 (-473):	5'-TCACGCAGCT TCCTTCCCTT TTCTGGGA-3'
VCAM-1 (-315):	5'-TGTCTCCATT TTTTCTCTCC CCACCCCC-3'
ITGB6 (-606):	5'-CTTCCCTAG CCTTCCCTTCT CATTACT-3'
Hey1 (-228):	5'-CCGCGCCTCC TCCTTCCCTT GAGTGCAG-3'

Although not comprehensive yet, the PyPu box is found in zyxin-regulated genes in SMC such as, e.g. the motif at the position -113 to -99 (5'CCT TCC CCT CCC CTT 3') of the calponin gene.

4.4.1 Zyxin association with the PyPu box:

To test whether zyxin really interacts with this PyPu motif, chromatin immunoprecipitation (ChIP) was performed for 9 stretch-sensitive genes, i.e. IL-8, Hey1, HMCN1, ET-1, ELF4, LAMC3, FOXO1, Notch2 and HMGCR. ChIP analysis revealed that zyxin in fact interacts with the promoter region around the PyPu box of these genes. Genes that are expressed independently of zyxin did not emerge with the B72 anti-sera employed for this assay (Figure 16).

(A)



(B)

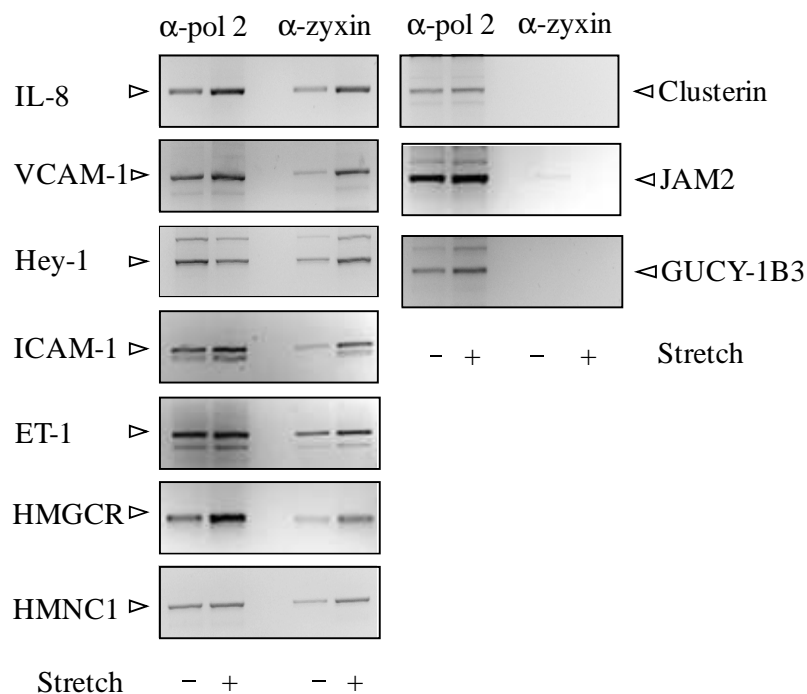


Figure 16: Zyxin-DNA interactions. Chromatin immunoprecipitation (antibodies used were against RNA polymerase II (positive control) and zyxin) analysis of 9 gene products. (A) Summary of 3 independent analyses (relative densitometric ratio of DNA bands from stretched vs static cells). Besides the zyxin-dependent genes IL-8, VCAM-1, HMNC1, Hey-1, HMGCR and ICAM-1, zyxin-independent gene products guanylate cyclase-1B3 (GUCY-1B3), clusterin/apolipoprotein J (CLU) and JAM2) and ET-1 are shown in exemplary agarose gels (B).

4.4.2 PyPu box mimicking decoy oligonucleotide (decoy ODN)

To further corroborate the above finding, cultured EC were pre-incubated with a decoy ODN that mimic the PyPu box sequence in the human prepro-endothelin-1 (ET-1) gene; *edn1*, 5'-GCA CTT CCT TCC TTT TCC CGA A-3'; position -163 to -136. As expected, the decoy ODN virtually abolished the stretch-induced expression of IL-8, as well as that of prepro-ET-1, another well-known stretch-sensitive gene whereas the scrambled control ODN did not show any effect on expression of these two stretch-sensitive genes (Figure 17).

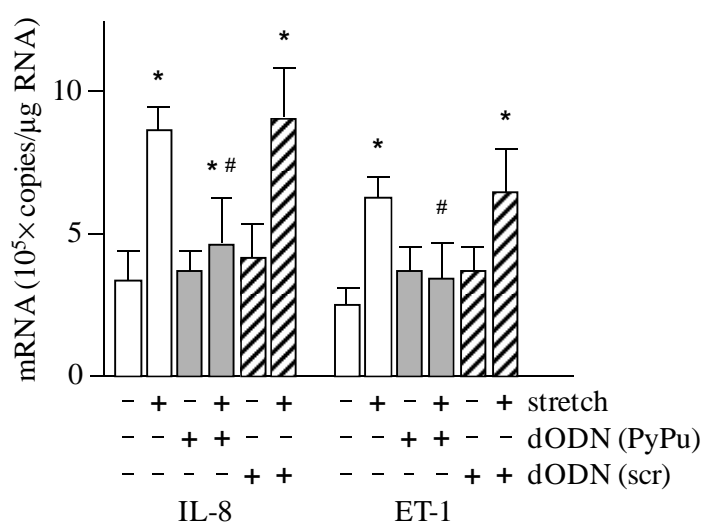


Figure 17: Effects of a PyPu-dODN on zyxin-dependent gene expression. Real time-PCR analysis of static and stretch-induced (6 hours) IL-8 and prepro-ET-1 mRNA expression in the absence (open columns) or presence of a decoy ODN (10 $\mu\text{mol/L}$; 1 hour pre-incubation) mimicking the PyPu box of the *edn1* gene (PyPu; filled columns) or a scrambled control ODN (scr; hatched columns) (* $p < 0.05$ vs. static control, # $p < 0.05$ vs. stretched control; $n = 6$).

Moreover, an electrophoretic mobility shift assay (EMSA) using a probe with a sequence identical to that of the decoy ODN finally confirmed that in human cultured EC exposed to cyclic stretch a nuclear protein–DNA complex forms that according to supershift analysis with two different zyxin-specific antibodies contain zyxin (Figure 18).

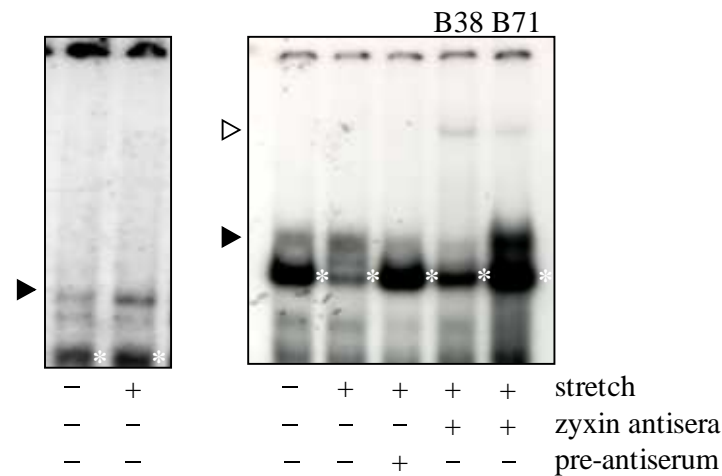


Figure 18: Electrophoretic mobility shift (EMSA). EMSA with the PyPu box-type promoter ODN of the *edn1* gene and nuclear extracts from static control or stretched (6 hours) EC, (Right panel), supershift analysis with two zyxin-specific polyclonal rabbit antisera (B71 and B72; the preantiserum used as a negative control was from rabbit B71) revealing that the retarded complex with nuclear protein from stretched EC contains zyxin (arrowhead). The strong unspecific band (*) was frequently detected but not stretch-related.

4.4.3 Optimisation of the stretch protocol

To analyse what the threshold for stretch-induced gene expression is, HUVEC were subjected to stretch of different frequencies (0.2-2 Hz) and elongation (2-20% Figure 19). IL-8 expression significantly increased with all the set frequencies and was found to be optimal at 0.5Hz. Also, it was observed that IL-8 expression significantly increased in EC stretched more vigorously with 10% and 20% elongation. Elongation beyond 25% stretch resulted in a disruption of the cells. IL-8 expression was thus dependent on both the frequency and magnitude of stretch in these cells.

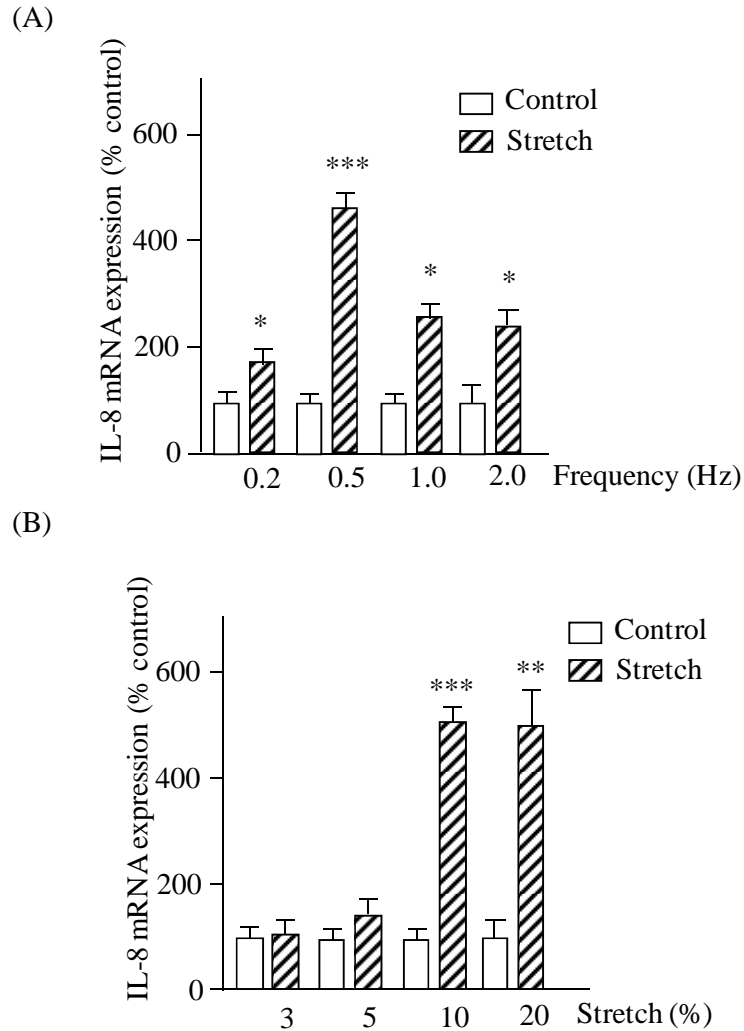


Figure 19: Analysis of the impact of the stretch protocol on IL-8 gene expression in cultured cells. (A) Real time-PCR analysis of static and stretch-induced (10%, 6 hours) IL-8 expression at 0.2 to 2 Hz. (* $p < 0.05$ vs. static control, $n = 3-10$). (B) Real time-PCR analysis of static and stretch-induced (0.5 Hz, 6 h) IL-8 expression at 3 to 20% stretch. Higher stretch levels ($\geq 25\%$) resulted in disruption of the cells (not shown) (* $p < 0.05$ vs. static; $n = 3-10$).

Mechanism of stretch-induced zyxin activation

After confirming that zyxin is crucial for stretch-induced gene expression in EC and SMC, the signalling events leading to stretch-induced zyxin activation moved into the focus of the project.

4.5 Components of the signalling cascade activated by wall tension

4.5.1 Effect of mechanosensitive pathway inhibitors on zyxin translocation

Initially, several inhibitors/agonists that are known to interact with mechanosensitive pathways in EC, SMC or cardiomyocytes were used for a preliminary analysis of components potentially involved in stretch-induced signalling in EC. The zyxin translocation dependent expression of the chemokine, interleukin-8 (IL-8) was used as read-out.

Table 21: Potential stretch induced pathways mediators and their blockers or stimulators. The above indicated concentration of each stimulator and/or inhibitor was used in cell culture.

Potential mediators	Blockers/Stimulators	Concentration
TRP channel blocker	Gadolinium chloride (Gd^{3+})	100 μ mol/l
B-type endothelin-1 (ET-1) receptor-specific antagonist	BQ788	10 nmol/l
protein kinase G (PKG) blocker	8-(4-Chlorophenylthio)-guanosine 3',5'-cyclic monophospho-thioate (Rp8)	100 μ mol/l
Rho associated protein kinase (ROCK) inhibitor	Y27632	3 μ mol/l
Endothelin-1 (ET-1)	-	10 nmol/l
Atrial natriuretic peptide (ANP)	-	1 nmol/l

Whereas most generic inhibitors or activators of these pathways (e.g., nitric oxide synthesis, p38-MAP kinase or ERK1/2, not shown) had no effect, the broad spectrum inhibitor of TRP channels blocker, gadolinium, the B-type ET-1 receptor antagonist BQ788 and the protein kinase G inhibitor, Rp8 all prevented zyxin translocation to the nucleus in EC (Figure 20).

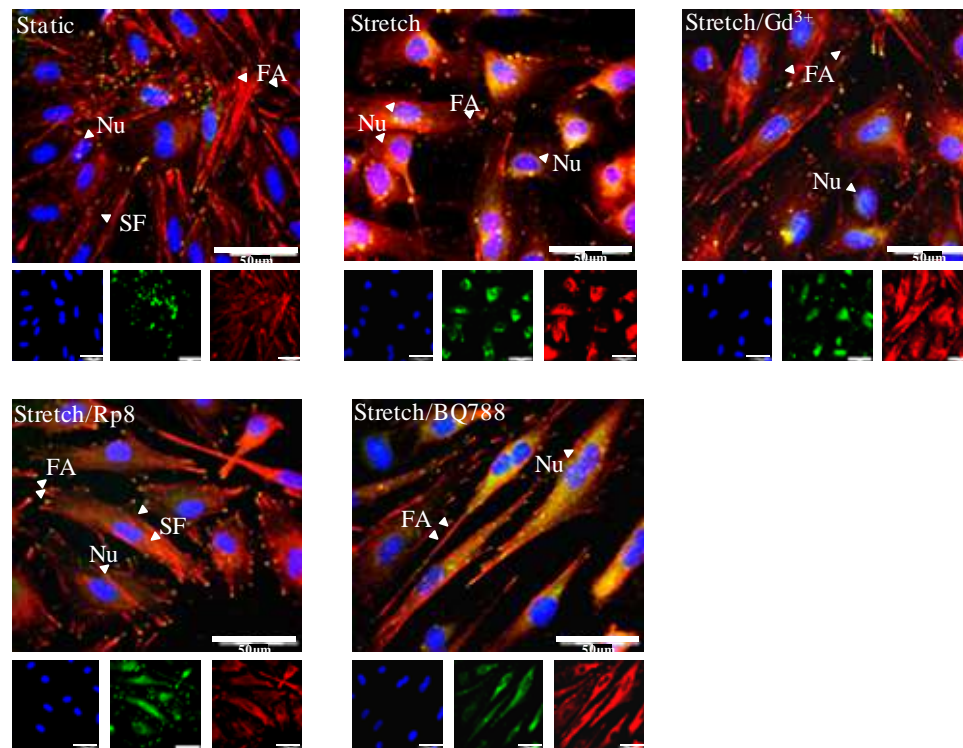


Figure 20: Representative confocal IFA showing zyxin localisation in endothelial cells treated with various inhibitors. HUVEC were treated with the TRP-inhibitor Gd^{3+} (100 $\mu\text{mol/l}$), the ET-1-receptor antagonist BQ788 (1 $\mu\text{mol/l}$) or the protein kinase G-inhibitor Rp8 (100 $\mu\text{mol/l}$). All three agents were applied 1 hour prior to the start of the stretch protocol (10%, 0.5 Hz for 6 h). The cells were further stained for zyxin (Cy3/red), paxillin (Cy2/green) and nuclei (DAPI/blue). Scale bar: 50 μm .

These findings implicated the involvement of TRP channels, ET-1 and as NO synthase inhibition had no effect, ANP in the zyxin signalling cascade. For quantitative analysis, the relative amount of nuclei positive for zyxin was counted in each group (Figure 21).

Furthermore, these three inhibitors also prevented zyxin-dependent IL-8 expression and secretion (Figure 22).

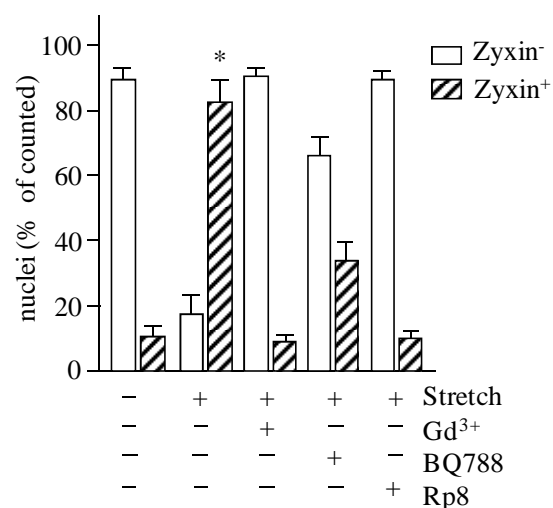


Figure 21: Statistical summary of zyxin localisation in stretched EC treated with Gd³⁺, the ET-1 receptor antagonist BQ788 or the protein kinase G-inhibitor Rp8. Nuclei were counted in 3 independent experiments (200 nuclei per experiment). As indicated in the diagram, blank columns represent zyxin-negative nuclei and hatched columns represent zyxin-positive nuclei. (* $p < 0.01$ vs. static control).

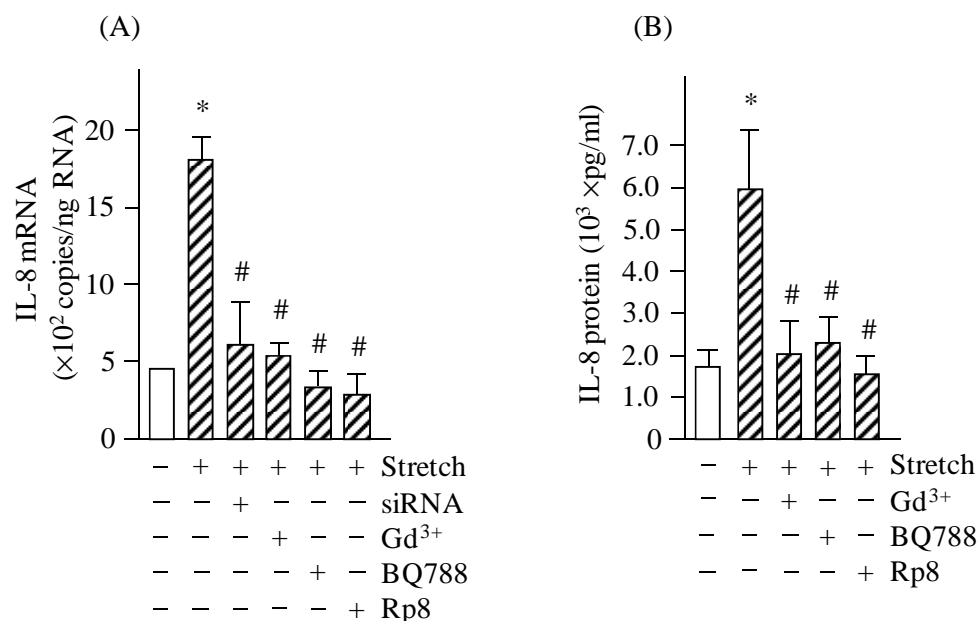


Figure 22: Effects of Gd³⁺, BQ788 and Rp8 on IL-8 expression and release in stretched EC. Analysis of stretch-induced IL-8 mRNA (A, real time RT-PCR) and protein (B, ELISA) expression. All agents were applied as described in Table 22. All three inhibitors repressed the stretch-induced release of IL-8 (* $p < 0.01$ vs. static control, # $p < 0.01$ vs. stretched cells, $n = 3$).

4.5.2 Effect of ANP and ET-1 on zyxin translocation

As inhibition of nitric oxide synthesis, another source of PKG-activation had no inhibitory effect, we hypothesized, that an endogenous (thus endothelium-derived) natriuretic peptide acting via one of its particulate guanylyl cyclase receptors (GC-A/B) might be responsible for stretch-induced PKG activation in an autocrine manner. As atrial natriuretic peptide (ANP) and the receptors GC-A and GC-B but not the brain (B-type) or C-type peptides or the C-type receptor are expressed in significant amounts in the cultured EC, the effects of ANP and ET-1 on zyxin activation were tested. In fact, both ET-1 (10 nmol/l) and ANP (1 nmol/l) mimicked the effects of stretch on the EC by leading to translocation of zyxin to the nucleus in a BQ788- and Rp8-inhibitable manner (doctoral thesis of Agnieszka Wojtowicz, Heidelberg, 2008).

To confirm these findings, EC were additionally treated with ET-1 and/or ANP, and immunofluorescence analysis was carried out to test if they mediate zyxin translocation to the nucleus. Indeed, ET-1 (10 nmol/l) as well as ANP (1 nmol/l) mimicked this effect of stretch on the endothelial cell phenotype, leading to nuclear accumulation of zyxin. This was inhibitable by BQ788 and Rp8 (Figure 23).

4.5.3 Effect of the TRP blocker gadolinium on stretch induced ANP and ET-1 expression in endothelial cells

To observe if gadolinium has an effect on stretch induced ET-1 and ANP mRNA expression, EC were treated with gadolinium as described before. Interestingly, gadolinium did not influence the stretch-induced expression of both mediators (Figure 24) suggesting that ET-1 and ANP mRNA expression in these cells is stretch but not gadolinium dependent and, hence, zyxin-dependent.

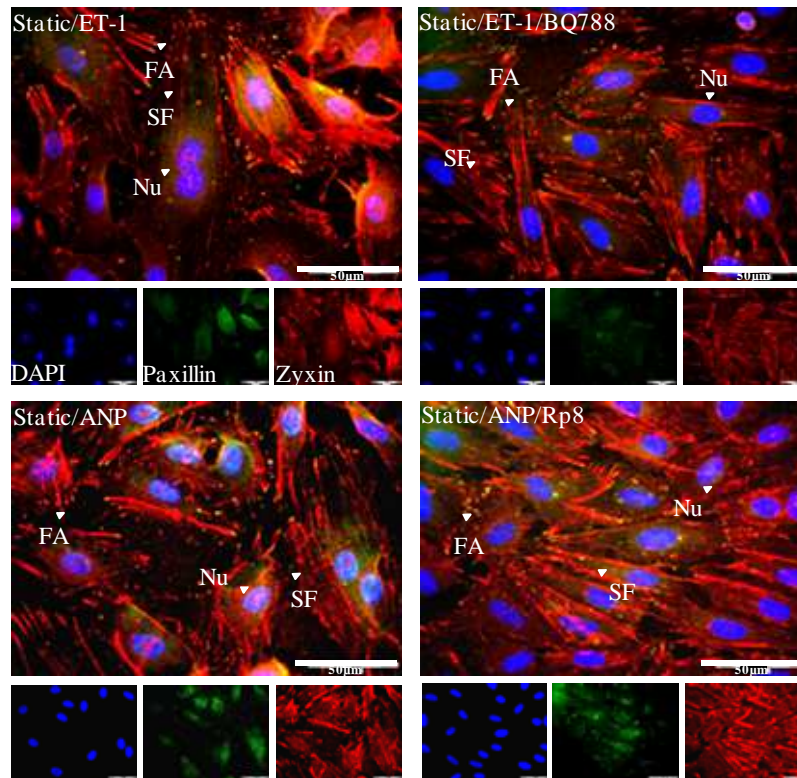


Figure 23: Representative confocal IFA of zyxin localisation in HUVEC. (A) The cells were treated with ET-1 (10 nmol/l), ANP (1 nmol/l), BQ788 (10 nmol/l), Rp8 (100 μ mol/l) alone or in combination for 6 hours. ET-1 (10 nmol/l) and ANP (1 nmol/l) caused the nuclear translocation of zyxin which was inhibited by BQ788 and Rp8, respectively. Scale bar: 50 μ m.

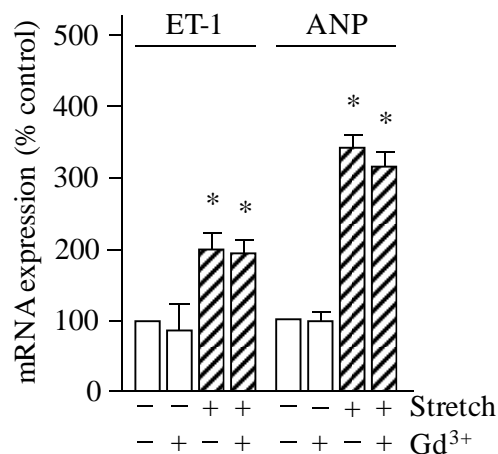


Figure 24: Real time PCR analysis of the effects of stretch and TRP channel inhibition on ET-1 and ANP mRNA expression in EC. Both, ET-1 and ANP expression is stretch-sensitive but insensitive to Gd³⁺ (100 μ mol/l). The cells were treated with Gd³⁺ and subjected to stretch protocol (10%, 0.5 Hz, 6 h). The mRNA expression of pro-ANP and ET-1 was analysed by real time PCR (* p < 0.01 vs. static control, n = 5).

In contrast, at the protein level, the release of both peptides was strongly inhibited by gadolinium (Figure 25). In conjunction with the mRNA expression data this suggests that the stretch-induced synthesis of both mediators but not their release from the EC is independent from zyxin. As both peptides are implicated in the stretch induced activation of zyxin, this outcome is not unexpected.

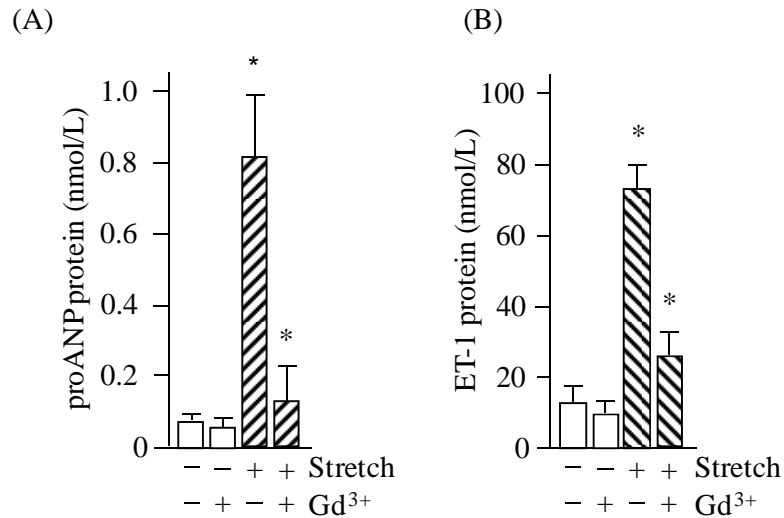


Figure 25: ELISA revealing the effects of gadolinium on stretch-induced proANP and ET-1 release from the EC. The cells were treated with Gd³⁺ and subjected to stretch protocol (10%, 0.5 Hz, 6 h). The supernatant was collected immediately after the stretch protocol and ELISA was performed for (A) pro-ANP and (B) ET-1 (**p* < 0.05 vs. static control, n = 3).

4.6 Hierarchy of TRPs, ANP and ET-1 in zyxin translocation pathway in endothelial cells

To further understand how TRP channels, ET-1 and ANP are involved in zyxin activation, complementation experiments were performed for zyxin translocation. Stretch-induced nuclear accumulation of zyxin was inhibited by gadolinium. However, gadolinium did not have an effect on stretch-induced migration of zyxin when the cells were treated with exogenous ET-1 and ANP, suggesting that TRP channels are upstream of ET-1 and ANP in the zyxin signalling cascade. Similarly, the ET_B-R antagonist BQ788 blocked zyxin translocation in stretched cells but exogenous ANP was able to bypass the BQ788 blockade of zyxin translocation

suggesting that ET1 is upstream of ANP but downstream of TRP channels (Figure 27).

Furthermore, a similar complementation experiment analysing zyxin induced IL-8 expression confirmed these results. Analysis of IL-8 mRNA also showed that stretch-induced IL-8 expression was inhibited by gadolinium but was bypassed by exogenous ET-1 or ANP. Similarly, ET_B-R antagonist BQ788 inhibited ET-1 induced IL-8 expression but did not influence the effect on ANP (Figure 26).

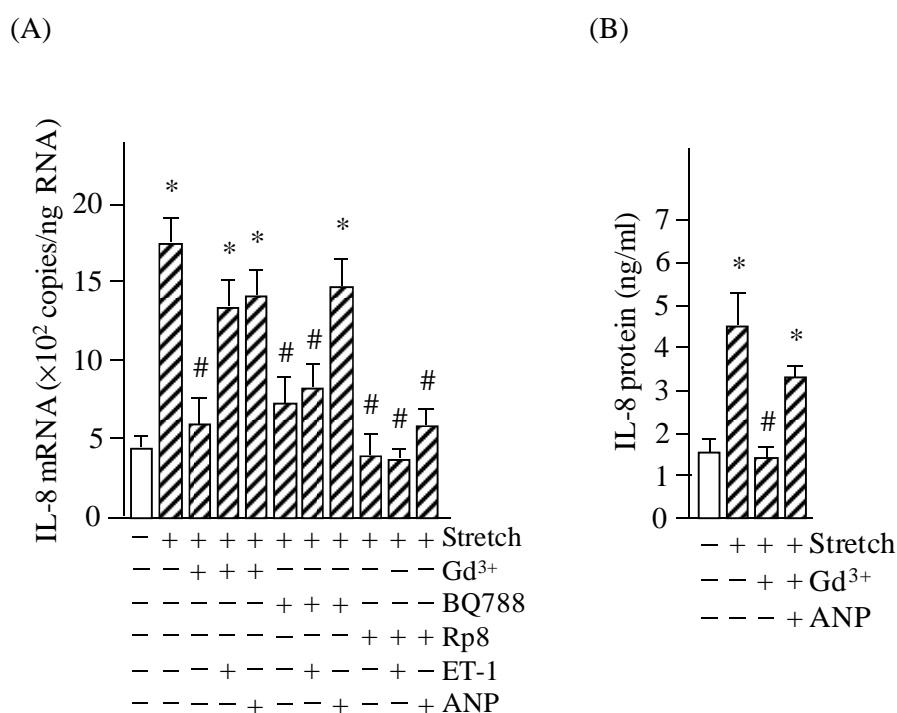
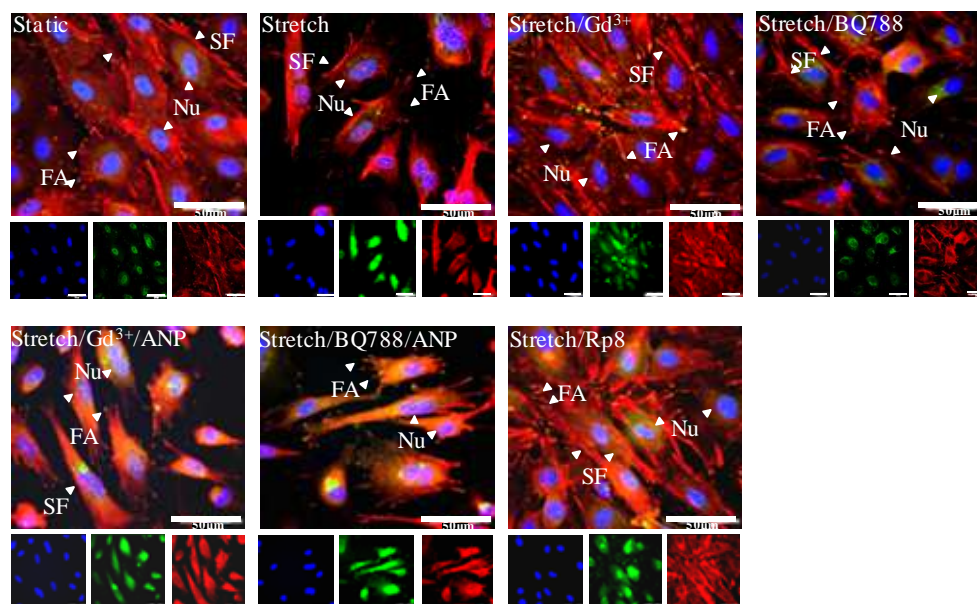


Figure 26: Real time RT-PCR and ELISA for stretch-induced IL-8 expression and release. Analysis of (A) IL-8 mRNA ($*p < 0.01$ vs. static control, $\#p < 0.01$ vs. stretched cells, $n = 5$) and (B) protein ($*p < 0.05$ vs. static control, $\#p < 0.05$ vs. stretched cells, $n = 3$) in the conditioned medium of the stretched cells in the absence or presence of combinations of Gd³⁺, BQ788, Rp8, ET-1 and/or ANP as indicated. Treatment with these substances started 1 hour prior the stretch protocol.

(A)



(B)

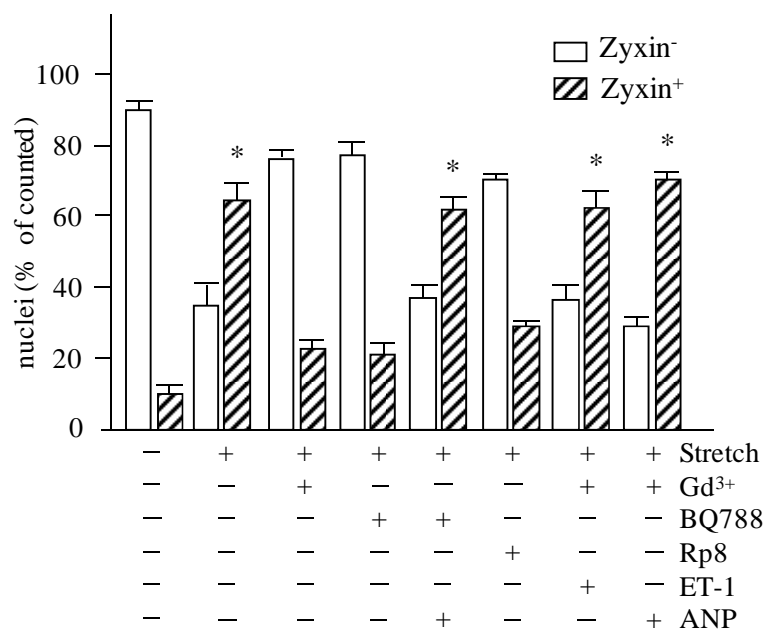


Figure 27: Representative confocal IFA (A) and statistical summary (B) of zyxin localisation in EC. IFA of zyxin The cells were pre-treated with Gd³⁺ (10 μmol/l), BQ788 (1 μmol/l) and/or ANP (1 nmol/l) as indicated in the pictures and subjected to stretch protocol (6 hours, 0.5 Hz, 10%). The cells were further stained for (Cy3/red), paxillin (Cy2/green) and nuclei (DAPI/blue) Scale bar: 50 μm. The statistical analysis was done as described before (ref Figure 21, **p* < 0.01 vs. static control, *n* = 3).

These data reveal that the effect of TRP inhibition can be overcome by the addition of exogenous ET-1 as well as ANP. Furthermore, the BQ788-mediated blockade of ANP-release and hence zyxin activation in stretched EC could be bypassed with exogenous ANP. Finally, neither ET-1 nor ANP was able to overcome the Rp8-mediated blockade of PKG, the effector kinase directly activated by GC-A/B-catalysed formation of cyclic GMP (Figure 26) suggesting that this step may be last before zyxin activation by PKG.

4.7 Zyxin translocation in smooth muscle cells

In order to elucidate whether zyxin translocation in SMC was induced in a similar manner as in EC, mouse cultured aortic SMC were exposed to same agents as the cultured EC. Thus SMC were treated with ET-1 (200 nmol/l), ANP (100 nmol/l) and BQ788 (10 μ M) alone or in combination as indicated in Figure 28 for 6 hours.

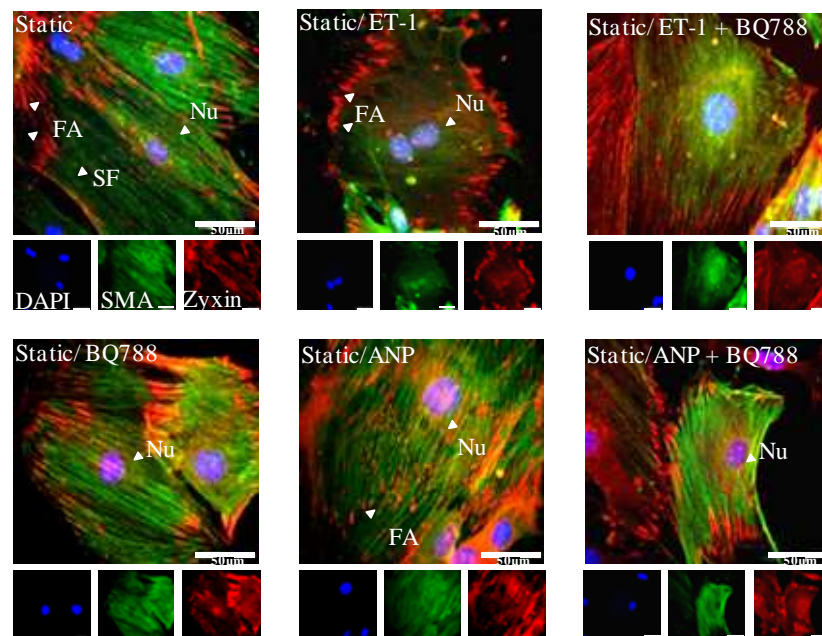


Figure 28: Representative confocal IFA of zyxin in SMC. The SMC were treated with ET-1, ANP and BQ788 alone or in combination as indicated at the concentrations mentioned in the text. The cells were further stained with zyxin (Cy3/red), smooth muscle actin (SMA/Cy2/green) and nuclei (DAPI/blue). Zyxin translocation to the nucleus was seen in the cells treated with ET-1 or ANP. The ET_B-R antagonist inhibited zyxin translocation to the nucleus and this effect was overcome by the addition of ANP. Scale bar: 50 μ m.

Although the concentration of ET-1 and ANP needed for zyxin translocation was higher in SMC, principally the same reaction was observed in both cell types.

4.8 TRP channels in endothelial cells

Several TRP channels are known to be expressed in EC and SMC (Nilius 2007). Expression of TRP channels in HUVEC was analysed using RT-PCR. Although in some cases there was a slight tendency towards increased expression following zyxin knockdown, no significant zyxin or stretch-induced changes in TRP expression were detected (Figure 29).

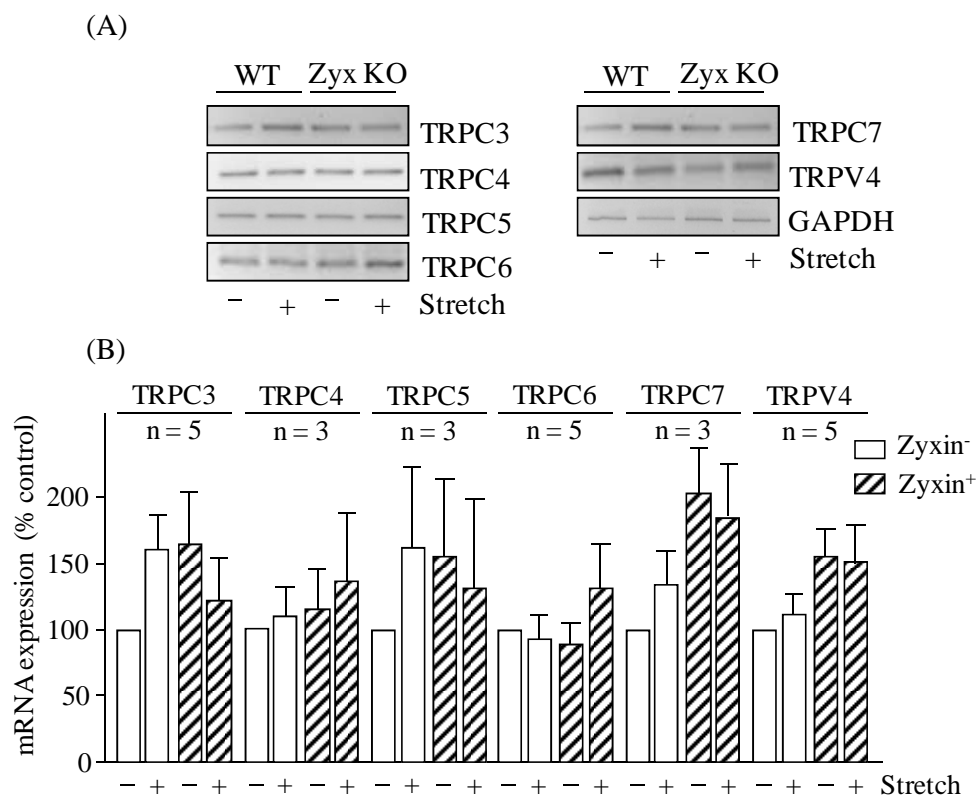


Figure 29: Expression of TRP channels in EC. (A) Exemplary RT-PCR analyses of EC revealing the expression of various TRP channels in EC with or without zyxin and (B) quantification of the expression of various TRP channels in human cultured EC with or without zyxin expression.

4.9 *In situ* perfusion analysis of femoral arteries derived from TRP- deficient mice

Although the effect of Gd^{3+} suggests the involvement of TRP channels, it was not clear whether a single or several channels are responsible for zyxin activation nor which potential candidate may be the stretch-inducible channel. Therefore, the effects of stretch on zyxin translocation in native EC of femoral arteries derived from mice deficient in TRPC1,4,5 as well in those deficient in TRPC3,6 were analysed (Figure 30).

Immunofluorescence analysis of cross sections of the perfused vessels from wildtype mice showed a clear nuclear translocation of zyxin in EC which was also observed in the femoral arteries of TRPC1,4,5 triple knockout animals. In contrast, there was no prominent nuclear translocation of zyxin with the corresponding vessel of TRPC3,6 double knockout mice after pressure perfusion (Figure 30) indicating that either TRPC3 or TRPC6 is necessary for translocation of zyxin to the nucleus during stretch.

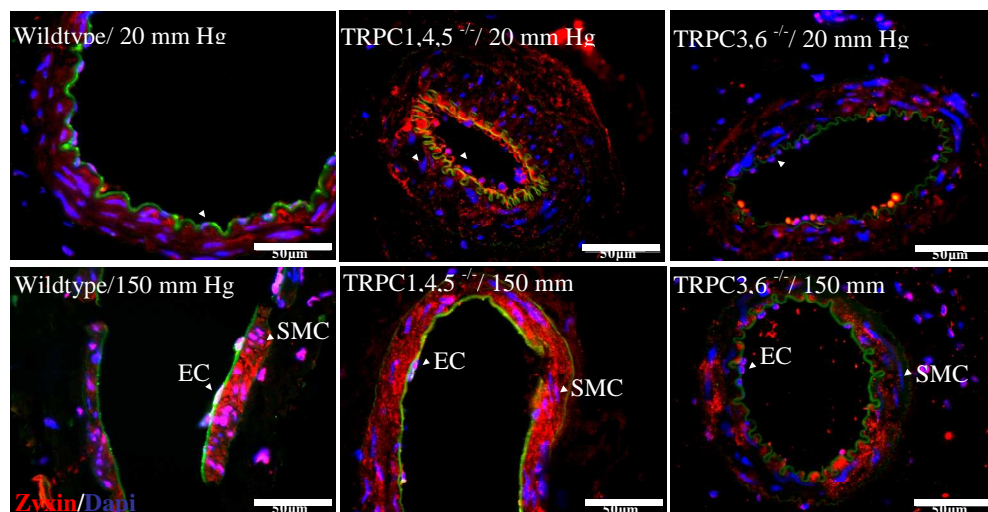


Figure 30: Representative confocal IFA images of zyxin localisation in mouse femoral arterial EC. Pressure perfusion (150 mm Hg) caused nuclear translocation of zyxin in arterial EC of the (A) wildtype and (B) TRPC1,4,5 deficient but not in the (C) TRPC3,6 deficient mice. Paraffin sections of these arteries were stained for zyxin (Cy3/red) and nuclei (DAPI/blue). The green channel depicts the auto-fluorescence of elastic vessel fibres. Scale bar: 50 μ m.

4.10 TRPC3 mediates zyxin activation

4.10.1 *In situ* analysis of TRP KO femoral arteries

To find out the specific TRP involved in zyxin translocation, femoral arteries from TRPC3 and TRPC6 single knockout mice were analysed after pressure perfusion at 150 mm Hg as described before. *In situ* analysis revealed that native EC from TRPC3 but not TRPC6 deficient femoral arteries were defective in wall tension-induced zyxin translocation (Figure 31).

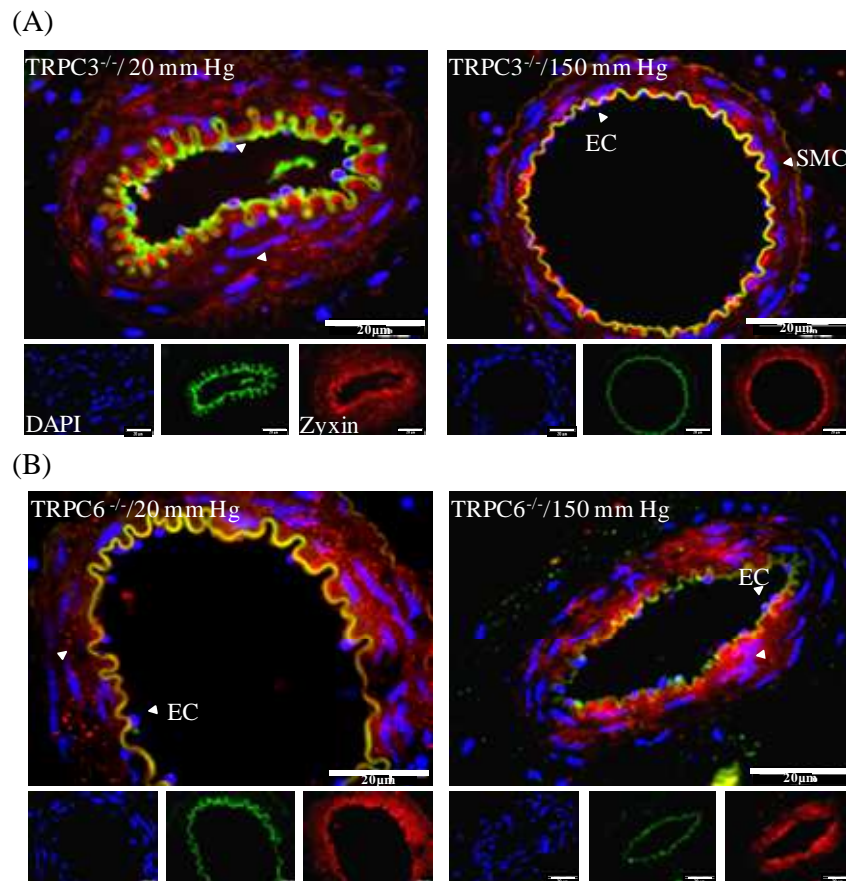


Figure 31: Representative confocal IFA images of zyxin distribution in EC of femoral arteries. Femoral artery sections were derived from (A) TRPC3 and (B) TRPC6 deficient mice and were stained for zyxin (Cy3/red) and nuclei (DAPI/blue). The green channel depicts the auto-fluorescence of elastic vessel fibres. Scale bar: 20 μm.

4.10.2 Analysis of TRP deficient SMC for zyxin translocation

In addition, aortic SMC were isolated from TRPC3 and TRPC6 deficient mice and subjected to cyclic stretch (12%, 0.5 Hz, 6 h). They were stretched at 12% (unlike

the EC which were normally stretched between 0 and 10%) because they are more resistant to stretch than EC (Figure 32).

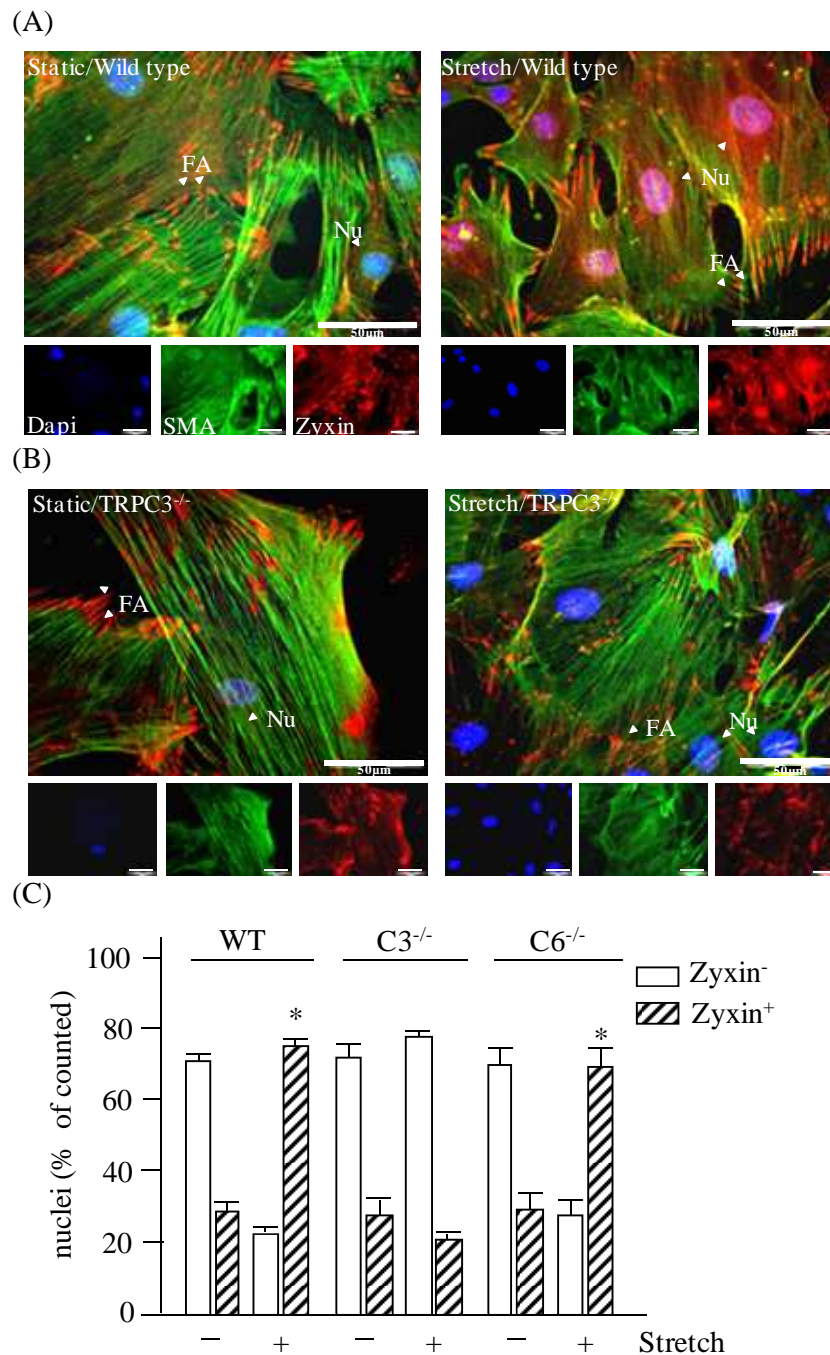
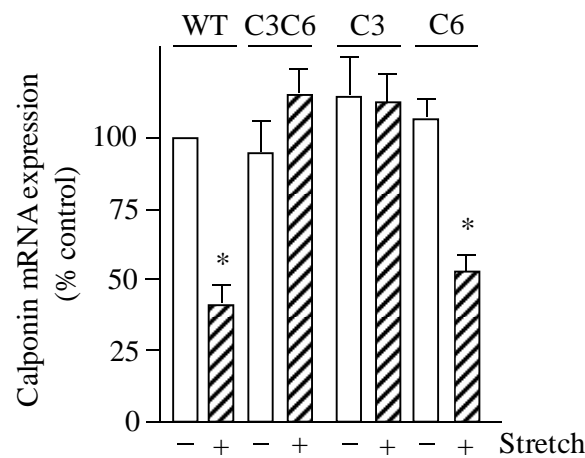


Figure 32: Representative confocal IFA images of zyxin in SMC derived from TRP deficient mice. SMC derived from aorta of (A) wild type mice and (B) TRPC3 deficient mice were subjected to the stretch protocol as described in the text and IFA was performed for zyxin (Cy3/red), α -actin (Cy2/green), nuclei (DAPI/blue). Scale bar: 50 μ m. (C) For the statistical summary, 100 randomly selected nuclei were counted. (* $p < 0.01$ vs. static control, $n = 3$).

In line with the vessel data, aortic SMC derived from TRPC3-deficient animals neither displayed stretch-induced zyxin translocation (Figure 32) nor expression of stretch-sensitive gene products in SMC such as calponin or thrombomodulin (Figure 33).

The expression of thrombomodulin increased upon stretch in the wildtype SMC whereas in the TRPC3 deficient mice, stretch-induced expression was suppressed. Furthermore, the stretch induced regulation of calponin expression was absent in TRPC3 deficient SMC.

(A)



(B)

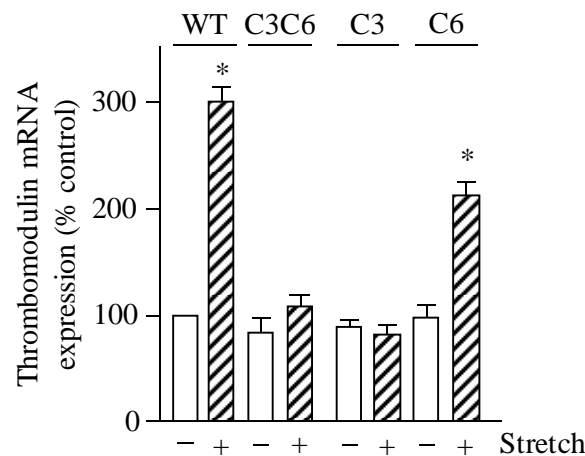


Figure 33: Real time RT-PCR analysis of (A) calponin and (B) thrombomodulin in SMC. The stretch-induced regulation of calponin and thrombomodulin was absent in the SMC derived from TRPC3,6 and TRPC3 deficient mice. Calponin ($*p < 0.01$ vs. static control, $n = 5$) and thrombomodulin ($*p < 0.01$ vs. static control, $n = 5$) mRNA expression was analysed in response to stretch (12%, 0.5 Hz for 6 h) in cells with a wild type genome (WT), deficiency in TRPC3,6 (C3C6), or deficiency in one of the channels (C3 and C6, respectively).

The stretch-induced regulation of these genes in TRPC3 deficient SMC is similar to their stretch-induced regulation in the zyxin deficient SMC additionally proving the role of the TRPC3 channel in zyxin translocation pathway.

4.11 GC-A mediates zyxin phosphorylation by PKG

4.11.1 *In situ* analysis of GC-A deficient femoral arteries

In a similar approach, it was tested which of the guanylate cyclase ANP receptor candidate, the A- or the B-type, respectively, was involved in mechanotransduction. Comparing nuclear zyxin translocation in femoral arteries derived from GC-A knockout mice with that of wildtype mice (Figure 34), revealed that GC-A is required for zyxin translocation because the EC of GC-A-deficient pressure perfused femoral arteries did not show a prominent nuclear translocation of zyxin (Figure 34).

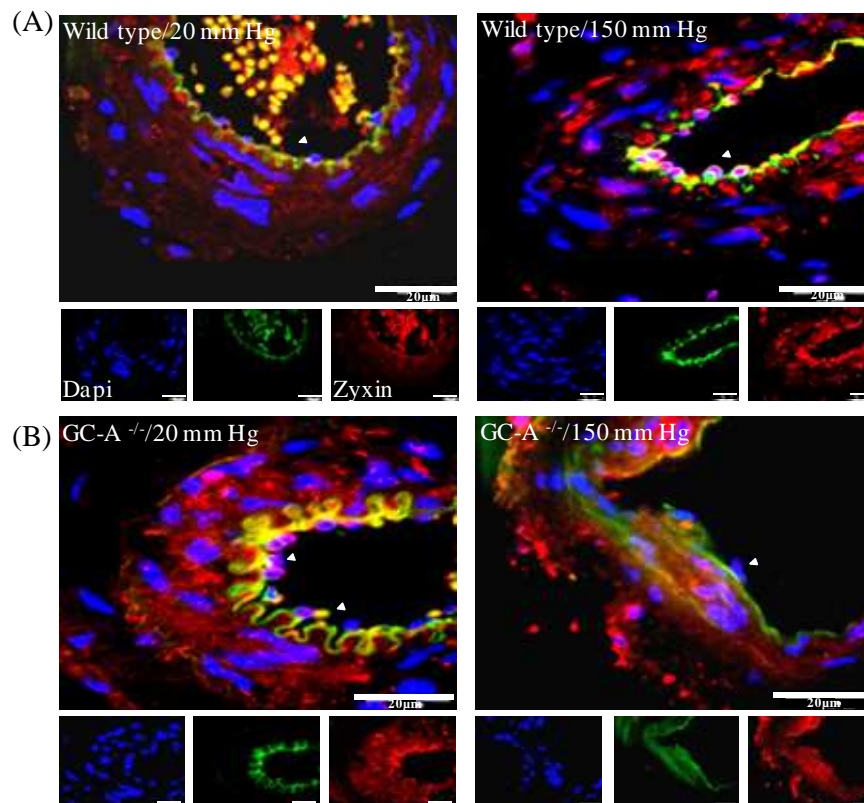


Figure 34: Representative confocal IFA images of femoral arteries. Femoral artery segments derived from (A) wild type mice showing the nuclear translocation of zyxin in arterial EC as opposed to arterial EC from (B) GC-A deficient mice. The arteries were perfused at indicated pressures and stained for zyxin (Cy3/red) and nuclei (DAPI/blue). The green channel depicts the auto-fluorescence of elastic vessel fibres. Scale bar: 20 μ m.

Additionally, the reactivity of pressure perfused GC-A knockout femoral arteries to vasoactive agents such as epinephrine, acetylcholine and ET-1 was similarly blunted as in the zyxin knockout arteries suggesting that a similar defect in stretch-induced signalling occurs in these vessels (Figure 35).

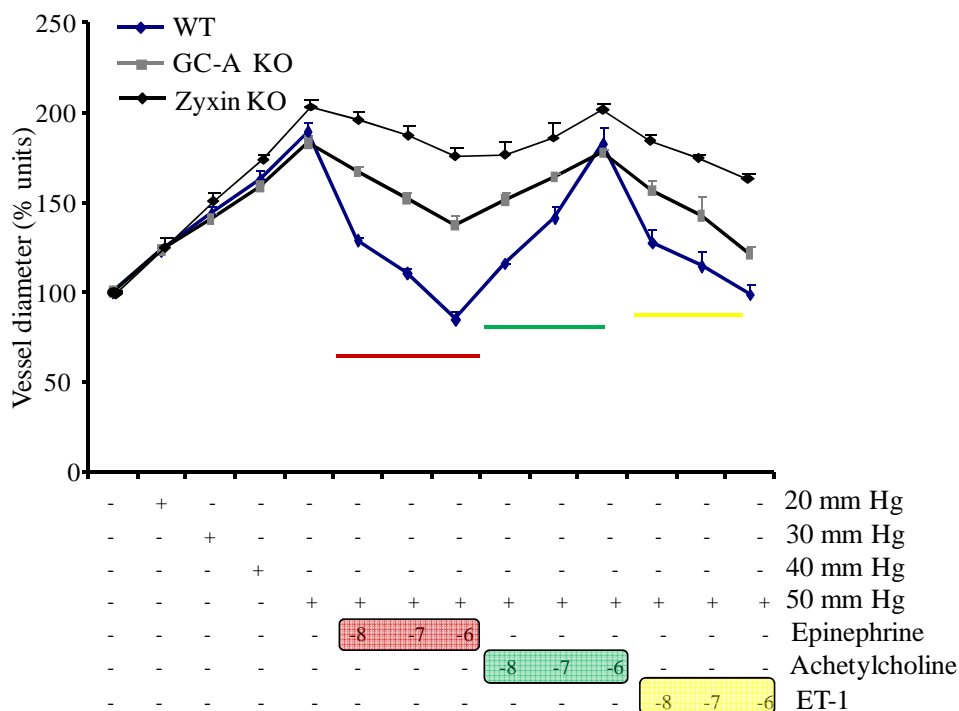


Figure 35: Response of GC-A or zyxin deficient femoral arteries to changes in hydrostatic pressure or to vasoactive agents: Intraluminal pressure was set to 50 mm Hg in order to allow both dilator and constrictor responses. Phenylephrine (at 10 nmol/l, 100 nmol/l and 1 μ mol/l, respectively), ET-1 (at 10 nmol/l, 100 nmol/l and 1 μ mol/l, respectively) and acetylcholine (10 nmol/l, 100 nmol/l and 1 μ mol/l) were consecutively added extra-luminally. The femoral arteries were isolated from 5-12 week old mice (* p < 0.05 vs. control, n = 5).

4.11.2 Analysis of GC-A deficient smooth muscle cell

Further, aortic SMC derived from GC-A knock-out mice were analysed in the same way as SMC derived from TRPC knockout mice (ref 4.10.2). The analysis revealed that the translocation of zyxin to the nucleus of stretched GC-A knockout SMC was significantly low as compared to the wild type SMC further confirming the role for GC-A in zyxin translocation to the nucleus in response to stretch (Figure 36).

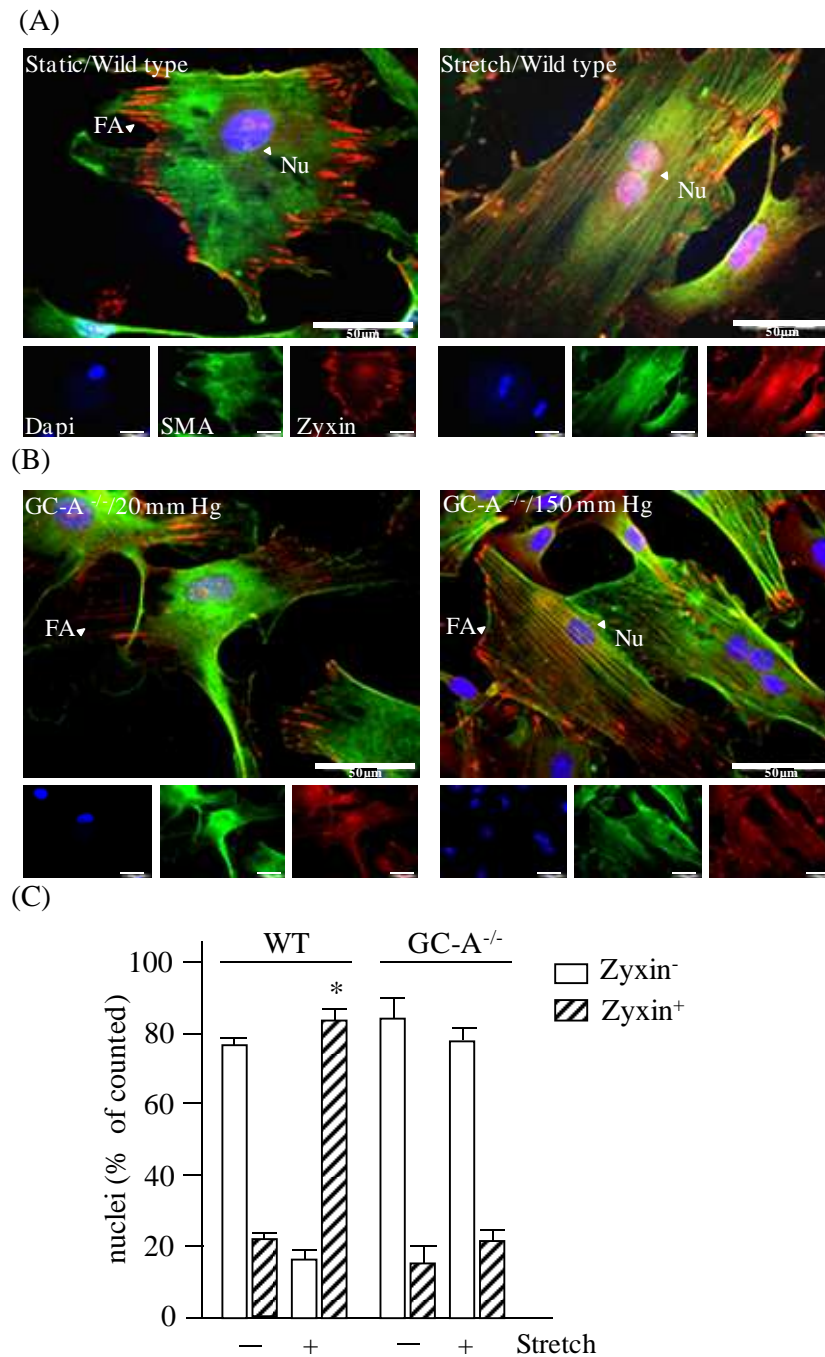


Figure 36: Representative confocal IFA images of zyxin in SMC derived from (A) wildtype and (B) GC-A deficient mice. The SMC were stretched (12%, 0.5 Hz for 6 hours) and stained for zyxin (Cy3/red) α -actin (Cy2/green), nuclei (DAPI/blue). The nuclear localisation of zyxin was seen in the wildtype stretched SMC as opposed to the stretched GC-A deficient SMC. Scale bar: 50 μ m. (C) For the statistical summary, 100 randomly selected nuclei from each of 3 independent experiments were counted ($*p < 0.01$ vs. static control).

Moreover, stretch-induced calponin (Cal) and thrombomodulin (TM) expression was blunted in these cells similar to SMC derived from zyxin-knockout mice (Figure 37).

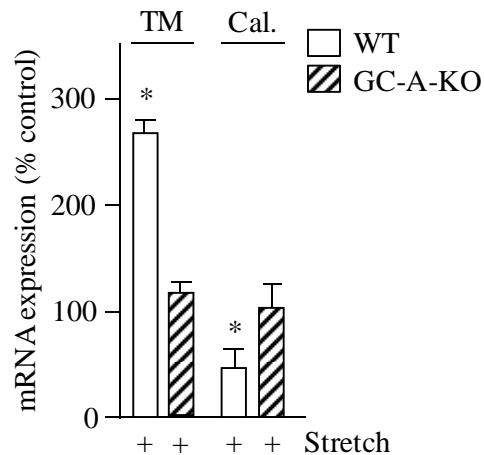


Figure 37: Real time RT-PCR analysis of thrombomodulin (TM) and calponin (Cal) in SMC. Stretch-dependent repression of calponin mRNA expression and up-regulation of thrombomodulin mRNA expression in SMC derived from age-matched wild type (WT) or GC-A-deficient animals (* $p < 0.001$ vs. static control, $n = 5$).

In summary, a hierarchical chain of signalling events starting with TRP activation leading to ET-1 release leading to ANP-release and concomitant activation of PKG could be defined not only by physiological inhibitors but also by genetic knockout of the key players of this cascade, TRPC3, GC-A and zyxin itself.

4.12 Analysis of phosphorylated amino acid residues in zyxin targeted by PKG

Presumably, ANP via its receptor GC-A leads to PKG mediated phosphorylation of zyxin. 2D gel-electrophoresis analysis of EC lysates and nuclear extracts were performed to characterise the stretch and ANP-induced phosphorylation pattern of zyxin through PKG. Stretching of EC in fact caused shift in pI of zyxin that was prevented by the broad range phosphatase (not shown). Moreover, zyxin was phosphorylated and co-purified with nuclear proteins only in extracts of stretched EC, whereas pre-treatment with the PKG-inhibitor Rp8 resulted in inhibition of both phosphorylation and translocation. Accordingly, ANP alone caused a PKG-dependent accumulation of zyxin in the nucleus (doctoral thesis of Agnieszka Wojtowicz, Heidelberg, 2008).

4.12.1 Generation eGFP-zyxin constructs

To probe for putative PKG target sites in the zyxin amino acid sequence, an *in-silico* phosphorylation site analysis was performed (<http://www.phosphosite.org>). Among others serine-142 (S142), serine-344 (S344) and threonine-352 (T352) were selected for mutation (ref Figure 38 and Table 22). To analyse which of these residues were in fact PKG targets, the eGFP-zyxin expression constructs were generated using eGFP-pcDNA 6.2 vectors and mutated or not at the above mentioned sites (ref 3.1.5).

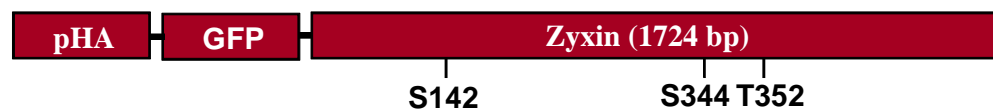


Figure 38: GFP-zyxin constructs. The N-terminal GFP-zyxin constructs were cloned into TOPO vectors and mutated at S142, S344 and T352. Sequences can be found in the Table 22.

4.12.2 Transfection of zyxin expression plasmids into HUVEC

Initially magnetofection was used to transfect HUVEC with the zyxin expression plasmids but the observed transfection efficiency was very low (1 - 3%) and alternative transfection methods with Lipofectamine (Invitrogen), Hi-perfect (Qiagen) and jetPRIME (poly-plus) were performed unsuccessfully. Finally, using polyethylenimine (PEI) transfection (ref 3.2.3) yielded a sufficient number of cells expressing eGFP-zyxin which was adequate for the analysis.

4.12.3 Effects of ANP on cells transfected with zyxin-wildtype and mutant constructs

The HUVEC were transfected with zyxin-wildtype and mutant constructs using PEI. As a first step to characterise the amino acid residue phosphorylated in response to stretch, eGFP-zyxin transfected HUVEC were exposed to ANP (Figure 39) as a surrogate stimulus for stretch. Forty eight hours post transfection, cells were exposed to ANP for 6 hours and fixed thereafter. Total zyxin was stained together with a nuclear counterstain (DAPI) to distinguish transfected from non-transfected cells. It was observed that transfected eGFP-wildtype zyxin was expressed in the focal adhesions, which coincides with the

endogenous zyxin and upon addition of ANP, zyxin translocated to the nucleus, which also matches the behaviour of endogenous zyxin.

Table 22: Wildtype and mutated zyxin constructs. The sequence of the mRNA with a single nucleotide mutation and the resulting amino acid is shown in the table. The official one letter nucleotide and amino acid code is given.

ID	Mutation
S142 Serine 142	mRNA: 570 agg gag aag gtg agc agt att gat ttg gag a 599 amino acid: R E K V S S I D L E 142
S142G Serine142 (AGC) to Glycine 142 (GGC)	570 agg gag aag gtg ggc agt att gat ttg gag a 599 R E K V G S I D L E 142
S142D Glycine-142 (GGC) to Aspartate-142 (GAC) Phospho-mimetic	570 agg gag aag gtg gac agt att gat ttg gag a 599 R E K V D S I D L E 142
S142E Aspartate-142 (GAC) to Glutamate-142 (GAG) Phospho-mimetic	570 agg gag aag gtg gag agt att gat ttg gag a 600 R E K V E S I D L E 142
S344 Serine 344	1170 aac caa aac cag gtg cgc tcc cct ggg gcc c 1200 N Q N Q V R S P G A 344
S344A Serine-344 (TCC) to Alanine-344 (GCC) Phospho-resistant	1170 aac caa aac cag gtg cgc gcc cct ggg gcc c 1200 N Q N Q V R A P G A 344
S344D Alanine-344 (GCC) to Aspartate-344 (GAC) Phospho-mimetic	1170 aac caa aac cag gtg cgc gac cct ggg gcc c 1200 N Q N Q V R D P G A 344
S344E Aspartate-344 (GAC) to Glutamate-344 (GAG) Phospho-mimetic	1170 aac caa aac cag gtg cgc gag cct ggg gcc c 1200 N Q N Q V R E P G A 344
T352 Threonine 352	1200 cca ggg ccc ctg act ctg aag gag gtg gag g 1230 P G P L T L K E V E 352
T352A Threonine 352 (ACT) to Alanine 352 (GCT) Phospho-resistant	1200 cca ggg ccc ctg gct ctg aag gag gtg gag g 1230 P G P L A L K E V E 352
T352D Alanine 352 (GCT) to Aspartate 352 (GAT) Phospho-resistant	1200 cca ggg ccc ctg gat ctg aag gag gtg gag g 1230 P G P L D L K E V E 352

In contrast to glycine or alanine mutants of S344 and T352 (not shown), the correspondingly modified S142 construct did not reveal any nuclear translocation upon addition of ANP, indicating that this amino acid residue is in fact the target of PKG in response to stretch. Moreover, conversion of S142 to glutamate residue partially mimicked the effect of endogenous S142 phosphorylation (Figure 39, right panel).

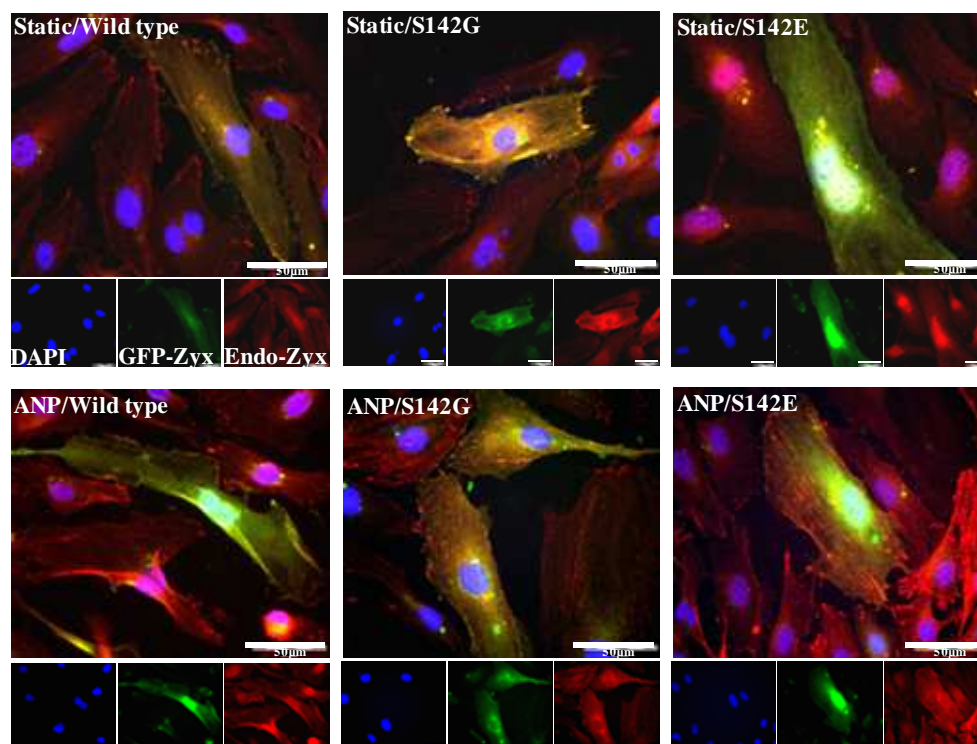


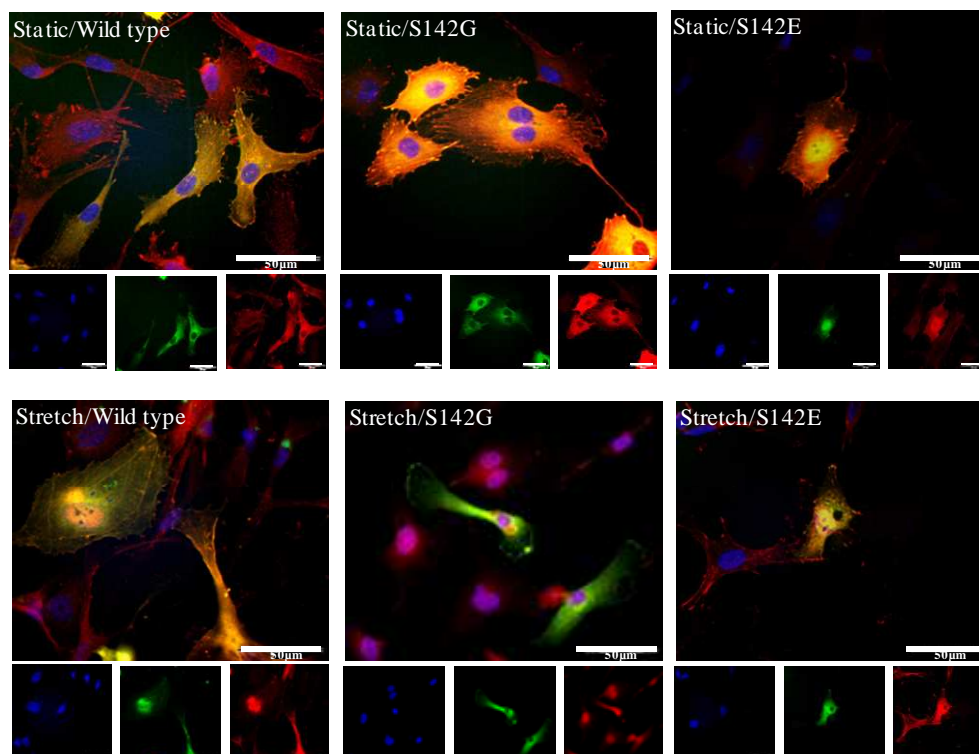
Figure 39: Exemplary confocal IFA of zyxin in EC transfected with eGFP-zyxin constructs. EC were transfected with eGFP-tagged plasmid constructs with a wild type (WT), or mutated (serine-142 to glycine-142/S142G, serine-142 to glutamate-142/S142E) sequence. Total zyxin (Cy3/red) was stained together with a nuclear counterstain (DAPI/blue) Scale bar: 50 μ m.

4.12.4 Effect of cyclic stretch on cells transfected with zyxin-wildtype and mutant constructs

Similar experiments were performed with cyclic stretch as the stimulus for zyxin translocation to confirm that S142 was the actual amino acid residue phosphorylated in response to stretch (Figure 40).

Mutating serine-142 to glycine resulted in a translocation-incompetent zyxin isoform. Moreover, conversion of serine-142 into a glutamate residue partially mimicked zyxin phosphorylation resulting in a significant stretch-independent translocation of this mutant indicating that in fact this amino acid residue is phosphorylated by PKG during cyclic stretch.

(A)



(B)

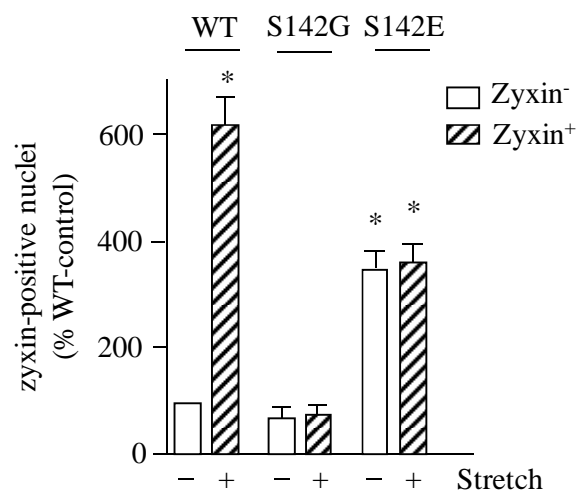


Figure 40: Exemplary IFA (A) and statistical summary (B) of the eGFP-zyxin transfected HUVEC. (A) EC were transfected with eGFP-tagged plasmid constructs with a wild type (WT) and mutant constructs as indicated. Total Zyxin (Cy3/red) is stained together with a nuclear counterstain with DAPI (blue). Whereas the wild type constructs translocate to the nucleus in response to stretch (6 hours, 0.5 Hz, 10 % elongation) essentially like the endogenous protein, S142G has lost the ability to translocate in response to stretch, whereas S142E to some extent mimics phosphorylation already in static cells. Scale bar: 50 μm. (B) A minimum of 50 transfected cells were counted for each condition (* $p < 0.01$ vs. static control $n=3$).

Furthermore, to understand how the zyxin constructs mutated at S344 and T352 act in response to stretch, these constructs were transfected into the HUVEC as described before. Independently of the respective mutation, these constructs were localised in focal adhesions under static condition and translocated to the nucleus upon exposure to stretch indicating that these amino acid residues do not play a role in stretch-induced nuclear translocation of zyxin (Figure 41).

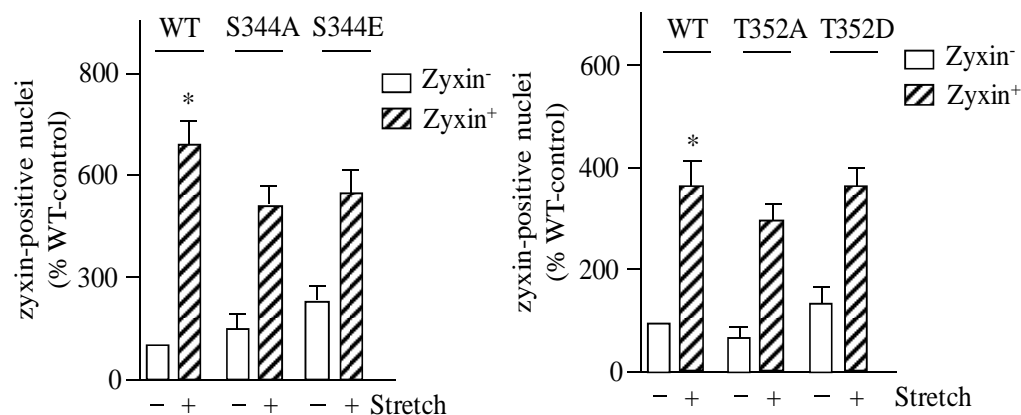


Figure 41: Statistical summary of cells transfected with S344 (A) and T352 (B). Both wild type and mutated S344 and T352 constructs translocated to the nucleus of the endothelial cells in response to stretch (6 hours, 0.5 Hz, 10%). A minimum of 50 transfected cells were counted for each condition (* $p < 0.01$ vs. static control $n=3$).

4.13 Effect of Rho associated protein kinase (ROCK) on zyxin translocation

Rho kinases, being the effectors of Rho play an important role in the formation of stress fibres and focal adhesions due to their effects on myosin light chain phosphorylation. To find out if ROCK plays a role in zyxin translocation, HUVEC were incubated with the ROCK inhibitor Y27632 and then subjected to the standard stretch protocol. The mRNA analysis of IL-8 revealed that Y27632 slightly inhibited stretch- induced IL-8 expression (Figure 42).

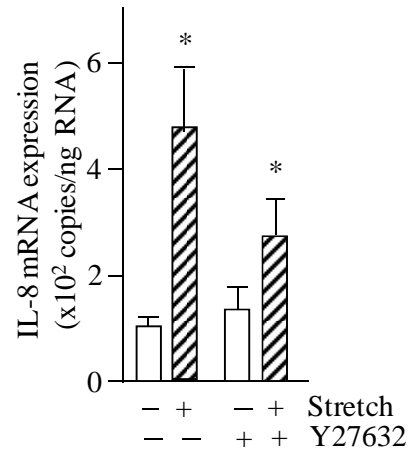


Figure 42: Real time RT-PCR analysis of stretch-dependent IL-8 expression. The cells were treated with the ROCK inhibitor Y27632 (3 μ mol/l) and subjected to standard stretch protocol. The rock inhibitor showed a moderate but insufficient repression of stretch induced IL-8 expression (* p < 0.05 vs. static control n=4).

5. DISCUSSION

Wall tension and vascular disease

Hypertension is a major risk factor for potentially fatal diseases such as stroke, congestive heart failure, myocardial infarction and kidney disease (Bahiru 2008). The reason for this causal relationship is that the chronically elevated transmural pressure leads to an increase in wall tension that causes stretching of both arterial EC and SMC and disables the contractile capacity of the affected blood vessels. In addition this increase in wall tension elicits certain phenotype changes in both cell types aimed at antagonizing the mechanical overload and, consequently, regain control on vascular tone.

Although the clinical manifestations of this pressure-induced vascular remodelling, a fixed increase in total peripheral resistance and a pro-inflammatory and synthetic SMC phenotype facilitating the development of atherosclerosis, are well described even in molecular details, little is known about the onset of this process. Consequently one aim of the present work was to characterise primary, thus specific, mechanisms of mechanotransduction in EC and SMC.

5.1 Models used to apply wall tension

As outlined in the introduction, wall tension is derived from the transmural pressure gradient, the diameter/radius and thickness of the vessel wall (see Fig. 1). Thus, an increase in either pressure or radius results in increased wall tension.

Wall tension translates to stretch in cultured cells

It is highly difficult to expose cultured cells to increased transmural pressure gradients. Therefore, EC as well as SMC used in this project were stressed via increasing the “radius-component” of WT, thus stretching them in a Flexercell unit. This model is well established and widely used to mimic wall tension *in vitro* (e.g., Shrinsky 1989; Cattaruzza 2004; Kakisis 2004; Lacolley 2004, Wojtowicz 2010). Data presented in these reports show that there is a good correlation with data derived from *in situ*- or *in vivo*-models.

The rhythmic or cyclic component of the stretch protocols used, however suggestive, should not be mistaken as an attempt to mimic the pulsatility of regular

blood flow. This manoeuvre is solely used to prevent a compensatory reaction of the cultured cells observed under conditions of static stretch, i.e., evasion of stretch by adhesion to new attachment points. Indeed, using the Flexercell unit, frequencies near to human (>1 Hz) or even mouse (5+ Hz) heart rate were found to be lethal, most probably due to the mechanical properties of the membranes used and development of heat.

Wall tension in perfused vessels

To mimic wall tension *in situ*, perfusion of freshly isolated mouse femoral arteries was used using a pressure myograph system, which allowed continuous control of temperature, pressure and vessel diameter. In this model, transmural pressure is used to also increase the vessel diameter and decrease wall thickness considerably, thus very efficiently increase wall tension. Perfusion in this model does not show any pulsatile component underlining the fact that maybe *in vivo* pulsatility of blood flow plays a role, e.g., at arterial bifurcations, but that wall tension *per se* must not be pulsatile to be effective as a stimulus for mechanotransduction.

In vivo analyses of zyxin-induced gene expression.

In this thesis no *in vivo* experiments have been performed; this was due to an insufficient supply of zyxin-deficient mice. However, as after extensive back-crossing with wild type mice, meanwhile mating of zyxin-deficient mice is successful, a major focus will be set in the future to confirm the importance of zyxin-induced gene expression after induction of hypertension in the living animal (see also below).

5.2 Gene expression regulated by zyxin

The zyxin-regulated transcriptome in EC and SMC

Microarray analyses comparing quiescent with stretched EC with or without siRNA-mediated zyxin knockdown (Wojtowicz 2010) and of aortic cultured smooth muscle cells derived from wild type and zyxin-deficient mice (in this thesis only a comparison of zyxin-controlled pathways in EC and SMC is given, see Table 19 and below) confirmed that in both cell types around 70% of all

stretch-sensitive genes in fact are controlled by zyxin. Most of these gene products can be arranged in pathways which are of special importance for pressure-induced vascular remodelling, e.g. cell migration, proliferation, differentiation or apoptosis. Many of the pathways regulated are very similar in EC and SMC (Table 19). In both cell types after 6 hours of stretch zyxin suppresses apoptosis as well as proliferation, and thus seems to stabilize a differentiated phenotype at least for relatively short periods of supra-physiological stretch. It will be of great interest to analyse the impact of zyxin on these pathways *in vivo* (see above) and after longer periods of time in cultured cells.

However, some pathways, e.g., muscle contraction (SMC) or TOLL-like receptor signalling (EC), are regulated in a cell type-specific manner. From a teleological point of view this seems comprehensible. From a mechanistic point of view, this finding suggests a more complex regulatory function of zyxin. At least, zyxin-dependent gene expression is not independent of the cell type-specific transcription machinery, but must interact with other, at this stage of the project unknown, transcription factors.

Interestingly, only two pathways are regulated antidromic in EC and SMC. Both are suggestive and might hint to a different assignment of EC and SMC during early phases of supra-physiological stretch. Whereas in SMC transcriptional activity is generally down-regulated, EC respond with an overall increase in transcription. Vice versa, besides increasing sugar and fatty acid metabolism, SMC seem to degrade several amino acids (the pathway depicted is just an example), whereas EC will even decrease protein turn over/amino acid metabolism. This may hint towards a more regulatory function of EC aimed to control SMC activity and metabolically highly active SMC trying to regulate vascular tone. However, at this point, this is quite speculative.

In conclusion, these microarray analyses are highly suggestive as for zyxin-dependent transcriptome that is similar to that in dysfunctional EC and/or synthetic SMC.

Zyxin as a transcription factor?

Zyxin binds to a promoter motif, a stretch of pyrimidine bases termed pyrimidine-purine box (PyPu box). This motif, which is not defined by an exact sequence but

by the base content, could be found in all gene promoters shown to be regulated by zyxin. Moreover, using specific decoy-ODN and EMSA, this motif could be shown to be functional. Thus, zyxin may act as a true transcription factor, most probably via its zinc finger LIM-domains, but it cannot be ruled out that the protein is coordinated to the PyPu-box by an up to now not unknown factor. Potential candidates may be the poly-pyrimidin tract binding protein (Sawicka 2008) and matrin 3 (Matsushima 1996; Valencia 2007; both proteins are known to bind to a stretch of pyrimidine bases.

5.3 The endothelial cell response to stretch – a defined signalling cascade

Analysis of the localisation of zyxin revealed that the protein was in fact localised exclusively to focal adhesions and stress fibres in both EC and SMC under basal conditions. However, upon exposure to cyclic stretch, zyxin associates more prominently with stress fibres (Cattaruzza 2004; Yoshigi et al, 2006) and, most intriguingly, rapidly translocates to the nucleus (Cattaruzza 2004, Wojtowicz 2010). Subsequently, this stretch-induced nuclear translocation of zyxin results in distinct changes of gene expression corroborating our assumption that zyxin in fact specifically transduces changes in wall tension to the nucleus.

In the course of this study the signalling events leading to the release of zyxin from focal adhesion contacts and its redistribution to the nucleus could be elucidated. A hierarchical chain of events leads to the nuclear translocation of zyxin in response to stretch namely, stretch-induced activation of TRPC3 induces ET-1 release from EC which through the ET_B-R elicits the subsequent release of ANP. ANP in turn elicits a GC-A-mediated rise in intracellular cGMP leading to protein kinase G (PKG) activation. Subsequent PKG phosphorylation of zyxin at serine-142 enables its dissociation from the focal adhesions and trans-location to the nucleus. This cascade is outlined below (Figure 43).

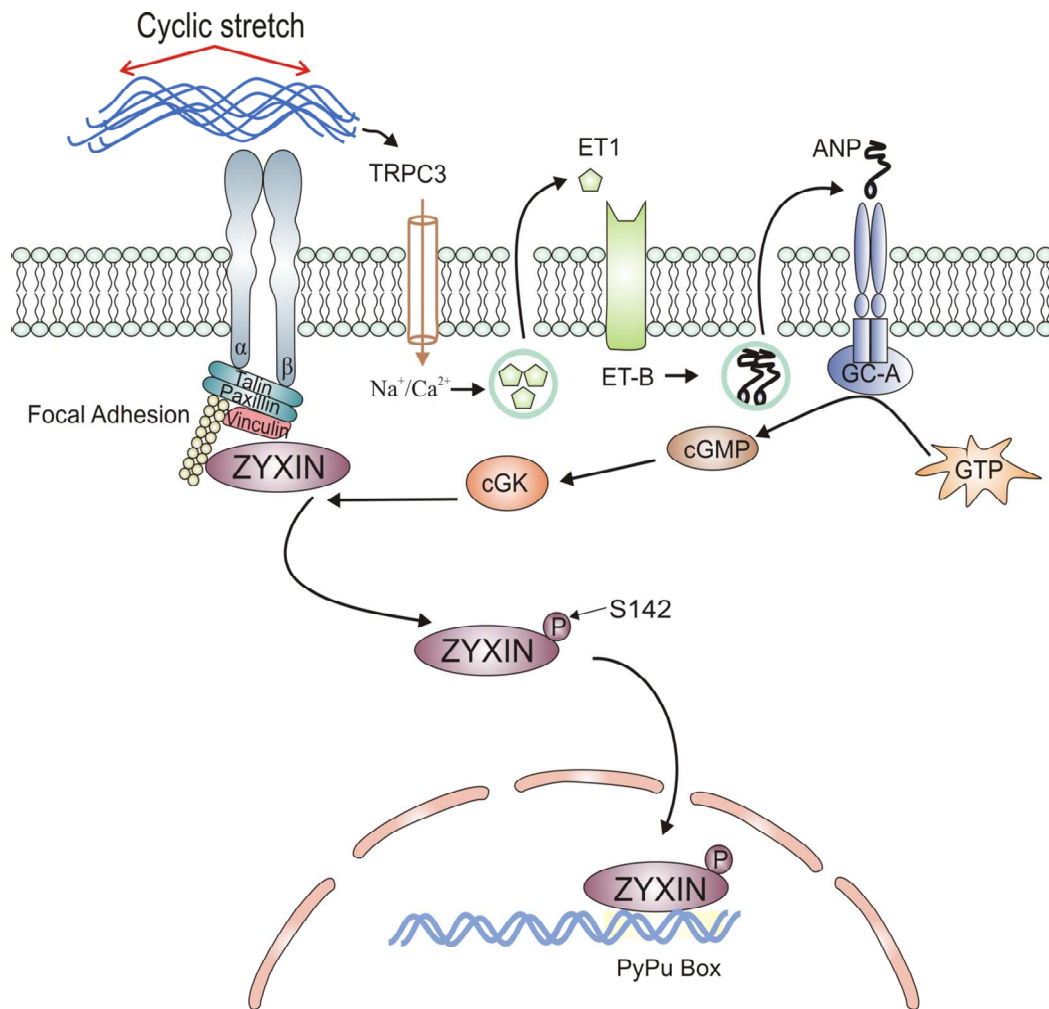


Figure 43: Stretch-induced signalling pathway leading to the nuclear translocation of zyxin. Stretch induces the TRP-C3-channel-induced release of endothelin-1 (ET-1) and, in an ETB-R-mediated manner, Atrial Natriuretic peptide (ANP). ANP through NPR-A receptor mediated the activation of the protein kinase PKG leading to phosphorylation of Zyxin at serine-142 and finally, nuclear translocation of Zyxin, it induces endothelial gene expression in response to stretch.

Although well defined, some aspects of endothelial mechanotransduction remain controversial. Among those is the actual sensing of stretch, the capacity of EC to release ANP and, finally, phosphorylation of zyxin by other kinases. These aspects will be shortly discussed below.

TRPC3 as a mechanosensor

Although the role of TRP channels in the pressure-induced myogenic response (Bayliss 1902; Davis & Hill 1999; Vennekens 2010) is well characterised, nothing is known about their role in early phases of pressure-induced vascular remodelling. Here we have analysed the role of TRPC3 in stretch-induced endothelial mechanotransduction. However, it could not be shown, whether TRPC3 is a genuine mechanosensor or whether the channel is activated by the true (upstream) sensor of stretch.

Principally, TRP channels can be mechanically *gated* and, thus, act as force sensors themselves (shown for TRPM3) or are mechanically *sensitive*, thus activated by second messengers downstream of the true force sensor(s) (TRPC6, Voets 2005; Shimizu 2007; Christensen 2007; Nilius 2007).

Some evidence suggests that mechanically *sensitive* channels are activated by signalling pathways downstream of a G-protein, namely G_q-protein-coupled receptors such as the angiotensin II type-2 receptor (AT₂) that may in fact be a real mechanosensor (Laher 1993; Schnitzler 2008). Intriguingly, the AT₂ receptor in this case is activated without its generic ligand-angiotensin II, leading to activation of phospholipase C and release of diacylglycerol, the TRPC-activating agent in this signalling process (Clapham, 2003, Hofmann et al, 1999; Schnitzler 2008).

In case of EC, TRPC3 and stretch it is an attractive speculation that a similar mechanism as described for TRPC6 and AT₂ may exist, placing the ET_B-R up- and/or downstream of TRPC3 (Figure 44).

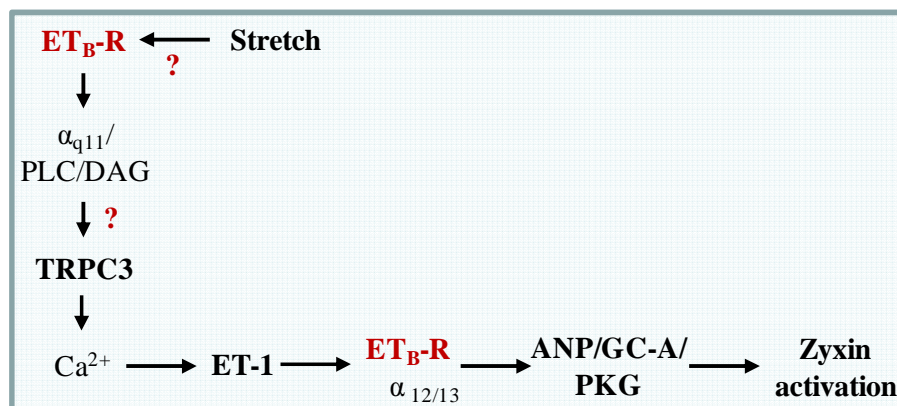


Figure 44: Model of a dual function of the ET_B-R in endothelial mechanotransduction. ET_B-R might play a role upstream of the TRPC3 channel via G_{αq} and also downstream to TRPC3 channel in eliciting the release of ANP.

Another attractive hypothesis how TRPC3 may be activated by stretch without being the actual mechanosensor is the recruitment of the receptor to the cell membrane. Again, this mechanism up to now cannot be analysed because no antibodies for, e.g. immunofluorescence analysis are available.

However, TRPC6 has been shown to respond to pressure stimuli in patches even in the presence of phospholipase-C blockers, arguing against the DAG-mediated activation (Spasova 2006). Therefore, the mechanism through which a TRP channel is activated and regulated is still controversial.

Endothelial release of ANP and the endothelial ANP system

Three natriuretic peptides (ANP, BNP, CNP) with three functionally distinct membrane receptors the guanylate cyclases GC-A and GC-B and the G-protein-coupled receptor NPR-C are known in mammals. Besides the systemic function of ANP, a decrease in blood volume via renal sodium/water secretion (described in the introduction), local ANP-systems have been characterised, predominantly in bone (Schulz 2005) and brain (Shirakami 1993).

Interestingly, the atrial release of ANP and BNP into the blood stream involves a wall tension-induced release of ET-1 from atrial endothelial cells that, in turn, causes ANP release from the cardiac myocytes by activation of the ET_A-R (Thibault 1994). ANP binds then to GC-A and GC-B in the kidney, the brain and several other tissues including the vasculature (Suga 1992; Abraham 1994). Thus, multiple cell types are involved in ANP-mediated volume control.

Intriguingly, systemic volume control by ET-1/ANP seems to be perfectly mimicked at the single cell level in EC with the exception of the effector mechanisms, sodium secretion vs. zyxin activation. However, endothelial release of proANP and its conversion to ANP is controversial as normally (pro)CNP (Chen 1998) is regarded to be the endothelial variant of natriuretic peptides, whereas ANP is thought to be strictly derived from the heart (Cody 1986; Dietz 2005). In contrast, our group was able to demonstrate proANP mRNA expression by and proANP-release from human cultured endothelial cells. This, however, was exclusively restricted to conditions of stretch. As in the literature, our EC did neither express nor release noteworthy amounts of ANP under static conditions. Therefore, it is comprehensible that our findings only seemingly contradict the commonly accepted view of EC as cells without ANP expression. However, as

HUVEC, used throughout the project are venous endothelial cells, it cannot be ruled out that in endothelial cells from other sources CNP may as well be responsible for mechanotransduction. Taken together, although the type of EC-derived natriuretic peptide may be controversial, this is of little consequence for the actual signalling pathway defined in this thesis.

The control of salt and water homeostasis and local vascular mechanotransduction thus seem to share basic signalling mechanisms in order to respond to the same stimulus: stretch.

Phosphorylation of zyxin by PKG at serine 142

Phosphorylation is a dynamic regulatory mechanism that affects the function of a protein (Cohen 2001; Pondugula 2009). During stretch, zyxin phosphorylation leads to its dissociation from the focal adhesions and translocation to the nucleus. Zyxin was found to be phosphorylated at serine-142 by PKG using transfection-based expression of phosphorylation-incompetent and phospho-mimetic zyxin isoforms. To render the zyxin translocation-incompetent, a phosphorylation resistant amino acid residue such as glycine was introduced instead of the wild type amino acid residue. The constructs mutated at S142 to G142 did not translocate to the nucleus upon addition of ANP or stretch (Figure 39 and 40). To confirm that this is not an unspecific reaction, the constructs were further mutated to phosphorylation-mimetic mutants by introducing an acidic residue such as glutamate (E142). Moreover, other mutations at serine-344 and threonine-352 did not have any effect on zyxin activation further confirming the specificity of serine-142 as the amino acid addressed by PKG.

As zyxin has been characterised as a phospho-protein previously, other kinases may be functionally interesting for zyxin activation. Among those, the kinase Akt (Chan 2007) stands out as it has been shown to phosphorylate zyxin at serine-142. Akt itself has been shown to be activated in response to fluid shear stress (Dimmeler 1998). Moreover, NO is well characterised to cause an increase in intracellular cGMP levels and, thus, activate PKG (Martin 1999). Surprisingly, recent experiments showed that HUVEC subjected to fluid shear stress do not respond with zyxin translocation while NO-donors, on the contrary, as a shear stress surrogate, inhibit zyxin translocation. This apparant paradox – expected from

a teleological point of view but surprising from the molecular perspective needs further experimental evaluation. At this point in time differential compartmentalization and up to now unknown protein-protein interactions seem to be the best hypotheses to explain these puzzling findings.

Rho-associated Protein Kinase (ROCK)

ROCK, a downstream effector kinase of the small GTPase Rho, plays an important role in EC signalling in response to inflammation (Mong 2009) and also in stretch (Tsuda 2002). Moreover, ET-1 activates the Rho-ROCK pathway via the G-protein $G_{\alpha_{12/13}}$ in SMC leading to contraction via phosphorylation of myosin light chain (Riento 2003).

The role of ROCK in endothelial mechanotransduction was tested using its inhibitor Y27632. Although to some extent effective in inhibiting stretch-induced IL-8 expression in EC, the results were not fully conclusive so that at this stage it cannot be decided whether the ET_B -R-mediated release of ANP is induced via activation of $G_{\alpha_{q11}}$ or $G_{\alpha_{12/13}}$ or maybe both G-proteins together (see also Figure 44 above).

The stretch response in other cell types

The experiments conducted on SMC using ANP, ET-1 and the same set of inhibitors revealed that SMC have the same signalling cascade for zyxin activation. Although this makes sense from a teleological point of view and, moreover, *in vivo* endothelium-derived ET-1 and ANP will be available, a question remains open:

How can SMC alone possess stretch-induced zyxin activation as these cells do not express ANP? This question is further substantiated as also epithelial cells and primary cultured SMC derived from the urinary bladder show stretch-induced zyxin activation as we could show in the group.

Besides technical reasons, as, e.g., EC co-cultured with primary SMC in our model (isolated perfused artery), it might be that (i) these cell types indeed can respond with ET-1/ANP expression in response to stretch (as at least known for epithelial cells (Novaira 2006) or that (ii) alternative kinases and, thus, endogenous stimuli may account for zyxin activation in these cells. The overall

mechanism, give or take molecular details, however, seems to be similar in many cell types experiencing high levels of wall tension *in vivo* such as lung epithelia, bladder SMC and, naturally vascular EC and SMC.

5.4 Stretch-induced zyxin activation and pressure-induced vascular remodelling

What is the impact of zyxin translocation on pressure-induced vascular remodelling? Although the results presented here and in other reports (Cattaruzza 2004; Wojtowicz 2010; Kato 2005; Nix 1997) plus preliminary findings from our group comparing vessels, the lung and the urinary bladder from wild type and zyxin-deficient mice hint towards a general role of zyxin in wall tension-induced signalling and organ-homeostasis in the face of mechanical (over)load, systematic analysis of the role of zyxin in hypertension and pressure-induced remodelling are necessary to proof the transferability of the *in vitro* data presented here into the *in vivo* situation. However, analyzing the changes in gene expression brought about by zyxin, a dual role of zyxin in early wall tension-induced signalling is highly suggestive. On the one hand, proliferation as well as apoptosis are attenuated and SMC are rendered more susceptible to exogenous constrictors such as ET-1 or norepinephrine and, on the other hand, pro-inflammatory and, in the long run, growth-promoting and de-differentiating pathways are activated.

5.5 Perspective

The present study provides a conclusive description of a specific wall tension-induced mechanotransduction mechanism in endothelial cells. Moreover, a stretch-sensitive promoter element (the PyPu-box) that coordinates zyxin-induced gene expression could be identified and characterised.

Based on these findings, several questions arise that will be addressed in the future:

1. What is the functional impact of zyxin activation *in vivo*? Having overcome the insufficient supply of zyxin-deficient mice in the last few months, this question will be approached by employing a simple hypertension model with wild type and zyxin-deficient mice.

2. What is the real mechanosensor? Although technically demanding, it will be attempted to analyse stretch-induced TRPC3 activation in EC.
3. Functional antagonism between fluid shear stress and wall tension. As shortly discussed above, the inhibitory effect of NO, hence fluid shear stress, on zyxin activation will be further explored: How do both hemodynamic forces interact at the level of mechanotransduction in EC?

6. REFERENCES

Abraham, WT and Schrier RW (1994). Body fluid volume regulation in health and disease. *Adv Intern Med* **39**: 23-47.

Airhart N, Yang YF, Roberts Jr CT, Silberbach M (2003). ANP induces natriuretic peptide receptor-PKG interaction. *J Biol Chem* **278**: 38693–38698.

Bahiru E and Kloner RA (2008). A Comparative Literature Review Exploring Hypertension Drugs that Lower Target Organ Damage Above and Beyond Reducing Blood Pressure Based on Research Studies Between 1992 and 2006. *Current Hypertension Reviews* **4**: 167-176.

Beckerle MC (1997). Zyxin: zinc fingers at sites of cell adhesion. *Bioessays* **19**(11): 949-957.

Birder LA (2002). Altered urinary bladder function in mice lacking the vanilloid receptor TRPV1. *Nature Neurosci* **5**: 856–860.

Black SM, Grobe A, Mata-Greenwood E, Noskina Y (2004). Cyclic stretch increases VEGF expression in pulmonary arterial smooth muscle cells via TGF-1 and reactive oxygen species: a requirement for NAD(P)H oxidase. *Conf Proc IEEE Eng Med Biol Soc.* **7**: 5053-5056.

Cattaruzza M, Lattrich C, Hecker M (2004). Focal adhesion protein zyxin is a mechanosensitive modulator of gene expression in vascular smooth muscle cells. *Hypertension* **43**: 726-730.

Cattaruzza M, Wagner AH, Hecker M (2011) Mechanosensitive pro-inflammatory gene expression in vascular cells. In: *Mechanosensitivity and Cytokines volume 5*, Kamkin A, Kiseleva I (Eds.). ISBN 978-94-007-2003-9.

Chan CB, Liu X, Tang X, Fu H, Ye K (2007). Akt phosphorylation of zyxin mediates its interaction with acinus-S and prevents acinus-triggered chromatin condensation. *Cell Death Differ* **14**: 1688-1699.

Chen HH, Burnett JC Jr (1998). C-type natriuretic peptide: the endothelial component of the natriuretic peptide system. *J Cardiovasc Pharmacol* **32** Suppl 3:S22-S28.

Cheng JJ, Wung BS, Chao YJ, Wang DL (2001) Sequential activation of protein kinase C (PKC)- α and PKC- ϵ contributes to sustained Raf/ERK1/2 activation in endothelial cells under mechanical strain. *J Biol Chem* **276**: 31368-31375.

Chrisman TD, Garbers DL (1999). Reciprocal antagonism coordinates C-type natriuretic peptide and mitogen-signalling pathways in fibroblasts. *J Biol Chem* **274**: 4293–4299.

Cody R J, Atlas SA, Laragh JH, Kubo SH, Covit AB, Ryman KS, Shaknovich A, Pondolfino K, Clark M, and y Camargo MJ (1986). Atrial natriuretic factor in

- normal subjects and heart failure patients. Plasma levels and renal, hormonal, and hemodynamic responses to peptide infusion. *J. Clin. Invest* **78**: 1362–1374.
- Cohen D, Koh GY, Nikonova LN, Porter JG, Maack T (1996). Molecular determinants of the clearance function of type C receptors of natriuretic peptides. *J Biol Chem* **271**: 9863–9869.
- Crawford AW, Michelsen JW, Beckerle MC (1992). An interaction between zyxin and α -actinin. *J Cell Biol* **116**: 1381-1393.
- Davies PF (1995), Flow-mediated endothelial mechanotransduction, *Physiol Rev*, **75**: 519–560.
- Davis MJ & Hill MA (1999). Signalling mechanisms underlying the vascular myogenic response. *Physiol Rev* **79**: 387–423.
- De Martin R, Hoeth M, Hofer-Warbinek R, Schmid JA (2000). The transcription factor NF- κ B and the regulation of vascular cell function. *Arterioscler Thromb Vasc Biol.* **20**: E83–E88.
- Demicheva E, Hecker M, Korff T (2008) Stretch-induced activation of the transcription factor activator protein-1 controls monocyte chemoattractant protein-1 expression during arteriogenesis. *Circ Res* **103**: 477-484.
- Dietrich A (2005). Increased vascular smooth muscle contractility in TRPC6 $^{-/-}$ mice. *Mol. Cell Biol* **25**: 6980–6989.
- Dietrich A and Gudermann T (2008). Another TRP to Endothelial Dysfunction TRPM2 and Endothelial Permeability. *Circ Res.* **102**: 275-277.
- Dietz, J.R (2005). Mechanisms of atrial natriuretic peptide secretion from the atrium. *Cardiovasc Res* **68**: 8-17.
- Dimmeler S, Assmus B, Hermann C, Haendeler J, Zeiher AM (1998). Fluid shear stress stimulates phosphorylation of Akt in human endothelial cells: involvement in suppression of apoptosis. *Circ Res* **83**: 334-41.
- Earley S, Gonzales AL, Crnich R (2009). Endothelium-dependent cerebral artery dilation mediated by TRPA1 and Ca²⁺-Activated K⁺ channels. *Circ Res* **104**: 987-994.
- Garbers DL (1991). Guanyl cyclase-linked receptors. *Pharmacol Ther.* **50**: 337-345.
- Glagov S, Zarins C, Giddens DP, Ku DN (1988) Hemodynamics and atherosclerosis. Insights and perspectives gained from studies of human arteries. *Arch Pathol Lab Med* **112**: 1018-1031.
- Griendling KK, Sorescu D, Ushio-Fukai M (2000). NAD(P)H oxidase: role in cardiovascular biology and disease. *Circ Res.* **86**: 494-501.

- Grimm C, Kraft R, Sauerbruch S, Schultz G and Harteneck C (2003). Molecular and functional characterization of the melastatin-related cation channel TRPM3. *J. Biol. Chem* **278**: 21493–21501.
- Guest TM, Vlastos G, Alameddine FM, Taylor WR (2006) Mechanoregulation of monocyte chemoattractant protein-1 expression in rat vascular smooth muscle cells. *Antioxid Redox Signal* **8**: 1461-1471.
- Guo WH, Wang YL (2007). Retrograde fluxes of focal adhesion proteins in response to cell migration and mechanical signals. *Mol Biol Cell* **18**: 4519-27.
- Heagerty, AM, Aalkjaer C, Bund SJ, Korsgaard N, Mulvany MJ (1993). Small artery structure in hypertension. Dual processes of remodelling and growth. *Hypertension* **21**: 391-397.
- Hecquet CM, Ahmmed GU, Vogel SM, Malik AB (2008). Role of TRPM2 Channel in Mediating H₂O₂-Induced Ca²⁺ Entry and Endothelial Hyperpermeability. *Circ Res.* **102**: 347-355.
- Hermann C, Zeiher AM, Dimmeler S (1997). Shear stress inhibits H₂O₂-induced apoptosis of human endothelial cells by modulation of the glutathione redox cycle and nitric oxide synthase. *Arterioscler. Thromb Vasc Biol* **17**: 3588-3592.
- Hishikawa, K., Oemar B.S., Yang Z., Luscher T.F (1997). Pulsatile stretch stimulates superoxide production and activates nuclear factor- κ B in human coronary smooth muscle. *Circ Res.* **81**: 797–803.
- Kakisis JD, Liapis Ch.D, Sumpio BE (2004). "Effects of cyclic strain on vascular cells. *Endothelium* **11**: 17-28.
- Kanchanawong P, Shtengel G, Pasapera AM, Ramko EB, Davidson MW, Hess HF, Waterman CM (2010). Nanoscale architecture of integrin-based cell adhesions. *Nature* **468**: 580-584.
- Kanungo J, Pratt SJ, Marie H, Longmore GD (2000). Ajuba, a cytosolic LIM protein, shuttles into the nucleus and affects embryonal cell proliferation and fate decisions. *Mol Biol Cell* **11**: 3299-3313.
- Kato T, Muraski J, Chen Y, Tsujita Y, Wall J, Glembotski CC, Schaefer E, Beckerle M, Sussman MA (2005). Atrial natriuretic peptide promotes cardiomyocyte survival by cGMP-dependent nuclear accumulation of zyxin and Akt. *J Clin Invest* **115**: 2716-2730.
- Kawashima S and Yokoyama M (2004). Dysfunction of endothelial nitric oxide synthase and atherosclerosis. *Arterioscler Thromb Vasc Biol* **24**: 998-1005.
- Kida T, Chuma H, Murata T, Yamawaki H, Matsumoto S, Hori M, Ozaki H (2010) Chronic treatment with PDGF-BB and endothelin-1 synergistically induces vascular hyperplasia and loss of contractility in organ-cultured rat tail artery. *Atherosclerosis.* **214**: 288-294.

- Kinlay S, Libby P, Ganz P (2001) Endothelial function and coronary artery disease. *Curr Opin Lipidol* **12**: 383-389.
- Klotz LO, Schroeder P, Sies H (2002) Peroxynitrite signalling: receptor tyrosine kinases and activation of stress-responsive pathways. *Free Radic Biol Med* **33**: 737-743.
- Lacolley P (2004). Mechanical influence of cyclic stretch on vascular endothelial cells. *Cardiovascular Res* **63**: 577-579.
- Lauth M, Wagner AH, Cattaruzza M, Orzechowski HD, Paul M, Hecker M (2000) Transcriptional control of deformation-induced preproendothelin-1 gene expression in endothelial cells. *J Mol Med* **78**: 441-450.
- Lehoux S, Castier Y, Tedgui A (2006), Molecular mechanisms of vascular responses to hemodynamic forces, *J Int Med* **259**: 381-392.
- Lehoux, S., Tedgui A (1998). Signal transduction of mechanical stresses in the vascular wall. *Hypertension* **32**: 338-345.
- Li, S., Moon J.J., Miao H., Jin G., Chen B.P., Yuan S., Hu Y., Usami S., Chien S (2003). Signal transduction in matrix contraction and the migration of vascular smooth muscle cells in three-dimensional matrix. *J Vasc Res* **40**: 378-388.
- Libby P (2007). Inflammatory mechanisms: the molecular basis of inflammation and disease. *Nutr Rev* **65**:S140-S146.
- Macalma T, Otte J, Hensler ME, Bockholt SM, Louis HA, Kalff-Suske M, Grzeschik KH, von der Ahe D and Beckerle MC (1996). Molecular characterization of human zyxin. *J Biol Chem.* **271**: 31470-31478.
- MacMahon S, Peto R, Cutler J, Collins R, Sorlie P, Neaton J, Abbott R, Godwin J, Dyer A, Stamler J (1990). Blood pressure, stroke, and coronary heart disease. Part 1, Prolonged differences in blood pressure: prospective observational studies corrected for the regression dilution bias. *Lancet.* **335**: 765-774.
- Malek AM, Alper SL, Izumo S (1999). Hemodynamic shear stress and its role in atherosclerosis. *JAMA* **282**: 2035-2042.
- Mäntymaa, P, Leppaluoto J, Ruskoaho H (1990). Endothelin stimulates basal and stretch-induced atrial natriuretic peptide secretion from the perfused rat heart. *Endocrinology* **126**: 587-595.
- Matsushima Y, Ohshima M, Sonoda M, Kitagawa Y (1996). A family of novel DNA-binding nuclear proteins having polypyrimidine tract-binding motif and arginine/serine-rich motif. *Biochem Biophys Res Commun* **223**: 427-433.
- Minke B and Cook B. (2002), TRP Channel Proteins and Signal Transduction, *Physiol Rev*, **82**: 429-472.

- Molavi B and Mehta JL (2004). Oxidative stress in cardiovascular disease: molecular basis of its deleterious effects, its detection, and therapeutic considerations. *Curr Opin Cardiol* **19**: 488-493.
- Mong PY, Wang Q (2009). Activation of Rho kinase isoforms in lung endothelial cells during inflammation. *J Immunol* **182**: 2385-2394.
- Mullis KB., F. F. A. (1987). Specific synthesis of DNA in vitro via a polymerase catalyzed chain reaction. *Methods Enzymol* **155**: 335-350.
- Nilius B, Owsianik G, Voets T, Peters JA (2007). Transient Receptor Potential Cation Channels in Disease. *Physiol Rev.* **87**: 165–217.
- Nix DA, Beckerle MC (1997). Nuclear-cytoplasmic shuttling of the focal contact protein, zyxin: a potential mechanism for communication between sites of cell adhesion and the nucleus. *J Cell Biol* **138**: 1139-1147.
- Novaira HJ, Ornellas DS, Ortiga-Carvalho TM, Zhang XM, Souza-Menezes J, Guggino SE, Guggino WB, Morales MM (2006). Atrial natriuretic peptide modulates cystic fibrosis transmembrane conductance regulator chloride channel expression in rat proximal colon and human intestinal epithelial cells. *J Endocrinol* **189**: 155-165.
- Nussenzveig DR, Lewicki JA, Maack T (1990). Cellular mechanisms of the clearance function of type C receptors of atrial natriuretic factor. *J Biol Chem* **265**: 20952–20958.
- Oancea E, Wolfe JT and Clapham DE (2006). Functional TRPM7 channels accumulate at the plasma membrane in response to fluid flow. *Circ. Res* **98**: 245–253.
- Pasterkamp G, de Kleijn DP, Borst C (2000). Arterial remodelling in atherosclerosis, restenosis and after alteration of blood flow: potential mechanisms and clinical implications *Cardiovasc. Res.* **45**: 843-852.
- Petit MM, Fradelizi J, Golsteyn RM, Ayoubi TA, Menichi B, Louvard D, Van de Ven WJ, Friederich E (2000). LPP, an actin cytoskeleton protein related to zyxin, harbors a nuclear export signal and transcriptional activation capacity. *Mol Biol Cell* **11**: 117-129.
- Piechota A, Polańczyk A, Goraca A (2010). Role of endothelin-1 receptor blockers on hemodynamic parameters and oxidative stress *Pharmacol Rep.* **62**: 28-34.
- Planells-Cases R, Ferrer-Montiel A (2007). TRP Channel Trafficking. In: Liedtke WB, Heller S, editors. *TRP Ion Channel Function in Sensory Transduction and Cellular Signaling Cascades*. Boca Raton (FL): CRC Press; Chapter 23.
- Pohl U (2009). Vascular Remodelling: *In Situ* vs. *Ex Vivo*. *Physiology* **24**: 270.

- Potter LR, Abbey-Hosch S, Dickey (2006). Natriuretic peptides, their receptors, and cyclic guanosine monophosphate-dependent signalling functions. *Endocr Rev* **27**: 47-72.
- Reinhard M, Zumbunn J, Jaquemar D, Kuhn M, Walter U, Trueb B (1999). An alpha-actinin binding site of zyxin is essential for subcellular zyxin localisation and alpha-actinin recruitment. *J Biol Chem* **274**: 13410-13418.
- Riento K and Ridley AJ (2003). Rocks: multifunctional kinases in cell behaviour *Nat Rev Mol Cell Biol* **4**: 446-456.
- Rottner K, Krause M, Gimona M, Small JV, Wehland J (2001). Zyxin is not colocalised with vasodilator-stimulated phosphoprotein (VASP) at lamellipodial tips and exhibits different dynamics to vinculin, paxillin, and VASP in focal adhesions. *Mol Biol Cell*. **12**: 3103-3013.
- Sadoshima J and Izumo S (2007). The cellular and molecular response of cardiac myocytes to mechanical stress. *Annual Review of Physiology* **59**: 551-571.
- Salvatore S, Vingolo EM (2011). Endothelin-1 role in human eye: a review. *J Ophthalmol*. PMID 354645, Epub ahead of print].
- Sawicka K, Bushell M, Spriggs KA, Willis AE (2008). Polypyrimidine-tract-binding protein: a multifunctional RNA-binding protein. *Biochem Soc Trans* **4**: 641-647.
- Schepers A, Eefting D, Bonta PI, Grimbergen JM, de Vries MR, van Weel V, de Vries CJ, Egashira K, van Bockel JH, Quax PH (2006). Anti-MCP-1 gene therapy inhibits vascular smooth muscle cells proliferation and attenuates vein graft thickening both *in vitro* and *in vivo*. *Arterioscler Thromb Vasc Biol* **26**: 2063-2069.
- Schiffrin, EL (1999). State-of-the -Art lecture. Role of the endothelin-1 in hypertension. *Hypertension* **34**: 876-881.
- Schulz S (2005). C-type natriuretic peptide and guanylyl cyclase B receptor. *Peptides* **26**: 1024-1034.
- Sharma SK, Sweeny J, Kini AS (2010) Coronary bifurcation lesions: a current update. *Cardiol Clin* **28**: 55-70.
- Shirakami G, Magaribuchi T, Shingu K, Suga S, Tamai S, Nakao K, Mori K (1993). Positive end-expiratory pressure ventilation decreases plasma atrial and brain natriuretic peptide levels in humans. *Anesth Analg* **77**: 1116-1121.
- Shrinsky VP, Antonov AS, Birukov K.G, Sobolevsky AV., Romanov YA, Kabeva N.V., Antonova G.N., Smirnov V.N (1989). Mechano-chemical control of human endothelium orientation and size. *J Cell Biol* **109**: 331-339.
- Stults JT, O'Connell KL, Garcia C, Wong S, Engel AM, Garbers DL, Lowe DG (1994). The disulfide linkages and glycosylation sites of the human natriuretic peptide receptor-C homodimer. *Biochemistry* **33**: 11372-11381.

- Suga S, Nakao K, Hosoda K, Mukoyama M, Ogawa Y, Shirakami G, Arai H, Saito Y, Kambayashi Y, Inouye K, Imura H (1992). Receptor selectivity of natriuretic peptide family, atrial natriuretic peptide, brain natriuretic peptide, and C-type natriuretic peptide. *Endocrinology* **130**: 229–239.
- Sumpio BE, Banes AJ, Link GW, Iba T (1990). Modulation of endothelial cell phenotype by cyclic stretch: inhibition of collagen production. *J Surg Res* **48**: 415–420.
- Sung HJ, Yee A, Eskin SG, McIntire LV (2007). Cyclic strain and motion control produce opposite oxidative responses in two human endothelial cell types. *Am J Physiol Cell Physiol*. **293**: C87–C94.
- Taskinen P., Toth M., Ruskoaho H. (1994). Effects of genistein on cardiac contractile force and atrial natriuretic peptide secretion in the isolated perfused rat heart. *Eur J Pharmacol* **256**: 251–261.
- Thibault G, Doubell AF, Garcia R, Larivière R, Schiffrin EL (1994). Endothelin-stimulated secretion of natriuretic peptides by rat atrial myocytes is mediated by endothelin A receptors. *Circ Res* **74**: 460–70.
- Thubrikar MJ and Robicsek F (1995). Pressure-Induced Arterial Wall Stress and Atherosclerosis. *Ann Thorac Surg* **59**: 1594–1603.
- Touyz RM, Yao G, Viel E, Amiri F, and Schiffrin EL (2004). Angiotensin II and endothelin-1 regulate MAP kinases through different redox-dependent mechanisms in human vascular smooth muscle cells. *J Hypertens* **22**: 1141–1149.
- Tsuda YOM, Uezono Y, Osajima A, Kato H, Okuda H, Oishi Y, Yashiro A, Nakashima Y (2002). Activation of extracellular signal-regulated kinases is essential for pressure-induced proliferation of vascular smooth muscle cells. *Eur J Pharmacol* **446**: 15–24.
- Uematsu M, Ohara Y, Navas JP, Nishida K, Murphy TJ, Alexander RW, Nerem RM, Harrison DG (1995) Regulation of endothelial cell nitric oxide synthase mRNA expression by shear stress. *Am J Physiol* **269**: C1371–C1378.
- Valencia CA, Ju W, Liu R (2007). Matrin 3 is a Ca²⁺/calmodulin-binding protein cleaved by caspases. *Biochem Biophys Res Commun* **361**: 281–286.
- Vennekens R (2011). Emerging concepts for the role of TRP channels in the cardiovascular system. *J Physiol* **589**: 1527–1534.
- Wang Y, Gilmore TD (2003). Zyxin and paxillin proteins: focal adhesion plaque LIM domain proteins go nuclear. *Biochem Biophys Acta* **1593**: 115–120.
- Welsh DG, Morielli AD, Nelson MT and Brayden JE (2002). Transient receptor potential channels regulate myogenic tone of resistance arteries. *Circ. Res.* **90**: 248–250.

- Wojtowicz A (2008). The focal adhesion protein zyxin mediates wall tension-induced signalling in vascular cells. *Dissertation*, University of Heidelberg.
- Wójtowicz A, Babu SS, Li L, Gretz N, Hecker M, Cattaruzza M (2010). Zyxin mediation of stretch-induced gene expression in human endothelial cells. *Circ Res* **107**: 898-902.
- Yamazaki T, Komuro I & Yazaki Y (1995). Molecular mechanism of cardiac cellular hypertrophy by mechanical stress. *J Mol Cell Cardiol* **27**: 133-140.
- Yanagisawa M, Kurihara H, Kimura S, Tomobe Y, Kobayashi M, Mitsui Y, Yazaki Y, Goto K & Masaki T (1988) A novel potent vasoconstrictor peptide produced by vascular endothelial cells. *Nature* **332**: 411-415.
- Yoshigi M, Hoffman LM, Jensen CC, Yost HJ, Beckerle MC (2005). Mechanical force mobilizes zyxin from focal adhesions to actin filaments and regulates cytoskeletal reinforcement. *J Cell Biol* **171**: 209–215.
- Yue TL, Wang X, Sung CP, Olson B, McKenna PJ, Gu JL, Feuerstein GZ (1994) Interleukin-8, A mitogen and chemoattractant for vascular smooth muscle cells. *Circ Res.* **75**: 1-7.

APPENDIX

Sequence analysis of zyxin mRNA and the corresponding amino acid. The amino acids targeted for mutation are highlighted in yellow.

```

1  ccgcgccct ctcttctccc tccctctccc ttccgtgtgt ccctccccgc cgggtggag
61  gctgctccgg accgggacgc agagtctgcg gaccggcgcg cgaggcggcc acccgagacg
121  cggcgcgcac gctccggcct gcgcagcccc gcccgccat ggcggccccc cgcccgtctc
181  ccgcgatctc cgtttccggtc tcggtccggt ctttttacgc cccgcagaag aagttcggcc
241  ctgtggtggc cccaaagccc aaagtgaatc ctttccggcc cggggacagc gagcctcccc
301  cggcaccggg ggcccagcgc gcacagatgg gccgggtggg cgagattccc ccgcccggcc
361  cggaagactt tcccctgect ccacctcccc ttgctgggga tggcgcagat gcagagggtg
421  ctctgggagg tgccttcccg ccgcccctc ccccgatcga ggaatcattt ccccctgccc
481  ctctggagga ggagatcttc cttccccgcg cgcctcctcc ggaggaggag ggaggccctg
541  aggcccccat accgccccca ccacagccca gggagaaggt gagcagtatt gatttgagga
      E A P I P P P P Q P R E K V S S I D L E
      142
601  tcgactctct gtccctactg ctggatgaca tgaccaagaa tgatccttcc aaagcccggg
      I D S L S S L L D D M T K N D P F K A R
661  tgtcatctgg atatgtgccc ccaccagtgg ccaactccatt cagttccaag tccagtacca
      V S S G Y V P P P V A T P F S S K S S T
721  agcptgcagc cgggggcaca gcaccctgct ctccttgtaa gtccccttcc agtcccagc
      K P A A G G T A P L P P W K S P S S S Q
781  ctctgccccca ggttccggct ccggctcaga gccagacaca gttccatggt cagccccagc
      P L P Q V P A P A Q S Q T Q F H V Q P Q
841  cccagcccaa gcctcaggtc caactccatg tccagtccca gaccagcct gtgtcttggg
      P Q P K P Q V Q L H V Q S Q T Q P V S L
901  ctaacaccca gccccgaggg ccccagcct catctccggc tccagcccct aagtttcttc
      A N T Q P R G P P A S S P A P A P K F S
961  cagtactcc taagtttact cctgtggctt ccaagttcag tctggagcc ccaggtggat
      P V T P K F T P V A S K F S P G A P G G
1021  ctgggtcaca accaaatcaa aaattggggc accccgaagc tcttctgtgt ggcacaggct
      S G S Q P N Q K L G H P E A L S A G T G
1081  cccctcaacc tcccagcttc acctatgccc agcagagggg gaagccccga gtgcaggaga
      S P Q P P S F T Y A Q Q R E K P R V Q E
1141  agcagcacc cgtgccccca ccggctcaga accaaaacca ggtgectccc cctggggccc
      K Q H P V P P P A Q N Q N Q V R S P G A
      344
1201  cagggcccct gactctgaag gaggtggagg agctggagca gctgaccag cagctaattg
      P G P L T L K E V E E L E Q L T Q Q L M
      352
1261  aggacatgga gcatcctcag aggcagaatg tggctgtcaa cgaactctgc ggccgatgcc
      Q D M E H P Q R Q N V A V N E L C G R C
1321  atcaaccctt ggcccggggc cagccagccg tccgcgctct agggcagctg ttccacatcg
      H Q P L A R A Q P A V R A L G Q L F H I
1381  cctgcttcac ctgccaccag tgtgcgcagc agctccaggg ccagcagttc tacagtctgg
      A C F T C H Q C A Q Q L Q G Q Q F Y S L
1441  agggggcgcc gtactgcgag ggctgttaca ctgacaccct ggagaagtgt aacacctcgg
      E G A P Y C E G C Y T D T L E K C N T C
1501  gggagcccat cactgaccgc atgctgaggg ccacgggcaa ggcctatcac ccgactgtct
      G E P I T D R M L R A T G K A Y H P H C
1561  tcacctgtgt ggtctgcgcc cgcccctgg agggcacctc cttcatctgt gaccagcca
      F T C V V C A R P L E G T S F I V D Q A
1621  accggccccca ctgtgtcccc gactaccaca agcagtagcg cccgaggtgc tccgtctgtct
      N R P H C V P D Y H K Q Y A P R C S V C

```

```

1681 ctgagcccat catgcctgag cctggccgag atgagactgt gcgagtggtc gccctggaca
    S E P I M P E P G R D E T V R V V A L D
1741 agaacttcca catgaagtgt tacaagtgtg aggactgcgg gaagcccctg tcgattgagg
    K N F H M K C Y K C E D C G K P L S I E

1801 cagatgacaa tggctgcttc ccctggacg gtcacgtgct ctgtcggaa gtcacactg
    A D D N G C F P L D G H V L C R K C H T
1861 ctagagccca gacctgagtg aggacaggcc ctcttcagac cgcagtccat gccccattgt
    A R A Q T
1921 ggaccaccca cactgagacc acctgcccc acctcagtta ttgtttgat gtctagcccc

1981 tccccatttc aaccctccc tagcatcca ggtgccctga cccaggaccc aacatggtct

2041 agggatgcag gatccccgcc ctggggctctg gtcctcgccc atcctgcagg gattgcccac

2101 cgtcttcag acaccccacc tgaggggggc accaggttta gtgctgctgc tttcactgct

2161 gcaccgcgc cctcggccgg cccccgagc agcctttgta ctctgcttgc ggagggctgg

2221 gagaccctcc aggacattcc caccctccc catgctgcca agttgtagct atagctacaa

2281 ataaaaaaaa accttgtttt ccagaaaaaa aaaaaaaaaa aaaaaa

```

Exemplary figures showing the nuclei of the cells considered for quantification.

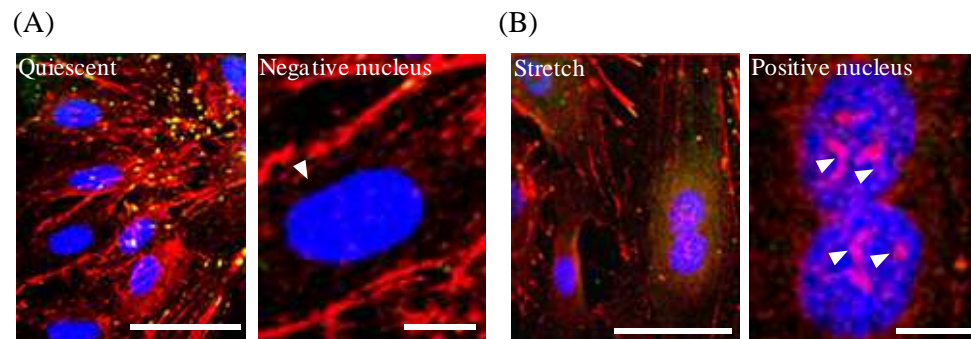


Figure 45: Representative confocal immunofluorescence analysis of zyxin localisation in (A) quiescent and (B) stretched HUVEC. The arrows depicting non-nuclear stress fibres over the nuclei of quiescent cells (thus, such nuclei are counted as negative) and the freckle-like pattern in the stretched nucleus (counted as zyxin-positive). The left panel always is an overview (Bar: 50 μ m), the right pictures are enlargements of nuclei. Scale bar: 10 μ m.

ACKNOWLEDGEMENTS

I would like to sincerely acknowledge Prof. Dr. Markus Hecker, firstly for providing me the opportunity to pursue my PhD studies at the department of cardiovascular physiology, and secondly for his consistent guidance throughout my thesis. I particularly thank him for our regular group discussions, which had a major influence on this thesis. His leadership, attention to details and urge for perfection has set an example that I would like to match some day.

The present thesis was simply not possible without the enthusiastic supervision of my mentor PD. Dr. Marco Cattaruzza. He virtually taught me everything; from making me understand the basic concepts of cardiovascular physiology, to having a perfect final draft of the thesis. The enthusiasm and dedication he has for research was highly motivational, especially during the tough times when I went for weeks without good results. I am indebted to him for showing confidence in me and always urging me to achieve greater heights.

I sincerely thank Prof. Dr. Stephan Frings for being my formal supervisor. I also thank PD. Dr. Andreas Wagner, PD. Dr. Thomas Korff and Dr. Oliver Drews for their valuable discussion and suggestions during the course of my PhD. I also thank Dr. Victor Ciocotisan for PEI transfection reagent. I warmly thank Kerstin Moeller and Cordula Rumig for their help with proof-reading the thesis.

It is my pleasure to acknowledge Renate Cattaruzza and Anja Feldner for their valuable guidance through different phases of my PhD. Technical expertise of Danijela Heide is deeply appreciated. Her precision and speed went a long way in getting my experiments done on time. I also thank my present and former colleagues, Mathilde Lorenz, Franziska Mohr, Larissa Pfisterer, Hannes Otto, Ender Serbest, Sviatlana Yakubenia, Oliver Adolph, Barbara Richards, Michaela Neidig, Juergen Czachurski, Agnieszka Wojtowicz, Jennifer Braun and Beate Berghoefer.

I am thankful to my best friends Santhosh Jayaraju, Sheethal Panchakshari, Deepa Damodaran, Hui Liu, and my roommate Pia Schmidt for always being there through my good and bad times.

Lastly, and most importantly, my utmost gratitude is reserved to my family: parents, Suresh Babu and Sujatha for their constant support and encouragement and sister; Sanjana Suresh for her keeping me light hearted with her jolly-well attitude towards life.